Master Thesis in Geosciences

Depositional environment, sequence stratigraphy and reservoir properties of an Eocene mixed siliciclastic- carbonate succession in the Ainsa Basin, Southern Pyrenees

Asfaw Tenna Woyessa

UNIVERSITY OF OSLO

FACULTY OF MATHEMATICS AND NATURAL SCIENCES

Depositional environment, sequence stratigraphy and reservoir properties of an Eocene mixed siliciclastic-carbonate succession in the Ainsa Basin, Southern Pyrenees

Asfaw Tenna Woyessa

Master Thesis in Geosciences

Discipline: Petroleum Geology and Geophysics

Department of Geosciences

Faculty of Mathematics and Natural Sciences

UNIVERSITY OF OSLO

01.05.2008

Tutor(s): Professor Johan Petter Nysuen, Professor Roy Gabrielsen and Dr. Micheal Heermans, UiO

This work is published digitally through DUO – Digitale Utgivelser ved UiO

http://www.duo.uio.no

It is also catalogued in BIBSYS (http://www.bibsys.no/english)

ACKNOWLEDGMENTS

I would like to express my deepest gratitude to my supervisor Professor Johan Petter Nystuen for his constant supervision, guidance, and valuable advices, without his support the research may not assume the present form. I am also very grateful to my co-supervisors Professor Roy Gabrielsen, Head of the Department of Petroleum Geology and Geophysics at the University of Oslo, and Dr. Micheal Heermans for their support.

I would like to thank Dr. Cai Puigdefabregas for his introduction to the studied area, guidance and invaluable descriptions of interesting features of the Ainsa Basin. I would also like to thank Erlend Morisbak, Gilbert Ako and Roger Flåt for the interesting discussions and the memorable times we spent together during the entire period of the Thesis work.

I am highly indebted to anyone who has given me any helpful comments and suggestions to any part of this Thesis work. I would also like to thank my parents and my sisters and brother who have given me every support I needed. I also thank my colleagues of the MSc student 2006-2008 class in Geosciences discipline for sharing experiences and knowledge during the time of study.

I would like to express my gratitude to my Scholarship sponsor, Norwegian State Education Fund (Lånekassen), for financing of my study at the University of Oslo.

Finally, I acknowledge NorskHydro AS (now StatoilHydro AS) for providing me financial support for field work of the study.

Oslo, June 2008

Asfaw Tenna Woyessa

Front Page: General overview of the study area (Observation direction: North to South).

LIST OF CONTENT

ABSTRACT

Mixed siliciclastic carbonate rocks of Lower Eocene age are studied in the eastern part of the Ainsa Basin, Southern Pyrenees. These deposits generally show an upward coarsening and shoaling trend followed by deepening trend. Nine facies identified in the study area have been grouped into four facies associations formed within a carbonate ramp platform. These are: (a) low-angle cross-bedded siliciclastic sandstone and micritic limestone; (b) cross-bedded to horizontally laminated carbonate rich sandstone; (c) amalgamated/interbedded carbonate rich sandstone; and (d) structureless siltstone and mudstone and micritic limestone. The succession has been classified into three informal units: the lower-, middle-, and upper-units. The lateral extent and the architectural style of the deposits in each unit are very variable.

Nummulites dominate the biota with minor occurrences of bivalves and plant fragments. Most part of the carbonates in the study area is interpreted to be produced by nummulites with some siliciclastic input in the shallower part of the platform. Nummulite shells were reworked, fragmented and redistributed later by basinal current processes. The platform has been divided into inner-, mid-, and outer-ramp positions. In the middle unit there is a systematic variation in depositional environment from northern- to southern- part of the study area that reflects northward shallowing and/or the existence of dominant oceanographic currents that drifted towards north, or a combination of both factors.

The middle unit represents a highstand systems tract with a possible highstand carbonate shedding into the deeper part of the basin. The deposits are interpreted to be controlled by both autogenic and allogenic factors. While *in situ* carbonate production by nummulites and oceanographic currents are included in the autogenic controls, tectonics, eustacy, and climate are thought to have played a major role in allogenic factors. Tropical to seasonal subtropical climatic condition of the study area during the Eocene, which created a conducive environment for nummulites, augmented by reduced siliciclastic sediment supply led to progradation for the mixed-siliciclastic carbonate deposits in the middle unit. Later, transgression must have occurred that caused deposition of carbonate rich mudstone of the upper unit, combined with shoreface retreat.

Poor vertical connectedness and lateral discontinuity of carbonate rich sandstones, very fine grain size and with most interparticle pore spaces filled by different minerals make this type of carbonate ramp platform succession to represent a low-permeability reservoir of restricted reservoir qualities.

1. INTRODUCTION

Carbonate rocks have got a strong focus due to their academic interest as rocks of especial origin and their great ecomonic importance in modern industry. Since these rocks constitute a significant part of the stratigraphic record, carbonates have been used to study the stratigraphy of the Earth. Carbonate rocks are used for construction purposes and as material in a series of industry product and for regulation of pH in agricultural soils. In addition, and not at least, carbonate rocks comprise reservoir rocks for around 40 % of the world's oil and gas reserves (Reading & Levell, 1996).

Shallow-marine mixed siliciclastic-carbonate deposits provide sensitive records of sea-level, tectonics, climate, and sediment supply. Nevertheless, mixed silciclastic-carbonate strata have generally received less attention than the carbonate and silciclastic end members. In addition, the controls on the sequence development of mixed-carbonate ramp systems are relatively poorly documented. Unlike siliciclastic or carbonate facies alone, the mixed lithology fill of foreland basins provide a more sensitive record of basin evolution, as the different sediment types respond differently to patterns of uplift and subsidence (Saylor, 2003). As concerns interpretation of depositional environment of shallow-marine mixed siliciclastic-carbonate deposits this creates problems because the influx of siliciclastic detritus to the shallow-marine realm generally inhibits or reduces biogenic carbonate production (e.g. Wright and Burchette 1996).

The shallow marine successions that crop out in the eastern part of the Eocene Ainsa Basin, Spanish Pyrenees, contain mixed siliciclastic-carbonate deposits. Such deposits are well exposed along the road which connects Feundecampo and Tierrantona localities, north to northeast direction of El Pocino. The quality of exposures in other sections of the study area is not very conducive due to vegetation cover.

The main objectives of this Thesis work are to (1) investigate the vertical and lateral facies successions and their architectural style; (2) determine the provenance of the deposits; and (3) describe and interprete the depositional environments of the study area, including processes which were active during and/or after the deposition. The objective of the Thesis

also includes the application of sequence stratigraphic concepts and to describe and interprete possible controlling factors which influenced the sequence development, and finally, to assess potential reservoir properties of this type of shallow marine deposits.

2. GEOLOGY

2.1 Regional Geological Setting

The shallow marine deposits selected for this study is found in the eastern part of the Ainsa Basin, in the Southern Pyrenees, northern Spain. During Cretaceous period, the relative movement of Euroasian and African plates had a strong influence on the paleogeography and sedimentation of the Iberia basin, but the initiation of the North Atlantic spreading decreased the sinisteral movement between Iberia and Africa (Ziegler, 1988) and later (from late Aptian to early Campanian) a counter clock-wise rotation (up to 30^0) of Iberia with respect to Europe resulted in the opening of the Bay of Biscay (Olivet, 1996). During this period, the South Pyrenean zone was part of the northern margin of the Iberian plate (Pomar et al., 2005). Basin widening due to extension occurred during Triassic followed by associated transtensional tectonics from Neocomian to Barremian (Puigdefabregas and Souquet, 1986). However, continental collision did not begin until Late Cretaceous and it was initiated in the eastern Pyrenees area (Gibbons and Moreno, 2002).

The Pyrenees is the result of the Cretaceous-Miocene collision of Afro-Iberian and European plates (Choukroune and Seguret, 1973; Fitzgerald et al., 1999). This collision created a compact two-sided orogen (Munoz, 1992) with paired fold and thrust belts developed in Mesozoic and Cenozoic sedimentary cover rocks, and foreland basins north and south of the Axial Zone (Pickering and Corregidor, 2005).

The Axial Zone, located in the central part of the Pyrenees, comprises antiformal stacks of Hercynian Paleozoic basement rocks and represents complex south-vergent duplex structures (Fitzgerald et al., 1999). Towards south of the Axial Zone, Mesozoic and Cenozoic rock successions of the Southern Pyrenean have been transported towards the south; whereas towards north of the Aixial Zone, the North Pyrenean contains the deep structural level of the belt which is characterized by N-verging asymmetrical folds (Choukroune, 1969; Choukroune et al., 1973b). Reconstructed Hercynian basement showed that 15 – 18 km of the Axial Zone antiformal stack were eroded to present day relief (Fitzgerald et al., 1999). The North Pyrenean Fault, which was formed due to sinisteral movement of Iberia with respect to Europe in Middle Cretaceous, bounds the basement antiformal stack to the north and is regarded as the boundary between the Iberian plate and

Europe (Choukroune et al., 1973a). The North Pyrenean zone and the sub-Pyrenean zone, consisting of Tertiary north-verging thrust sheets (Puigdefabregas and Souquet, 1986), were exposed north of this fault; whereas the southern zone consists of a succession of Tertiary south-verging thrust sheets (Munoz, 1985). The south Pyrenean thrust sheets, which make up the South Pyrenean Central Unit (SPCU), consists of the Bóixols, Montsec, and Sierras Marginales units (Puigdefabregas et al., 1992) (Figure 2.1).

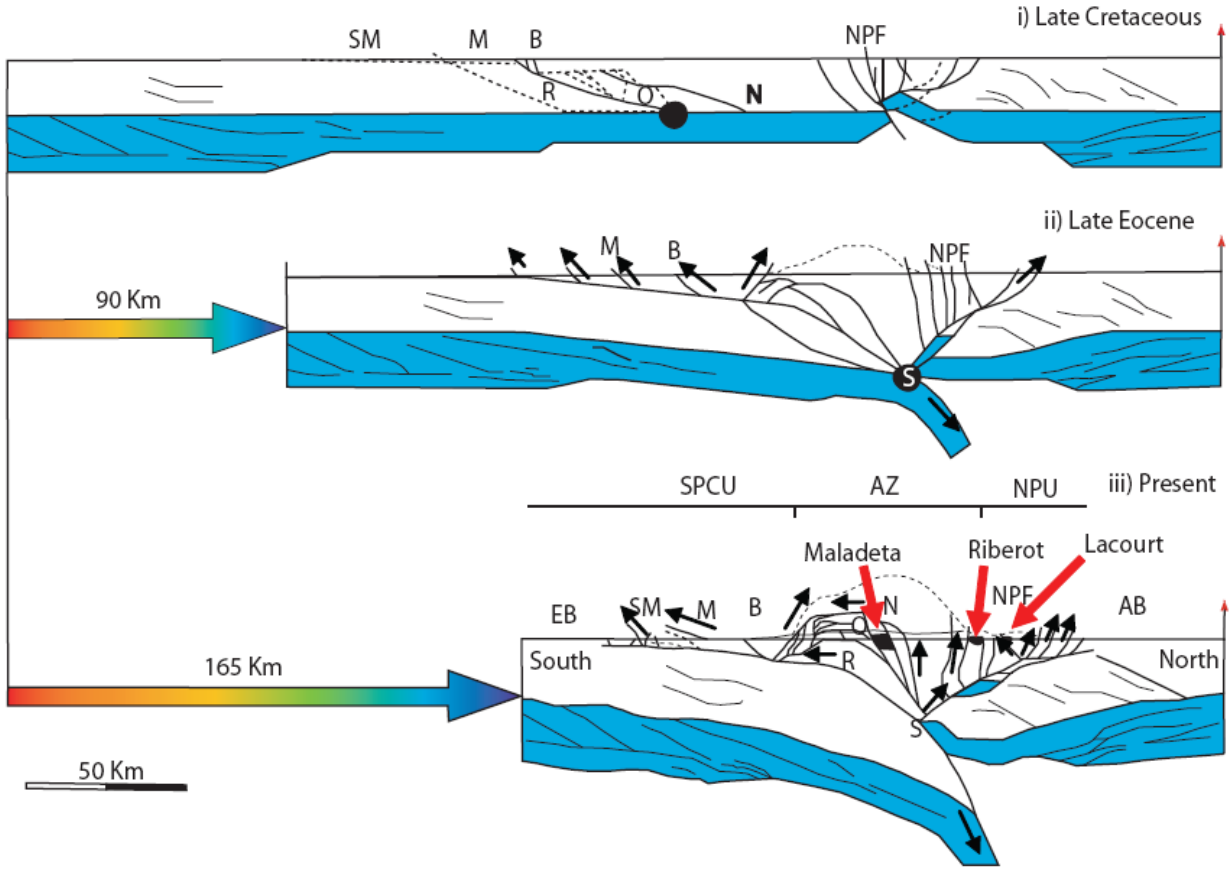

Figure 2.1: Late Cretaceous to Present tectonic evolution of the Pyrenean crust along the ECORS line (Modified after Fitzgerald et al., 1999). SPCU= South Pyrenean unit; NPU= North Pyrenean unit; AZ= Axial Zone; NPF= North Pyrenean Fault; SM= Serres M Marginals; *M*= Montsec; *B*= Bóixols; *R*= Rialp; *O*= Orri; *N*= Nogueres; *EB*= Ebro Basin; *AB*= Aquitane Basin. The shaded portion represents lower crust.

Fitzgerald et al. (1999) using apatite fission track thermochronology showed the younging of the Pyrenees from north to south and its asymmetric pattern that made the authors suggest the existence of severe exhumation to the south**.**

Munoz (1992) suggested the shortening of the Pyrenees by approximately 147 km in the central part where the majority of the shortening was directed southward. According to Verges et al. (1998) maximum rates of shortening and thrust front advance were coincident with the maximum rates of subsidence in the foreland basin during late Lutetian. However, about half of the total shortening was contemporaneous with the burial of the thrust belt and the exhumation of the Axial Zone (Munoz et al., 1997). According to ECORS Pyrenees Team (1988) to the east of $1^0$20' west longitude, orogenic shortening was accomodated by limited subduction of the lower Iberian crust beneath Euroasian crust, whereas to the west of $1^0$40' west longitude Grimaud et al. (1982) showed that the Euroasian crust of the Bay of Biscay was subducted beneath the Iberian margin.

Tectonic inversion of the Mesozoic basins during Alpine compression resulted in a foreland basin that contains several large thrust sheets (Seguret, 1972). Gavarine and Guarga thrust sheets contain imbricate fans and extensive decollement folds along their southern margins (Anastasio, 1992) and are included in the west central foreland (Camara and Klimowitz, 1985). The decollement zone of the Guarga thrust sheet is variable in thickness and it consists mainly of evaporite rich Kueper facies (Diegel, 1988). The Bóixols anticline comprises lower Cretaceous syn-rift and upper Cretaceous post-rift deposits and forms a south-directed asymmetric fault-propagation fold (Grelaud et al., 2003).

Two-tiered thrust networks have been developed in the Spanish Pyrenees: the lower and upper network. The lower network consists of a basement duplex with a roof of thrust in Triassic evaporites that served as the decollement for the upper network. The upper network, on the other hand, consists of several tier thrust sheets that carried the preorogenic roof sequence and synorogenic piggyback basins southward (Camara and Klimowitz, 1985; Deramond et al., 1985). Following thrust-sheet development, a series of basins formed in the south-central Pyrenees, including the initial thrust-sheet-top basins of Eocene age (the Tremp-Graus, Ainsa, and Inner Jaca sub- basins) and a later late Eocene-Oligocene thrust sheet-top basin (the Outer Jaca Basin) (Mutti et al., 1988). The Ainsa Basin is a segment of a Lower Eocene foredeep which lies to the west and south of the Montsec thrust sheet (Fernandez et al., 2004; Falivene et al., 2006).

2.2 Sediment infill of the South Pyrenean foreland basin

The aysmmetric fault-bounded small basins formed during Post-Hercynian (Permian) extension were filled by alluvial fan deposits, red mudstones and abundant volcaniclastics. The tectonic extension that occurred during Triassic led to the development of a widespread braided system. During the Jurassic, extensive carbonate sequences were deposited over most of the Pyrenees and surrounding areas (Puigdefabregas and Souquet, 1986; Pomar et al., 2005). Discontinuous sedimentation caused by sea-level fall and the change to transtensional tectonics, and local erosion characterise the Late Jurassic – Early Cretaceous period. At the turn from the Aptian to the Early Albian, the N-S extension and its associated transtension resulted in a rift system which was later filled by “marnes noires” formation in the deeper part, Urgenian carbonates along their margins, and onlapping a discontinuous bauxite fringe belt (Puigdefabregas and Souquet, 1986).

The deeper wrench troughs formed during Middle Albanian- Early Cenomanian were filled by the Pyrenean flysch. During this time, the basement was exposed and eroded, and gave terrigeneous sediments to shallow marine environments. From Middle Cenomanian to Middle Santonian, as a result of global sea-level rise (Cenomanian transgression), carbonate turbidites filled the deeper part of the basin. Paleocene events in the eastern Pyrenees area were dominated by non-marine sedimentation, represented by alluvial fan conglomerates and red mudstones; but the red beds facies were also extended to the northeast and to all parts of the southern foreland. The facies distribution during this period suggests the formation of the first foreland basin geometry in the eastern Pyrenees (Puigdefabregas and Souquet, 1986). From Eocene to Oligocene (Figure 2.2), piggyback deposition occurred in several of the thrust sheets formed. The accumulation of the deep marine Ainsa Basin sediments was contemporaneous with the tectonic subsidence of the foreland basin (Verges et al., 1998). Farther to the south, the largely Miocene Ebro foreland basin deposits represent the last stage of the basin filling (Weltje et al., 1996). Finally, erosional excavation exhumed the Pyrenees during mid to late Miocene to their present relief (Coney et al., 1996).

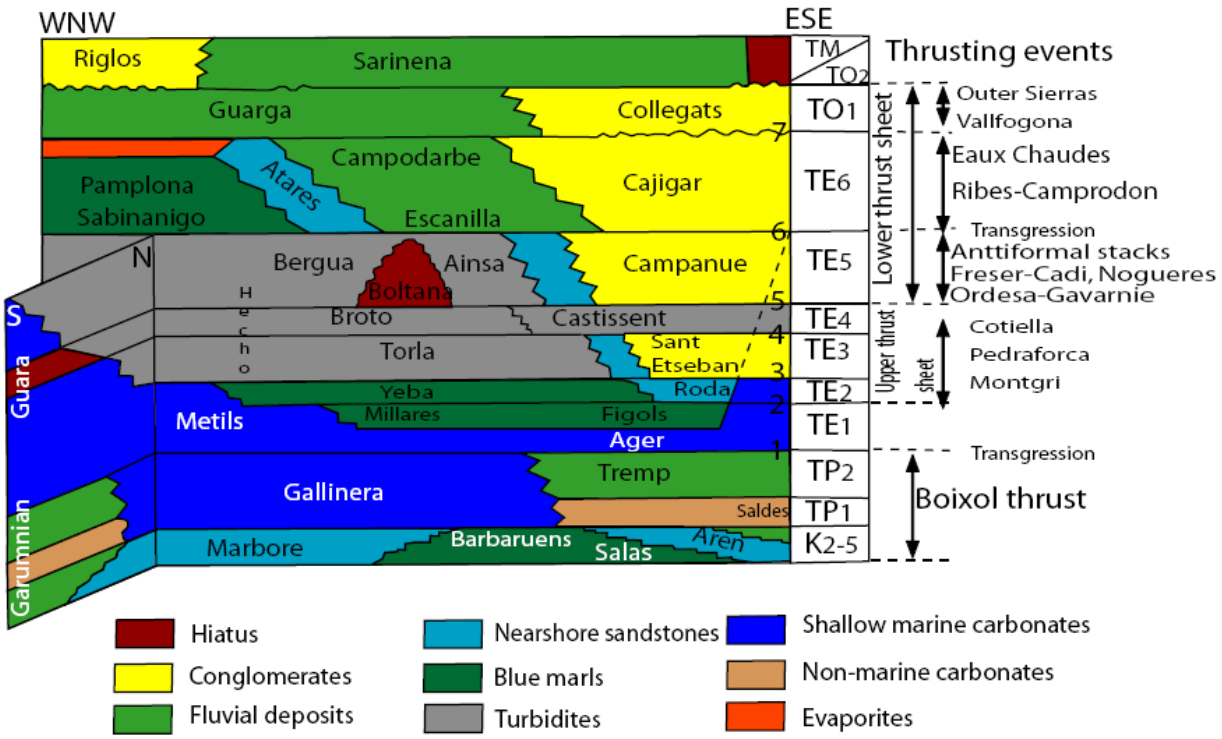

1- Cadi-Ager sequences; 2- Corones - Roda sequence; 3- Armancies - Esteban sequence; 4- Campdevanol - Castissent sequence; 5- Bellmunt - Campanue sequence; 6- Milany - Campodarbe sequence; 7- Solsona sequence

Figure 2.2: Longitudinal E-W correlation chart of Tertiary lithostratigraphic units, depositional sequences and thrusting events in the southern Pyrenees. TE1 to TE4 are of Early Eocene age. TE5 and TE6 roughly correspond to the Middle and Late Eocene (Modified from Puigdefabregas and Souquet, 1986).

3. THE AINSA BASIN

The 25 km wide and 40 km long (Dreyer et al., 1999; Arbues et al., 1999) Eocene Ainsa Basin is located on top and the easternmost part of the Gavarnie thrust-sheet complex (Munoz, 1992). According to Dreyer et al. (1999) the Cuisian – Lutetian transition due to flexural subsidence of the area laterally adjacent to the active south Pyrenean central thrust sheet resulted in the development of the Ainsa Basin. The incorporation of the basin into the hanging wall of the Gavarine-Sierras Exteriores thrust occurred during middle Eocene, as the thrust front propagated toward the foreland and evolved into a piggyback setting (Fernandez et al., 2004).

Four main north-south trending anticlines, Mediano, Anisclo, Boltaña, and Olson, have affected the Ainsa Basin (Fernandez et al., 2005). To the south, the basin is associated with the generally east-west trending Sierras-Marginales thrust (Munoz, 1992); whereas the Mediano anticline and its associated structures belonging to the South Central Pyrenees Unit (Munoz et al., 1994) bounded the northern and eastern part of the basin. The western margin is defined by a syn-sedimentary structural feature, the Boltaña anticline (Figure 3.1) (Dreyer et al., 1999).

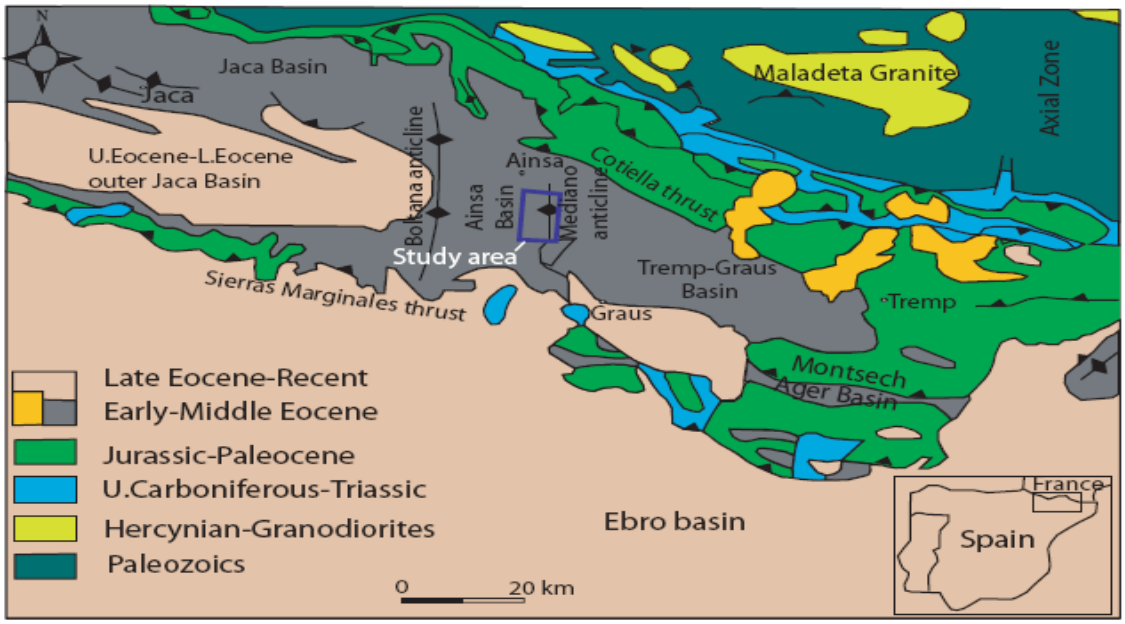

Figure 3.1: Location of the Ainsa Basin and the main structural elements within the context of the South Pyrenean Foreland Basin of northern Spain (Modified from Dreyer et al., 1999).

3.1 Structure

The eastern part of the Ainsa Basin is characterized by the embryonic Mediano anticline (Fernandez et al., 2004), an east-verging detachment fold (Poblet et al., 1997) which plunges and dies northward in Ainsa Basin. The basin is bounded to the west by the west-verging fault-propagation fold, i.e., the Boltaña anticline. Both of these anticlines are north-south trending, and are detached over the Triassic evaporites (Fernandez et al., 2004). The deep marine fills of the Ainsa Basin are deformed at different scales, where the scale of deformation decreases upward until the Guaso depositional system. In the Buil syncline, which is a north-south trending open syncline (Fernandez et al., 2004), the overlying Sobrarbe deltaics are deformed slightly (Pickering and Corregidor, 2005).

Based on paleomagnetic study and identification of unconformities, Holl and Anastasio (1993) suggested the initiation of the Mediano anticline at ~ 52 Ma, with main development by ~ 42 Ma. The N-S trending folds are superposed (overlain) by the late Eocene underthrusting of the basement units (Munoz, 1992). This thrusting was responsible for the folding of the Gavarnie – Sierras Exteriores thrust sheet into Jaca syncline (Fernandez et al., 2004).

Halotectonic related transverse folds, the Boltaña and Anisclo anticlines, localized the Gavarnie thrust sheet (Holl and Anastasio, 1995). The Anisclo anticline is a west-verging fault propagation fold. Besides these large scale anticlines, there exist small scale gentle folds (e.g. Arcusa anticline) in the Ainsa Basin, which have been interpreted by Dreyer et al. (1999) as growth structures (Figure 3.2).

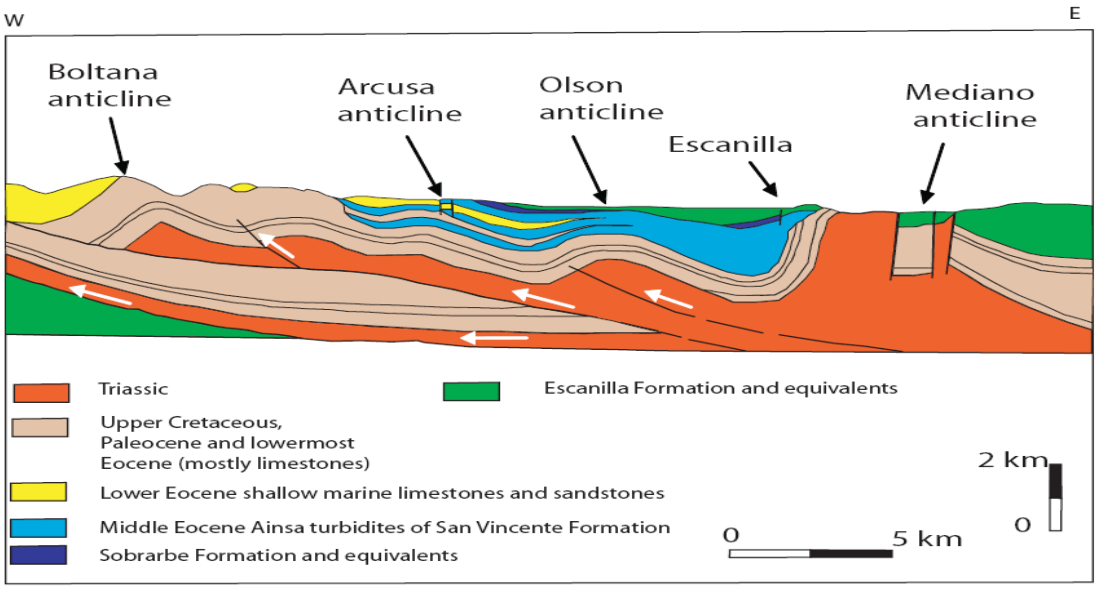

Figure 3.2: Structural cross-sections across the southern part of Ainsa Basin. Note also growth structures, Arcusa and Olson anticlines (modified from Dreyer et al., 1999).

3.2 Stratigraphy

Overlying the Triassic shales and evaporites that acted as detachment for the thrusts and folds, there are as much as 1500 m of shelfal carbonates and siliciclastics that accumulated between Mesozoic and Paleocene prior to thrusting of the Ainsa Basin (Garrido-Megias, 1973). This was followed by Ypresian Alveolina limestone, representing a wide transgression event just before the onset of thrusting in the Ainsa Basin (Fernandez et al., 2004).

The deep marine Ainsa Basin sediments were accumulated contemporaneously with the maximum rates of tectonic subsidence and thrust front advance in the foreland basin during late Lutetian (~41Ma) (Verges et al., 1998). These sediments are ~ 4 km thick and occur as four unconformity- bounded depositional cycles or depositional systems (Figure 3.3) (Arbues et al., 1998) that took ~ 10-12 million years duration during early to middle Eocene (Fernandez et al., 2004; Pickering and Corregidor, 2005). According to Bentham et al. (1992) the deep marine fill thins and pinches out towards west against the Boltaña anticline. To the east, the Ainsa Basin is separated from Tremp-Graus Basin by Mediano anticline, a detachment fold developed in the transitional foredeep phase of the Ainsa Basin (Dreyer et al., 1999). The deep marine deposits of the Ainsa Basin were accumulated during the

development of the Mediano anticline in upper to mid bathyal (~ 400 to 600 m) water depths (Pickering and Corregidor, 2005).

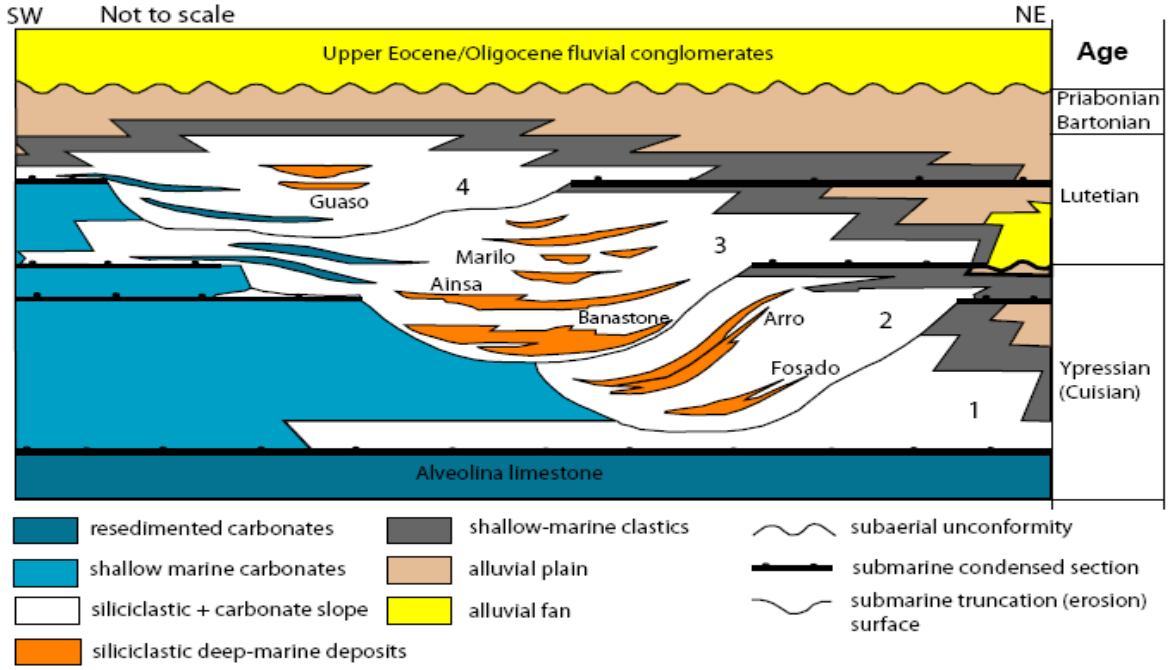

Figure 3.3: General Stratigraphy of the Ainsa Basin (not to scale). The four unconformity bounded units / cycles are indicated by numbers 1 – 4. (Modified from Arbues et al., 1999, in Fernandez et al., 2004).

Controlled by thrust activity, the northeastern margin of the Ainsa Basin was a site of lower to middle Lutetian slope deposition (Munoz et al., 1994). This thrusting propagated towards the west in the middle Lutetian and Bartonian (Dreyer et al., 1999), and the sole thrust broke in several places in the Ainsa Basin. This changed the Ainsa Basin from transtensional foredeep to a thrust-top basin (Remacha et al., 1998). During the transtensional foredeep stage, the Ainsa Basin received sediments from the west (Munoz et al., 1994) mainly from the large axial sediment dispersal system (Puigdefabregas and Souquet, 1986). On the other hand, during thrust-top stage the Sobrarbe deltaic complex was formed. This deltaic complex is bounded below and above by San Vincente Formation and Olson member, respectively (Dreyer et al., 1999). According to Puigdefabregas et al. (1992) Mediano and Boltaña anticlines represent the surface expressions of the thrust-top stage.

The Sobrarbe deltaic complex occurs at the transitional zone between alluvial plain of the Tremp-Graus Basin and the basin plains of the Jaca Basin (Dreyer et al., 1999) and it is part of the axial sediment dispersal system in the southern Pyrenean Foreland basin (Puigdefabregas and Souquet, 1986).

As its deposition records two major events, the Castisent Group (50.5-49.5Ma; Millington and Clark, 1995) represents one of the most significant stratigraphic units in the fill of the Ainsa Basin. These two events are: the onset of Cotiella Nappe, which controls the early configuration of the Castisent basin; and the growth of the Mediano anticline in the southern margin (Mutti et al., 1988). In addition to substantial submarine erosional surface that can be correlated across the central sector and parts of the eastern sector of the basin, the Castisent Group consists of two major unconformities. These unconformities bounded the Group (Millington and Clark, 1995). The submarine erosional surface within the Castisent Group divides the Group into two: CS1 (the lower part of the Castisent Group) and CS2 (the upper part of the Castisent Group) (Mutti et al., 1988). The shallow marine deposits, which are the main focus of this Thesis, are interpreted to represent part of the upper part of the Castisent Group (CS2).

Tropical to seasonal sub-tropical climate with moderately high rainfall patterns are suggested by Pickering and Corregidor (2005) in the Ainsa Basin using palynological and microfaunal data during the Eocene. Similar climatic condition was also suggested by Haseldonckx (1972).

3.3 Tremp-Graus Basin

Separated by the Mediano anticline, the Tremp-Graus Basin is located to the east of the Ainsa Basin. Tremp and Tremp (Ager) basins are separated by the thrust wedge of the Montsec Range (Nijman, 1998) but during Eocene time, the Montsec thrust was not expressed on the surface and, therefore, the two basins are considered as one sedimentary basin (Nijman, 1998).

Three successive lithostratigraphic units, the Vallcarga Formation, the Aren Sandstone Formation, and the lower part of the Trump Formation, representing overall prograding megasequences, were deposited in Tremp Basin during middle Campanian-Maastrichtian period (Simo and Puigdefabregas, 1985).

The Montanana Group consists of lower to middle Eocene fluviodeltaic sedimens that were deposited on top of a moving Southern Pyrenean Central Unit (SPCU) (Weltje et al., 1996). According to Ori and Friend (1984) the Montanana Group represents the fill of a piggyback basin, which is called the Tremp-Graus basin (Nijman and Nio, 1975) and it was drained by

a west-northwestward flowing axial fluvial system (Nijman and Nio, 1975). The three sediment dispersal mechanisms that have been suggested by Nijman and Nio (1975) are marine processes that acted on the delta platform, fluvial systems in southern-central part of the basin, and a complex of alluvial fans and fan deltas to the north-eastern part of the basin. The Montanana Group was deposited in contemporaneous with the turbidite systems of the Hecho Group in the South Pyrenean Foreland Basin (Mutti et al., 1988).

The Montanana Group is divided into three: Lower, Middle, and Upper Montanana Groups (Figure 3.4). These Groups have been subdivided into eight major, flooding surface and unconformity bounded, megasequences (Nijman and Van Oosterhout, 1994), having a thickness range of between 148 m and 404 m (Nijman, 1998). Nijman and Van Oosterhout (1994) suggested the shifting of the basin axis towards north during the development of the megasequences and they also suggested that the shifting was controlled by tectonics. During deposition of the Montanana Group, Haseldonckx (1972) suggested a change of climatic conditions from tropical humid conditions (during deposition of the Lower Montanana Group) to seasonal subtropical climate (during deposition of the Upper Montanana Group).

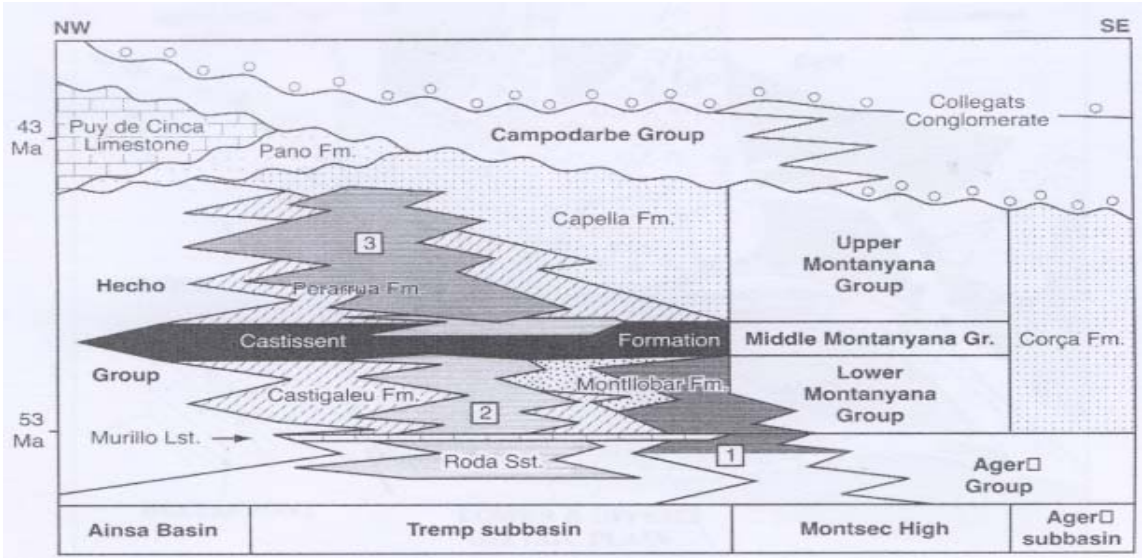

Figure 3.4: Scheme of stratigraphic nomenclature of the Tremp-Ager Basin. Stratigraphic names in italics refer to units outside Montanyana Group. Within it, greys refer to alluvial fans, coarse stippling to fluvial and upper deltaic plain; oblique hatching to lower deltaic plain and delta front (taken from Nijman, 1998).

4. LOCATION AND METHODOLOGY

4.1 Location

The study area is located in the eastern part of the Ainsa Basin, Spanish Pyrenees. It is bounded between UTM coordinates of 31274000 and 31276000 east and 4697000 and 4699000 north with minimum and maximum elevations of 500 and 920 meters above sea-level, respectively. The studied section is located few kilometers (1-2 kms) away from El Pocino in the north to northeast direction, and ~ 12.5 km from the Ainsa town with an approximate ESE direction (Figure 4.1a and b).

4.2 Field and laboratory methods

The field work was carried out between July 09, 2007 and August 05, 2007. The data and interpretations presented in this Thesis are based on the record of about an altogether 200 m thick vertical succession. The methods employed to achieve the objectives of the Thesis are described below.

4.2.1 Field work

During the actual field work, to meet the objectives of the Thesis, nine sedimentological logs were made. Even though vegetation cover created a problem in describing certain sections, a well exposed hillside and roadside exposures allowed detailed study of the area. A total of nine large scale (1: 50) sedimentological logs were measured to document bed thicknesses, grain size variation, sedimentary structures, ichnofossils, bioturbation and paleocurrents. From the nine sedimentary logs that have been made, five of them are thick (> 12 m) and can cover a significant part of the succession. Lateral spacing between these logged sections range from 400-600 m. The remaining four logs, which had a lateral spacing of 50-100 m, were measured to capture lateral facies changes. From all the logged sections, the 54 m thick road section outcrop logging was performed on a high-quality road cut exposure. At each of the logged sections, the direction of sediment transport was inferred from flute casts and dip azimuths of the foresets of cross-bedded units. To reconstruct the paleogeography,

palaeocurrent indicators (rarely present) and facies changes were recorded along the depositional strike of the study area.

Bioturbation classes (BC) were assigned by comparing intact sedimentary structure with that of bioturbated by using the method described by Nagy (2007), where BC I= intact lamination and bedding; BC II= reduced lamination and intact bedding; BC III= reduced lamination and bedding; BC IV= reduced lamination and absence of bedding; and BC V= absence of both lamination and bedding. In addition, ten rock samples of appropriate size from stratigraphic positions of interest have also been collected for a detailed study. To understand the vertical and lateral faunal variation and to give an approximate quantitative estimation, faunal counting (particularly for nummulites) was undertaken in randomly chosen beds.

4.2.2 Materials used

Equipments used during the field work were simple hand tools. The start and end of each log section was located in its respective position by the help of a Magilan GPS receiver. Relative variation in elevation was also measured with a help of this GPS. SILVA compass, on the other hand, was used to measure the attitude of the beds and orientation of sedimentary structures, e.g. cross lamination and flute casts. Hammer, hand lens, meter tape, shovels, and brushes were among the instruments and tools which were used during the field work. Topography map at a scale of 1:25,000 was employed as a base map. Log stations have been plotted and these locations are shown in Figure 4.1 (c)**.**

4.2.3 Laboratory work

The thin sections from the sampled rocks were investigated under high resolution microscope at the University of Oslo to investigate different parameters of interest, including mineralogy, grain size and shape, porosity and permeability, biostratigraphy, etc. The percentages of mineralogical and biological/fossil assemblages have been determined by counting an average of 500 counts per thin section under transmitted and reflected fluorescence-light microscopy.

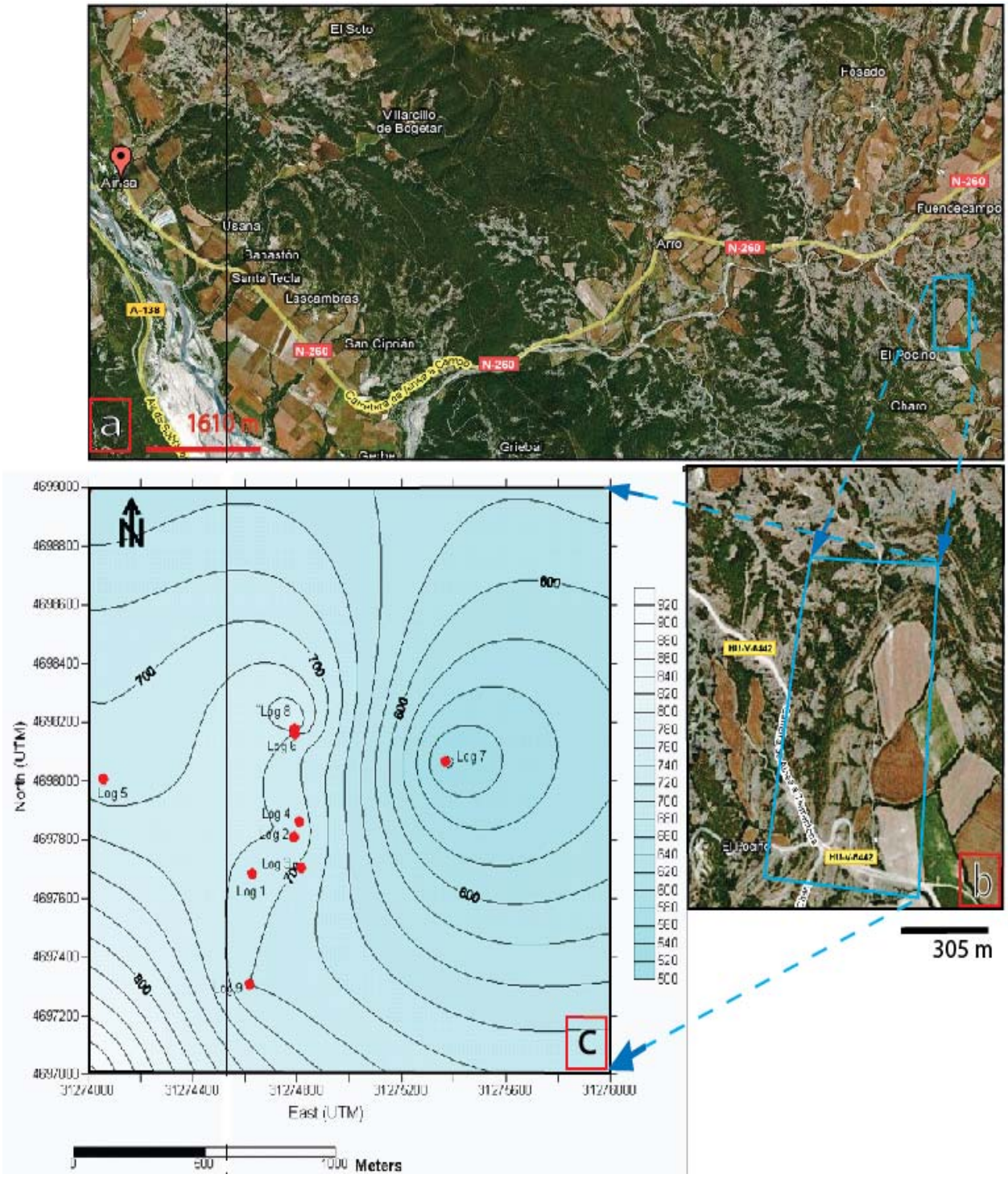

Figure 4.1: Location map of the study area. Figure (a) and (b) show the roads connecting Ainsa town and Feundecampo, and Feundecampo and El Pocino, respectively. The two pictures also show the topography and location of the study area. Figure (c) shows the contour map prepared using the software called Surfer and the nine log locations in the study area (for log correlation refer Appendix B). Figures (a) and (b) are taken from Google Earth ™.

4.3 Thesis writting

With certain modifications, the methods of Walker (1992) have been followed to organize the Thesis work from facies definition to controlling factors approaches (Figure 4.2). To make easier the environmental interpretations, the facies associations of the study area have been defined using the definition of Collinson (1969, p. 207) on the concept of *facies association* as "groups of facies genetically related to one another and which have some environmental significance". The definition of Mitchum et al. (1977) (in Van Wagoner et al., 1988, p. 39) to define sequence stratigraphy has been used; where sequence stratigraphy is defined as "a stratigraphic unit composed of a relatively conformable succession of genetically related strata bounded at its top and base by unconformities or their relative comformities".

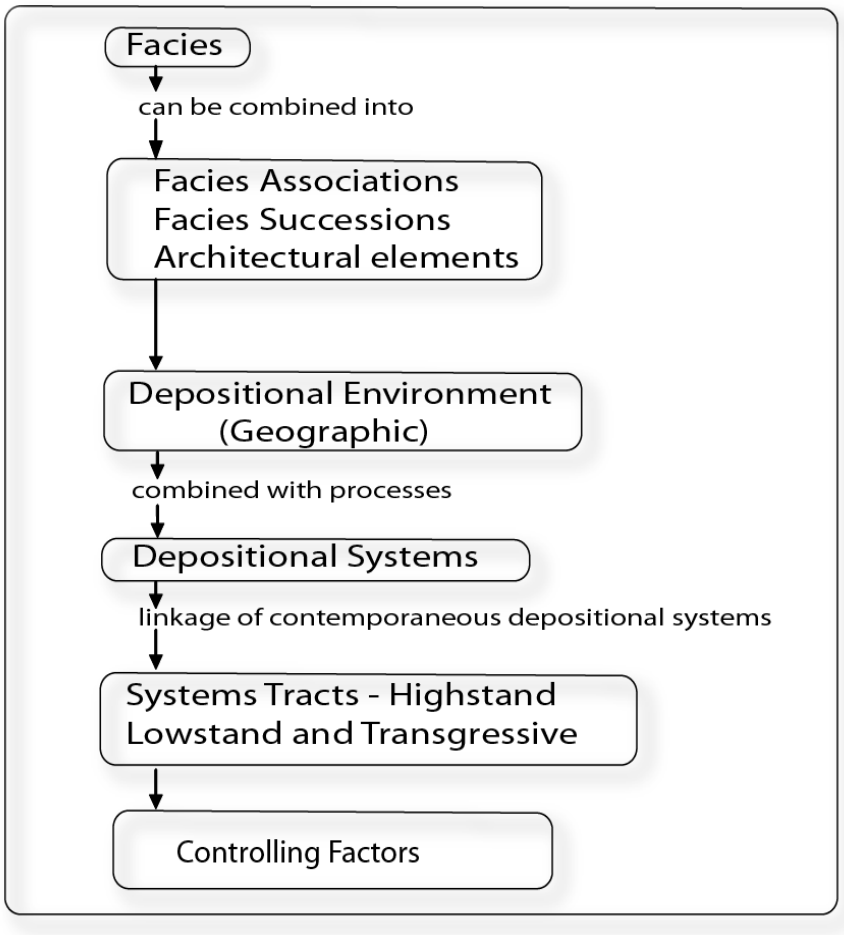

Figure 4.2: Relations between facies, depositional environments and systems, sequence stratigraphic approaches and controlling factors (modified from Walker, 1992).

4.4 Limitations

Below are pointed some possible errors that could possibly occur both during the actual field work and during petrographic analysis of the thin sections.

Most rocks of the study area are inclined towards ESE with an average dip angle of 20 - 30^0. During logging of the whole succession there was a difficulty of acquiring data in one stratigraphic column; hence a zigzag logging pattern has been applied. In addition, some parts of the outcrop were covered with vegetation which made the logging difficult. In such cases the logging was shifted to a nearby outcrop which had a better exposure. In such covered outcrops, tracing bounding surfaces and observing 3D architecture of the deposits were also a problem. The zigzaging approach and shifting to a better exposure are, therefore, expected to have created some possible errors on the data acquired. In addition, the section that crops out in the northern part of the study area has been overturned and the deposits show steep dip angles which vary from 50-75^0. Therefore, the palaeocurrents measured on this section are expected to have certain uncertainities.

As the rock types are very fine-grained, mineral identification from thin-sections was very challenging; therefore, possible errors are also expected during the point counting processes. Further petrographic studies, for instance by SEM, XRF, XRD and microsonde analysis, were beyond the scope defined for this Master Thesis.

5. FACIES

A rock facies (Gressly, 1883) is a body of rock with specified characterisitics. It may represent a single bed, or a group of multiple beds. Ideally, it should be a distinctive rock that formed under certain conditions of sedimentation, reflecting a particular process, set of conditions, or environment (Middleton, 1973). Facies definition is quite objective and the key to interpretation of facies is to combine observations made on their spatial relations and internal characteristics with comparative information from other well-studied stratigraphic units, and particularly from studies of modern sedimentary environments (Middleton, 1978). Based on sedimentary structures and texture, the sedimentary succesions of the study area have been divided into nine lithofacies. Below are presented the description and interpretation of the various lithofacies identified in the study area (Table 5.1).

Table 5.1: Summary of sedimentary facies of the study area

Facies	Description	Grain Size	Interpretation
A	Low angle cross-stratified siliciclastic sandstone with current rippled top. Assymmetric	Fine grained	High energy environment, probably current generated bedform or deposition from migration of 2D dunes in a shallow shelf setting
B	Cross-stratified and cross-laminated carbonate rich sandstone	Very fine to fine sand	Deposition in foreshore-shoreface environment
C	Plane parallel laminated carbonate rich sandstone	Very fine to fine sand	Deposition in relatively high to moderate energy shoreface environment
D	Hummocky cross-stratified carbonate rich	Coarse silt to fine	Storm dominated deposit

	sandstone	sand	in offshore-transition zone
E	Structureless (massive) carbonate rich sandstone with a very weak HCS and horizontal lamination	Very fine to fine sand	Rapid deposition from suspension or/and intense bioturbation by organisms
F	Micritic limestone with a strong variation in fossil content	Very fine grained (micritic) to medium crystalline (in the welded marine part)	Deposition in increased carbonate production environment where terresterial sediment input is restricted
G	Structureless (massive) Siltstone	Silt sized	Rapid deposition from suspension in a very low energy, quiet, relatively deep water environment or/and intense bioturbation by organisms
H	Structureless (massive) mudstone	Silt + clay	Rapid deposition from suspension or/and intense bioturbation by organisms
I	Fissile mudstone (‘’paper shale’’)	Silt + clay	Weathering of very finely parallel laminated mudstone which is rich in clay or micaceous particles

The average percentages of the different facies identified in the study area are shown below (Table 5.2). Large parts of the study area are covered by facies D, E, F & H, where as the rest part is covered by the remaining facies.

Table 5.2: Percentage of the different facies observed in the study area

	Facies A	Facies B	Facies C	Facies D	Facies E	Facies F	Facies G	Facies H	Facies I
%	0.44	1.1	1.0	3.9	17.8	17.4	2.0	56.0	0.58

5.1 Facies A: Low-angle cross-stratified siliciclastic sandstone

Description

Fine grained siliciclastic sandstone is (Figure 5.1) found in the central part of the study area. This deposit is laterally discontinuous and present as ~ 22 cm thick unit in the upper part of upward thickening succession. The lensoid depositional unit of this facies has a rounded straight-crest with a general SE crestal axis orientation. The spacing between the crests varies from 1.55 to 2 meters, with a shorter lee side (50 cm – 60 cm) and longer stoss side (95 cm to 140 cm). The cross strata of this bed are oriented NE direction. The foresets of the examined cross-bed are parallel and show current ripples on top. The siliciclastic layer is always found on top of micritic limestone and has a sharp top and bottom contact.

Interpretation

The siliciclastic sandstone is interpreted to be found at the boundary between retrogradational muddy units and carbonate rich sandstone intervals. Based on their spacing (wavelength), and relief dimensions (bed thickness), these deposits are interpreted as dunes. The low-angle stratification and asymmetric nature of the dune and the presence of current ripples on top indicate that the deposits were formed in a high energy environment followed by low energy conditions, as a bedform generated during storm events when siliciclastic

material was brought into the otherwise carbonate dominated shallow shelf environment, succeded by ripple-drift during slack-water or fair-weather conditions.

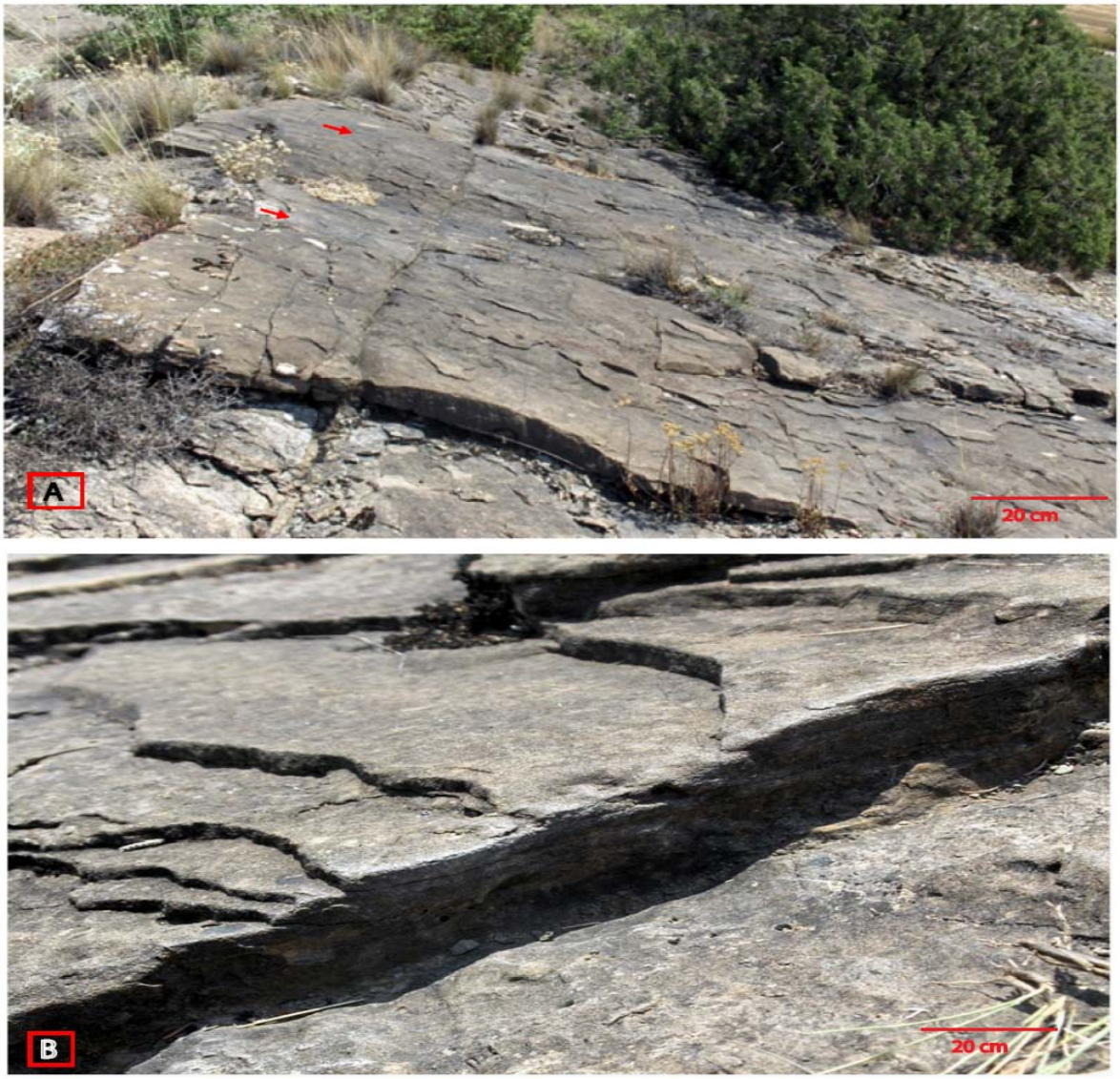

Figure 5.1: Examples of facies A. a) sand dune observed on the top of micritic limestone with a general SE crestal axis orientation (shown by red arrows), in log section 2, height 7.5 m, b) low angle cross stratification observed on the same bed.

5.2 Facies B: Cross-stratified and cross-laminated carbonate rich sandstone

Descreption

Facies B comprises ~ 1.1 % of the studied section and is mostly recorded in the overturned beds in northern part of the study area (section 7). In this section, the cross-stratified carbonate rich sandstone beds recorded have a thickness which varies from 24 cm to 38 cm, with a mean thickness of 30 cm. This facies is overlain and underlain by structureless mudstone (facies H) and structureless carbonate rich sandstone (facies E). It is characterized by dark gray color, normal grading, tabular geometry, sharp top and bottom contacts, regularly spaced foresets**,** and cross-lamination occurring in very fine to fine grained sandstone. While most of the regularly spaced foresets show paleocurrent directions towards NNW, few others show reverse paleocurrent direction dipping towards SW. It also consists of dominant symmetrical ripples, but asymmetrical ripples were also recorded (Figure 5.2a). Locally, the 28 cm thick bed at a log height of 30.5 meters shows a sharp transition from low angle cross-lamination to horizontal (plane parallel lamination (PPL)) lamination (Figure 5.2b). This facies records some burrowing organisms but a very rare amount of fossils content (mainly nummulites) ranging from zero to 5% have been recognized.

Interpretation

Facies B is interpreted to be deposited in a foreshore environment. The positive relief morphology and the internal structure of the sandstones indicate that they developed as linear bars and were formed by vertical aggradation and lateral accretion of 3D and / or 2D ripples and dunes, as those dune structures described by Chaudhuri & Howard (1985). The cross-lamina is interpreted to be developed in sand as a result of ripple migration. The dominance of symmetrical ripples on top of the sandstone bodies identify them as marine bars deposited within wave dominated foreshore-shoreface zones, as also described form other areas by Mukhopadhyay & Chaudhuri (2003). According to Miall (1996) abrupt changes in grain size and bedforms may be caused by rapid changes in flow velocities. Therefore, the sharp transition observed in one bed from low angle cross-lamination to horizontal (PPL) lamination suggests a sharp decrease in flow velocity. The normal grading

may be due to deposition from suspension, when the large particles tend to fall to the bottom first (Collinson & Thompson 1982).

5.3 Facies C: Plane parallel laminated carbonate rich sandstone

Description

The very fine to fine grained plane-parallel laminated carbonate rich sandstone is found in sections 3, 6, and 7. In the studied section, about fourteen plane parallel laminated beds, more than half of them in section 7, have been recorded. Some of the parallel laminae often show gentle undulation (Figure 5.3). This facies tends to occur in a thickness range of 12 cm to 42 cm, the average thickness being 18 cm. The sandstone of this facies is dark gray colored. Texturally it varies from very fine to fine grained. Unlike the dominant normal grading, ungraded (blocky) textures are only recorded in very few beds. This facies is commonly bounded above and below by structureless carbonate rich sandstones (facies E) and rarely by structureless mudstones (facies H). The dominant sedimentary structure is parallel lamination obseved in tabular to wedge shaped beds. Nummulites (benthic forminifera) are the only fossil type recorded in this facies. Its content varies from zero to 30 %, mostly < 10 %.

Interpretation

Facies C is interpreted to be deposited in a relatively high energy environment, most probably in the foreshore environment. The abundant planar lamination is interpreted as representing wave wash in a relatively flat beach foreshore zone**.** These may also represent deposition by storm-generated currents on the shoreface, as proposed by Brenchley et al. (1993) for similar facies and structures.

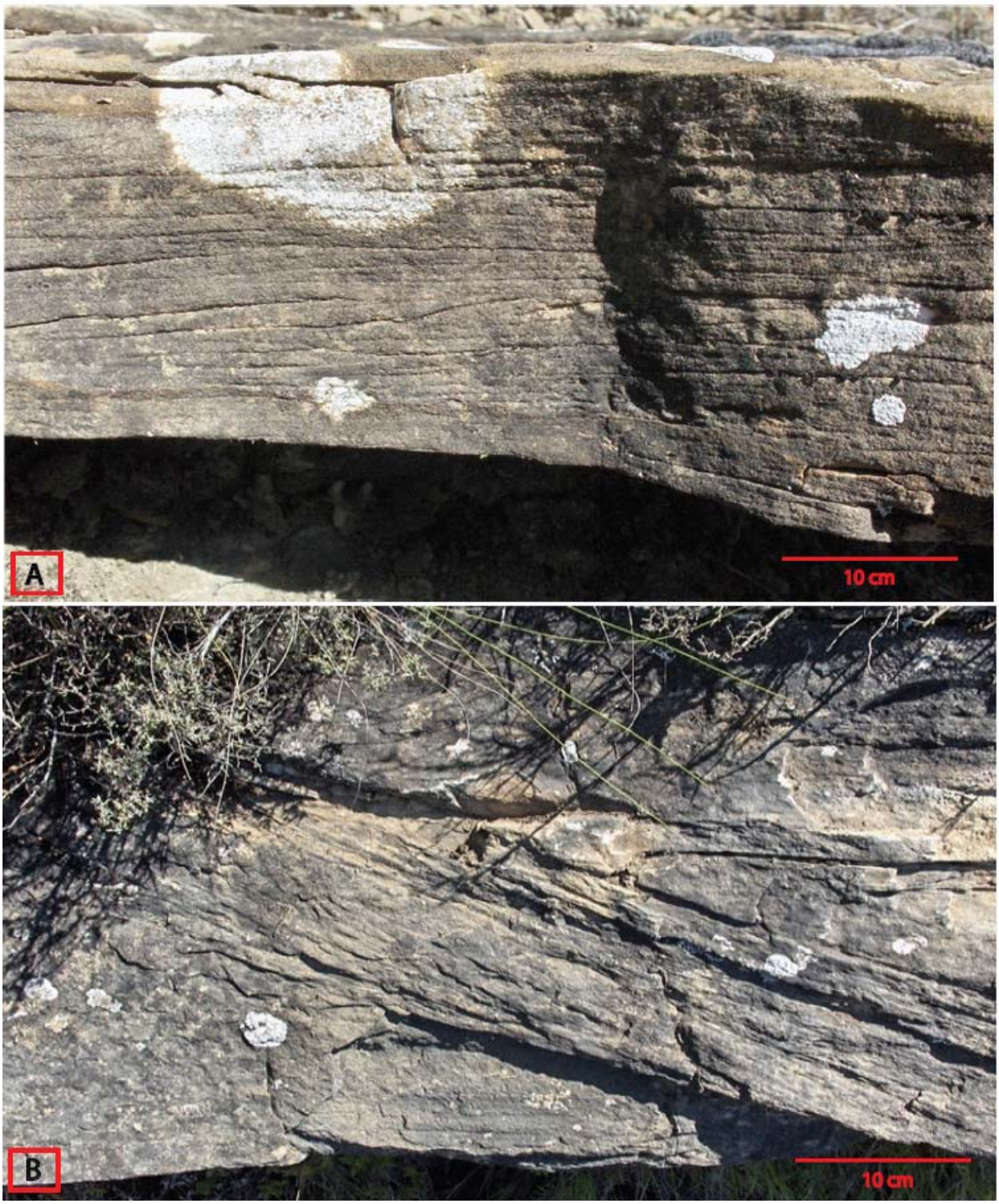

Figure 5. 2: Outcrop photographs of facies B. (a) ripple cross-lamination on 10 cm thick carbonate rich sandstone (4 m, section 5). (b) Sharp transition from cross-lamination to horizontal lamination (PPL) observed on 28 cm thick carbonate rich veryfine sandstone (30.5m, section 7)

Figure 5.3: Example of plane parallel laminated (slightly undulating) on 20 cm thick carbonate rich sandstone (24.75m, section 7).

5.4 Facies D: Hummocky cross-stratified (HCS) carbonate rich sandstone

Description

Coarse silt- to very fine-sand- grained, dark gray colored, carbonate rich sandstones of facies D occurs in almost all logged sections (outcrops) except in northern part of the study area (i.e. sections 7 and 8). This facies, together with facies E, is the most common variety among sandstone deposits. Beds are 5 cm to 90 cm thick and dominantly normally graded, but blocky (ungraded) textures have also been recorded. In few beds, e.g. log section 1 height 17 m, bedforms like parallel lamination and massive carbonate rich sandstone pass vertically into HCS. The hummocks' are usually not very well stratified and can not be easily recognized. In places they are also present in a very small scale, as micro hummocks (MHCS).

This facies is commonly interbedded with facies I (in the middle part of section 1**,** refer Appendix B) and facies H (e.g. section 1 and section 6) (Figure 5.4). The lower and upper boundaries are commonly sharp (planar to uneven), but in places beds of the facies grade

upward into beds of facies H and facies I. Fossils are rare, and it comprises nummulites (0-5 %) and plant fragments**.** Near the tops of some beds, vertical bioturbations have been observed.

Interpretation

HCS is considered to form under conditions of strong storm-wave oscillatory flow with a superimposed unidirectional geostrophic current (Colquhoun, 1995). In agreement with the grain size recorded in this facies, Duke (1990) noted that classic HCS storm beds and their variants are largely restricted to the fine to very fine sand fractions. The carbonate rich sandstone beds containing parallel lamination and HCS is considered to represent frequent episodes of high energy storm deposition above storm wave base (Dott & Bourgeois, 1982b). According to Brenchley (1985) this is typical in the lower shoreface or offshore-transition zone, close to fairweather wave base (usually 5-15 m deep, Walker, 1984). HCS also occurs in deltaic systems dominated by rivers in flood and therefore by hyperpycnal flows (Mutti et al., 2007). The rare bioturbation recorded in some beds and thin mudstones interbedded with HCS carbonate rich sandstone indicates water depths at which storms of average intensity would erode the bottom deeply enough to destroy evidence of every day infaunal activity (Bourgeois, 1980). The degree of bioturbation also reflects the time between storm events (Sepkoski et al., 1991).

Figure 5.4: Thin sandstone beds with HCS (facies D) interbedded with structureless mudstone (facies H) (4-4.25m, section 6)

5.5 Facies E: Structureless (massive) carbonate rich sandstone

Description

This is the most dominant carbonate rich sandstone facies recorded in most of the logged sections. It accounts ~ 17.8 % of the studied total stratigraphic succession. The facies is abundant in the middle part of sections 1, 4, 5, 6 and 7. The facies occurs in beds with a thickness range of 9 cm to 250 cm. In fresh outcrops, beds of this facies have dark gray color, but in weathered sections the carbonate rich sandstone appears light gray. Individual beds show both sharp (some of them uneven) and gradational contacts with overlying and underlying beds (mostly with facies D and H).

The carbonate rich sandstone is coarse silt to very fine grained, and occur in tabular to wedge shaped beds, laterally continuous at outcrop scale, structureless (massive), and displays normal grading, reverse grading and blocky (ungraded) textures. In some of the logged sections, the uppermost part of beds are very weakly hummocky cross-stratified and horizontally laminated. Mudclasts are rarely recorded. Erosional structures are also seldom; flute casts have been found at the base of some beds. In section 1, for example, the measured flute casts give variable paleocurrent directions of NW and NE whereas in

sections 6 and 7 they are directed to NW. Very rare horizontal burrows, with an average length of 12 cm are recorded at the bottom of some beds. In the middle and upper parts of other beds, 2 to 13 cm long vertical to near vertical burrows have been recorded. The bioturbation tubes are filled with the same (host) material as of the bed itself. Nummulite content varies from zero to 65%.

Interpretation

Structureless carbonate rich sandstone (facies E) may have resulted from rapid deposition from suspension currents that prevented the development of tractional bed structures, or original sedimentary structures may have been destroyed by intense bioturbation. The rare occurence of weak HCS in the top part of some of the beds indicates that oscillatory-dominant waves induced by storm currents were occassionally prevalent over unidirectional flows, as generally suggested by Duke et al. (1991). The observed inverse grading may be due to increasing flow velocity during deposition, but if the increase in velocity was too high, it would have resulted in erosion (cf. Bjørlykke, 1989). This can also have been caused by increased supply of a relatively coarse material during transport and deposition. Flute casts are interpreted to be formed by static vortices in the water above the sediment surface. As well as being a valuable indicator of 'way-up' in deformed sequences, flutes are amongst the most abundant and important indicators of paleocurrent direction (Collinson & Thompson, 1982).

5.6 Facies F: Micritic limestone

Description

This facies comprises ~ 17.4 % of the studied outcrop. The thicker micritic limestone beds are observed in section 2 and tend to occur with a thickness variation of 8 cm to 285 cm. Beds of this facies have also been observed in the upper most part of the rest of the logged sections in variable thicknesses, but generally thinner than the one observed in section 2. Sharp lower and gradual top contacts (boundaries) and tabular geometry are the most abundant boundary features, but other combinations of contacts and thinning in one direction have also been observed.

Though these deposits are very fine grained (micritic), medium crystalline (sparry) textures have been recorded in the upper most part. Like other facies, normal grading is the main texture, but reverse grading and blocky textures are also recognized. Of all the facies observed in the study area, micritic limestone is very rich in nummulites and the highest percentage recorded is around 90 % (Figure 5.5a). The size and the abundance of nummulites increase towards the upper part of sections 7 and 9**.** In a single bed, vertical and lateral variations in nummulite content have been observed. In the upper part of section 9, for example, a 60 cm thick micritic limestone bed shows 20 % and 85 % nummulite content in the lower and upper parts, respectively. Bivalves are also recorded in some of these beds.

In fresh and weathered outcrops, micritic limestone has dark gray and light brown colors, respectively. The facies is massive and is interbedded with structureless mudstone (facies H) in the deeper part of the total stratigraphic section (e.g. upper part of section 9) and carbonate rich very fine sandstone (facies E) and structureless mudstone (facies H) in the shallower part (e.g. section 2, 3 and 4). Lateral continuity of these beds for a long distance together with the abundance (high concentration) of nummulites makes them to serve as a marker bed.

Interpretation

The deposition of micritic limestone and the abundance of nummulites indicate the absence of significant terrigeneous sediment input into the basin, thus allowing the carbonate producers to dominate in the shelf environment. The increase in concentration and size of nummulites in the deeper part may be caused by reworking of shallow water environment by storm currents, causing nummulite shells to be carried by suspension currents basinward and then to settle in deep environments**.**

5.7 Facies G: Structureless (massive) siltstone

Description

This is the least common facies recorded in the study area. It is mainly observed in the uppermost part of the logged sections 7 and 9 (Figure 5.5b). At least 9 siltstone beds have

been recorded. The thickness varies from 9 cm to 70 cm and the average thickness is 30 cm. Mostly, there is a gradational passage from beds of this facies into overlying and underlying beds, which are usually mud and micritic limestone. The facies is usually found interbedded with mudstone in thick bedsets. No sedimentary structures are preserved, thus, the bed attains massive texture. The prevailing color in fresh outcrops is whitish (light colored)**.** Nummulites are very rare; the recorded percentage ranges from zero to 5%.

Interpretation

The fine grain size and homogeneous nature suggests deposition in a very low energy, quiet, relatively deep water environment. The lack of sedimentary structures might be caused by intense bioturbation.

5.8 Facies H: Structureless (massive) mudstone

Description

This is the most abundant facies in the study area and comprises 56 % of all lithofacies. Structureless mudstone is recorded in the lower and upper parts of the studied sections. No sedimentary structures were recorded in beds of this facies. Nummulites are abundant in structurelss mudstone in the upper part of sections 7 and 9. Bivalves have also been recorded in some of the beds.

Beds and bedsets of this facies are 7 cm to 12 meters thick and show variable silt content. The thickest units were observed in the lower parts of section 1 and lower and upper parts of sections 8 and 9. These mudstone units are commonly interbedded with facies D, E, and F. In the lower part of the total measured section, both sharp and gradational contacts with the overlying carbonate rich sandstone beds are common. Only in the lower part of section 1 this beds of this facies display gradational contacts with overlying structureless carbonate rich sandstone beds (facies E). In the middle (shallower) part of the total section beds of structureless mudstone are interbedded with beds of facies D and E.

Based on the amount of intact bedding and lamination (cf. Nagy, 2007), bioturbation class of this facies have been determined and it is observed to vary from III to V. The structureless

mudstone facies is mainly gray in color but alternations of light gray and dark gray color bands have been observed in some intervals. This facies do not display any sedimentary structures and hence appears massive. Among the mudstone beds observed in different parts of the study area, the highest percentage of nummulites are recorded in the upper part of section 9, which is 60 %.

Interpretation

Lack of structure in this facies may be due to a very homogeneous and possibly rather rapid depositional process in a very low energy environment or lack of platy grains. The original layering might have also been destroyed later by the mottling effects of burrowing organisms. The variation in silt content documents minor fluctuations in current flow energy during deposition. The color banding observed in some beds is interpreted to be caused by a slight difference in grain size. As a general rule, lighter colors indicate coarser-grained sediment in mud rocks, but there are cases where the opposite is true (Collinson & Thompson, 1982). Predominantly low-energy suspension sedimentation on a shelf that was generally below storm-wave base is generally indicated by lack of primary physical sedimentary structures (or the existence of reminant parallel laminae), the dominance of very fine-grained material (mudstone), high degree of bioturbation and by the existence of brief storm events (Colquhoun, 1995). The variation in intensity of bioturbation most probably reflects fluctuating rapid and slow rates of suspended sediment supply. The lighter gray color of the mudstone and the presence of bioturbation also suggest that bottom sediments were at least partially oxygenated.

5.9 Facies I: Fissile mudstone (“paper shale’’)

Description

The fissile mudstone is observed in the middle part of section 1 and is found always interbedded with facies D beds. The beds are thinly laminated and dark colored. Fissile mudstone beds with small scale HCS at the top are also recorded. Beds of this facies have an average thickness of 11cm, and mostly show sharp contacts with the overlying and underlying bed units. No bioturbation has been detected in this facies.

Interpretation

The fissility is interpreted to have formed due to weathering of finely parallel laminated mudstone which is rich in clay or micaceous silt. Small scale HCS recorded on thin intervals indicates the influence of the storm-induced currents. Generally, laminated mudstones result from suspension fallout from a standing water during slack water conditions (Uba et al., 2005). The lack of any obvious grain-size difference in very-fine-grained fissile mudstones suggests that grain orientation is responsible for the fissility. Clay minerals, chlorites, and micas commonly occur as platy grains which, during mechanical compaction, are squeezed into a texture of parallel orientated flat mineral grains (Collinson & Thompson, 1982). Fissile mudstone ("paper shale") is likely to indicate transition between shoreface to inner shelf, below storm wave base (Potter et al., 1980). Dark color (high content of organic matter) and the absence of visible bioturbation may suggest anoxic or dysoxic conditions at the sediment water interface (Brenchley et al., 1993).

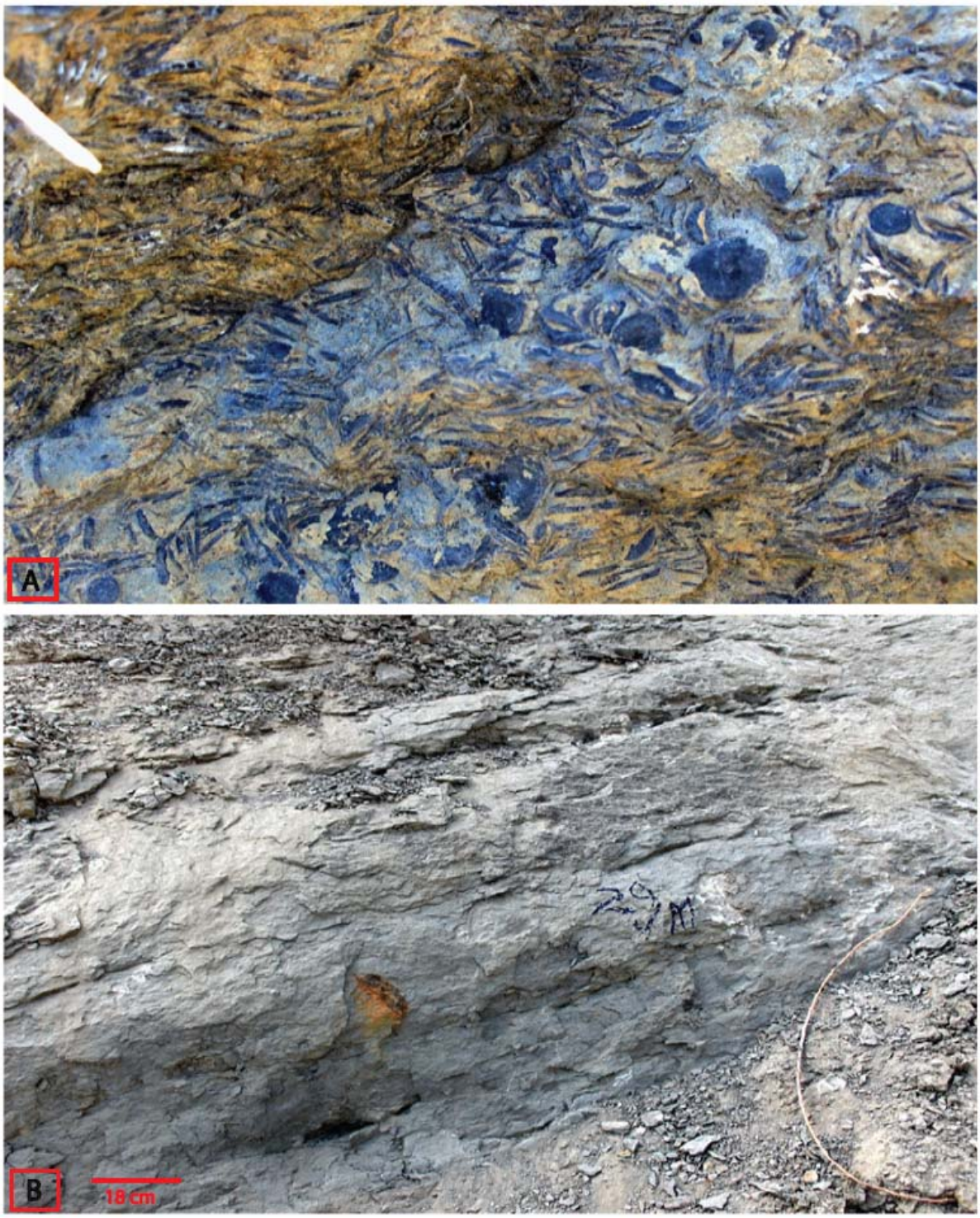

Figure 5.5: Outcrop photographs of facies F & G. a) Micritic limestone rich in nummulites (30.75 m, section 9). (b) Structureless siltstone overlain and underlain by structureless carbonate rich sandstone (facies E) (29.5 m, section 9).

6. FACIES ASSOCIATION

Facies associations are "groups of facies genetically related to one another and which have some environmental significance" (Collinson 1969, p. 207). The facies association provides additional evidence which makes environmental interpretations easier than treating each facies in isolation (Reading and Levell, 1996).

The nine facies described above reveal considerable variation in stratal packages both vertically and laterally. Depositional environments of the study area are interpreted by considering the sedimentary succession in the following four associations (Table 6.1).

Table 6.1: Description and suggested interpretation of the four facies associations of the study area

Facies Association	Description	Facies	Depositional environment
FA1	Low-angle cross-bedded siliciclastic sandstone and micritic limestone	A, F	Foreshore deposits
FA2	Cross-bedded to horizontally laminated carbonate rich sandstone	B, C, F	Shoreface deposits
FA3	Amalgamated/interbedded sandstone	D, E, I	Offshore-transition zone deposits
FA4	Structureless carbonate rich sandstone, siltstone & mudstones, and micritic limestone	E, F, G, H	Offshore deposits

The following table (Table 6.2) and the pie chart (Figure 6.1) show the percentage distribution of the four facies associations recorded in the study area. The background mudstone together with micritic limestone (FA4) covers most part of the study area (63.2 %), whereas the association of siliciclastic sandstone and micritic limestone (FA1) covers the least part of the succession (0.48 %).

Table 6.2: Percentage distribution of the four facies associations identified in the study area

Facies associations	Percentage (%)
FA1	0.48
FA2	13.14
FA3	23.2
FA4	63.2

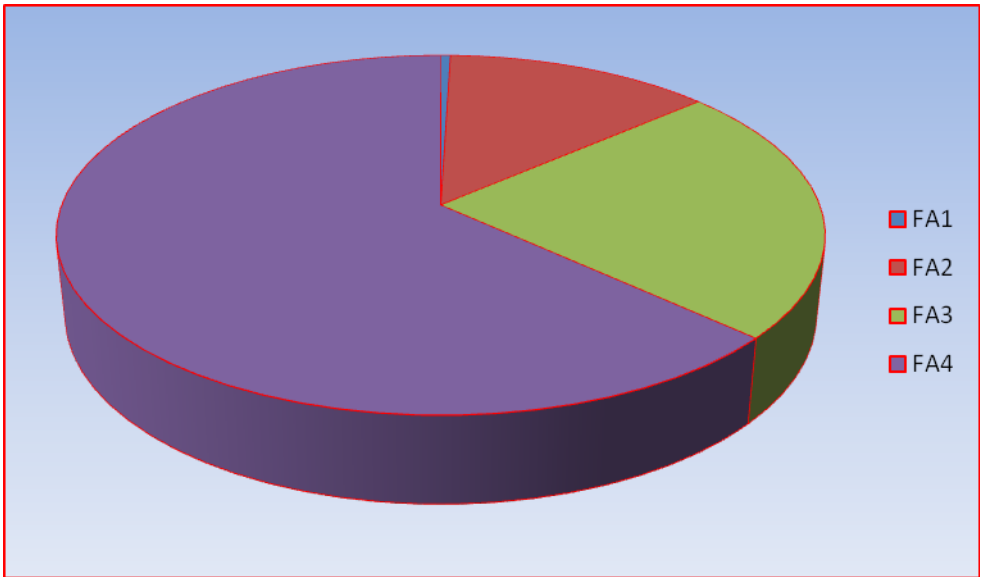

Figure 6.1: Pie chart showing percentage distribution of the four facies associations

6.1 FA1: Low-angle cross-bedded sandstone and micritic limestone

Description

Facies association 1 is mainly documented on the upper part of upward thickening and slightly upward coarsening successions and represents the middle part of the whole stratigraphic succession of the studied section. The association consists of fine grained siliciclastic sandstone and micritic limestone and comprises 0.48 % of the studied section. The thickness of the unit varies from 18 cms up to 1.50 meters and attains lenticular geometry, but it shows lateral discontinuities due to erosion. In various outcrops FA1 always occur as a single unit. In sections 2, 4 & 5 this facies association shows thickness variations between 18 and 48 cm; whereas in section 3 it has a thickness of 1.50 m. The sandy facies is characterized by low-angle cross-stratification with current ripples at the top and very rare (no) fossil content. The bottom bed of each unit, which is micritic limestone (facies F), has an average nummulite content of about 25 %, but in some logged sections the decrease in abundance upwards has been noticed. In some parts micritic limestone shows abundant vertical burrows, of which some are filled with sand and others are open, which is most probably caused by the weathering out of calcite fill that might have filled the bores. This vertical facies succession, therefore, gives a coarsening upward trend for FA1. The lower bounding surface of FA1 is conformable (both gradational and sharp) and, in some sections, it is underlain by massive mudstones (facies H) of FA4. The upper boundary is undulating and is always sharp with the overlying FA4.

Interpretation

The sedimentary structures on the siliciclastic sandstone and its grain size suggest that FA1 represents deposition in very shallow water. FA1 may be interpreted as a foreshore deposit with the low-angle cross-stratification and abundant vertical burrows suggesting a high energy condition. This could also be in the breaker zone, particularly in the upper flow regime, which produces a planar facies which in vertical section will appear as very low-angle cross-bedding (Reineck and Singh, 1980).

Biogenic and inorganic precipitaion from seawater results in carbonate sediment production. This is determined by interrelated factors such as water temperature, hydrodynamic energy, water salinity, terrigeneous sediment input, illumination, and

availability of nutrient elements (Hallock and Schlager, 1986). The principal control is siliciclastic sediment input; it has to be minimal for carbonate to accumulate (Reid et al., 2007). The association of micritic limestone with the overlying silciclastic deposit could therefore suggest that there might have been either a sea-level (eustacy) falls or source area uplift or both that might have resulted in the transport of siliciclastics across the exposed carbonate edifice and into the basin (Emery and Myers, 1996). Vertical and irregular burrows with structureless fill (e.g., Skolithos) suggest escape traces of upward burrowing small bivalves or polychaete worms following rapid sedimentation of the enclosing sandstone beds. Skolithos varies from marine to non-marine but is more abundant in marine and marginal marine strata (Ekdale et al., 1984).

The association of coastal-pain sediments such as those of lagoons and marshes with those influenced by waves, storms and tides, together with relatively mature sandstone composition, indicating derivation from the sea are the principal criteria used for recognising ancient linear silciclastic shorelines (Reading & Collinson, 1996). However, in the studied section coastal-plain sediments have not been recorded, therefore there are uncertainities in interpreting this association as a foreshore deposit.

6.2 FA2: Cross-bedded to horizontally laminated sandstone

Description

Facies association 2 is composed of 6 to 62 cms thick beds of cross-bedded carbonate rich sandstone (facies B), and cross- and parallel-laminated carbonate rich sandstones with a minor amount of mudstones, hummocky cross-stratified and massive carbonate rich sandstones (Figure 6.2). It has been well observed in sections 6 & 7 and comprises ~13 % of the total stratigraphy. Facies association two occurs in ~ 17 - 18 meters thick succession and is mostly overlain and underlain by FA1 and FA3 units, respectively. Rarely, it is also overlain and underlain by FA4 in sections 7 and 8, respectively. The lateral extent of this facies association is difficult to quantify as the area in which it crops out is mostly covered with vegetation, but locally lateral discontinuities have been recognized.

Two units of FA2 have been identified. Each unit is characterized by massive sandstone at the bottom, followed by wavy (undulating) and parallel (horizontal) lamination with symmetrical ripples in the middle. The notable feature of this facies association is the common occurrence of cross-bedding at the top most part/surface of each unit. The units show upward thickening trend from, for example, 7 meters in the lower unit to 10 meters in the upper unit. The grain size also increases moderately up through the unit. In some part of the logged sections, individual upward fining sandstone beds are stacked, whereas ocassionally they are separated by centimeters to decimeters thick structureless mudstone (facies H).

FA2 units have slightly erosive to gradational lower boundaries and planar / comformable upper boundaries. Fossils present include zero to 35 % nummulites (commonly < 10 %) and plant (leaf and/or root) fragments. It also displays vertical to sub-vertical burrows.

Interpretation

The observed sharp based sandstone beds with parallel lamination, at places grading into ripple lamination, resemble deposits of distal storm-related currents in the inner shelf-lower shoreface environment, as proposed by Myrow and Southard (1996) for similar structures. The presence of planar lamination, undulatory lamination and symmetrical ripple marks could also suggest wave action in the offshore to lower shoreface transition (Allen and Leather, 2006). The wavy bedding pattern may indicate deposition by the migration of small to medium wave ripples.

No structures have been observed that indicate deposition in the surf zone or subaerial exposure. This suggests that this facies was deposited on the shoreface above wave base but below the beach, as Mutti et al. (1996) proposed for similar deposits. Parallel lamination is the dominant sedimentary structure in the nearshore facies (Howard & Reinech, 1981). The interbedded rare HCS sandstone beds might suggest the occurrence of intermittent storm currents at this depth. Howard and Reinech (1981), for example, in their studies on the California Shelf found that small scale ripple lamination in the sea beds between the mean low-water line and 9.3m water depth. The slight increase in grain size of the sand grains and the upward thickening trend of individual beds might indicate a shallowing trend toward the top of the unit. Therefore, the gradual upward coarsening and thickening of FA2

might suggest progradation of a wave-dominated shoreface deposits, as described from other areas by Allen and Leather (2006).

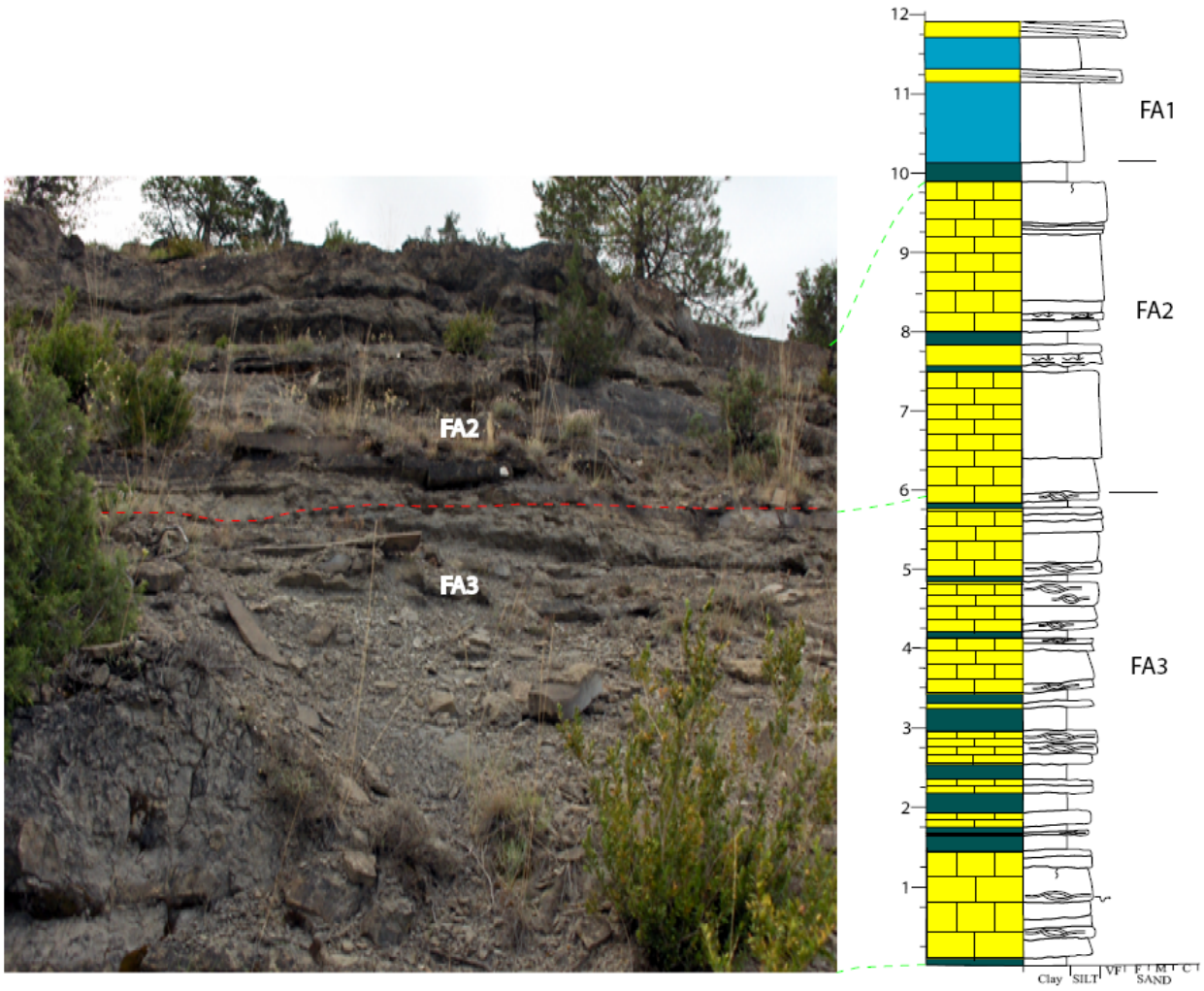

Figure 6.2: Outcrop photograph of facies from log section 6. The lower part is dominated by FA3 which passes upward into FA2. The picture also shows the upward thickening trend of FA2.

6.3 FA3: Amalgamated/interbedded sandstone

Description

Facies association 3 is comprised of HCS carbonate rich sandstone (facies D), structureless carbonate rich sandstone (facies E) and fissile mudstone (facies I), with sporadic occurrence

of massive mudstone (facies H) (Figure 6.3). It represents 23.2 % of the studied section. FA3 sandstone is very well exposed in the middle part of the road section (section 1). Although the quality of exposure is highly hampered by weathering and vegetation cover, this facies association has also been obseved in the hill side exposure of section 6. The unit is characterized by cycles of hummocky cross-stratified (HCS) and/or massive carbonate rich sandstone (facies D & E) and fissile mudstone (facies I). Occassionally the sandstone beds are separated by bioturbated massive mudstone (facies H). Carbonate rich sandstones dominate the association as massive and hummocky cross-stratified, and inplaces as hummocky cross-laminated beds. In section 7, the HCS beds are rarely documented.

The fissile mudstone constitutes a minor part of this association and shows occassional HCS top. In the lower part of the road section outcrop (section 1**),** about 31 meters thick succession consisting of alternations of carbonate rich sandstone and fissile mudstones observed. Individual sandstone beds show sharp to gradational contacts, HCS, mainly normal grading, and locally the massive beds are capped by hummocky cross-stratified to parallel laminated tops. These beds are separated by few centimeters thick mudstones (Figures 6.4a and 6.4b).

FA3 shows gradational to sharp contacts with the overlying cross-bedded to horizontally laminated carbonate rich sandstone (FA2). The lower contact varies from commonly sharp (uneven) to gradational and always occurs above FA4 wherever this facies association is observed. The general paleocurrent direction determined from storm-emplaced sandstone beds having flute casts indicate NW direction.

Interpretation

FA3 is interpreted as offshore-transition zone deposits based on the presence of hummocky cross-stratified sandstone interbedded with shale or mudstone. In transition zone hummocky bedding persists as the most significant primary sedimentary structure, with small scale oscillation-ripple lamination (Howard and Reineck, 1981) as the next common structure. Hummocky cross-stratified beds show deposition in a zone affected by storm waves but still below fair weather base.

Hummocks' can be formed by hurricanes (Duke, 1985) or severe winter storms. In some units the massive appearance of sandstone beds with sporadic hummocky cross-

stratification could be due to intense bioturbation. The extent of bioturbation and thus preservation of storm-generated structures can give records of the magnitude and frequency of storms, and the overall sedimentation (Reading and Collinson, 1996). Bioturbated mudstone beds indicate a long period of quiescence prior to emplacement of the overlying sand bed.

According to Duke (1985) the presence of hummocky cross-stratified sand, homogeneous sand with rare HCS, laminated sand interbedded with both bioturbated and fissile mudstones indicates that sometimes the influence of wave reworking was the most significant process at these depths, but at other times biogenic activity was the dominant influence. This could be an indication of the interplay between fairweather and storm conditions (Howard and Reineck, 1981). The sharp-based graded beds could probably be deposited from waning, storm generated flows whereas the muddy portion of each bed is probably partly storm emplaced, and partly reflects pelagic deposition between storms, as similar deposits described in other areas by Walker and Plint (1992).

Although it is hard to define clearly, the upper boundary of FA3 could probably represent the most typical day-to-day position of wave base, whereas the lower boundary may approximate storm wave base. Therefore, the occurences of FA3 generally have been interpreted as representing an alternation between rapidly emplaced storm deposited sandstones and slowly deposited hemipelagic mudstones, which can suggest sedimentation in water depths below fairweather wave base but above storm wave base (Dott & Bourgeois, 1982b). The directions of sand transport from the shoreface to its depositional site can be perpendicular, oblique or parallel (Walker and Plint, 1992). Duke (1991) noticed that the paleocurrent direction determined from flute casts that were made by the instantaneous action of waves are typically shore-perpendicular. Therefore, from flute cast paleocurrent measurement, the inferred most probable local shoreline strike direction of the study area would be ENE to WSW.

Figure 6.3: Outcrop photograph of FA3 showing interbedded sandstone and mudstone beds (part of the road section outcrop). The hammer used for scaling is 40cm long.

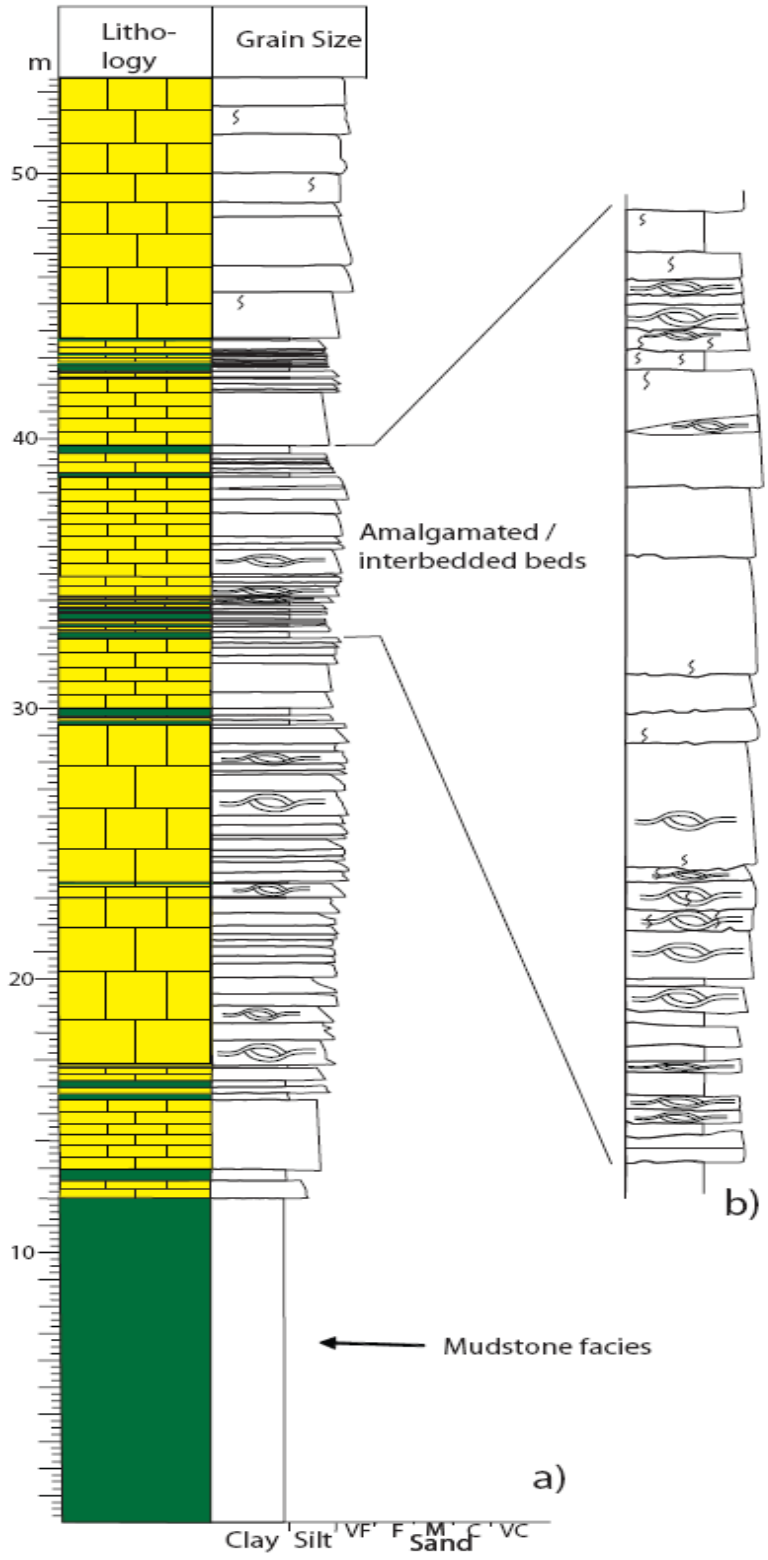

Figure 6.4: Sedimentary log of part of the road section. (a) The vertical sequence of facies recorded in the outcrop. (b) The nature of bounding surfaces and type of internal stratification observed in individual beds. Please refer appendix B for legends of sedimentary structures.

6.4 FA4: Offshore deposits

Description

This facies association is widely recorded in the upper part of the total stratigraphic section (e.g. log sections 7 & 9). It consists of micritic limestone (facies F), massive siltstone (facies G) and massive mudstone (facies H) and covers 63.2 % of the studied section (Figure 6.5a). The massive siltstone beds, which occur at an average thickness of 30 cm, forms a minor part of this facies association and has been observed only in some parts. In uneroded sections, except siltstone beds, this facies association forms laterally extensive deposit that can be traced for long distances along the depositional strike. In some exposures some siltstone beds are observed grading laterally into mudstones.

FA4 usually occurs in units with a thickness range of 1.75 meters to 12 meters, and such units become thicker up in the vertical succession. 7 centimeters to 1.22 meters thick, light gray to light brown colored micritic limestone comprises ~ 12 % of this facies association. Thin massive carbonate rich sandstones (facies E) are also recorded in some parts / sections. Sedimentary structures are generally absent. In the upper part of the stratigraphic seccession, both the micritic limestone and structureless mudstone beds of this association are rich in nummulites (average ~ 45 %) and the size and abundance (percentage) of nummulite content increases towards the top.

A vary rare bivalve fossil recorded in the study area are exclusively recorded in this facies association (Figure 6.5b). In some individual beds vertical variations in nummulites content have been noticed. This facies association is usually underlain by FA1 and rarely by FA2 units. Contacts with beds of the underlying facies are always sharp and are mostly planar. 5.5 to 12 meters thick massive mudstone beds with some siltstone beds, without micritic limestone; have also been recorded in the lower part of the studied section (e.g. lower part of log sections 1 & 7). These mudstone beds do not contain any fossil and shows sharp to gradational contacts with the overlying massive carbonate rich sandstones (facies E).

Interpretaion

The depositional style and large lateral extent of the mudstones and micritic limestones of this facies association along the strike suggest that these facies were deposited in offshore

environment. The presence of beds of micritic limestone in massive mudstone may indicate deposition that is influenced by distal storm flow or winnowing in habitats around or below maximum storm wave base (Dott & Bourgeois, 1982b). Thickening up trends of the units can be explained by a general increase in accommodation. The grain size could be the main reason that would likely permit the high nummulite content to be preserved. Bivalve shell might have been transported to this environment via storm activity. But in interpreting accumulations of larger foraminifera, biological factors may be as important as the hydraulics of the depositional environment (Aigner, 1985). Biological factors may complicate biofabric interpretations. Physical and biological structures in deposits like FA4 are commonly difficult to study in outcrop as physically formed structures have been partly or completely destroyed by the burrowing and grazing activities of orgainisms (Walker and Plint, 1992).

Figure 6.5: (a) FA4: intercalation of structureless mudstone and micritic limestone with sporadic massive sandstone and siltstone bed (part of log section 7 outcrop, overturned section). (b) Nummulites and bivalve recorded on micritic limestone (95.5m, log section 7). Pencil for scale (14 cm long).

7. FACIES SUCCESSION

A vertical succession of facies characterized by a progressive change in one or more parameters, e.g., abundance of sand, grain size, or sedimentary structures gives rise to what is know as facies succession (Walker, 1992). Lithofacies of the study area can be divided into three broad informal units (Figure 7.1) based on sedimentary facies, sedimentary structures and stratigraphic position. These are: lower-, middle-, and upper- unit.

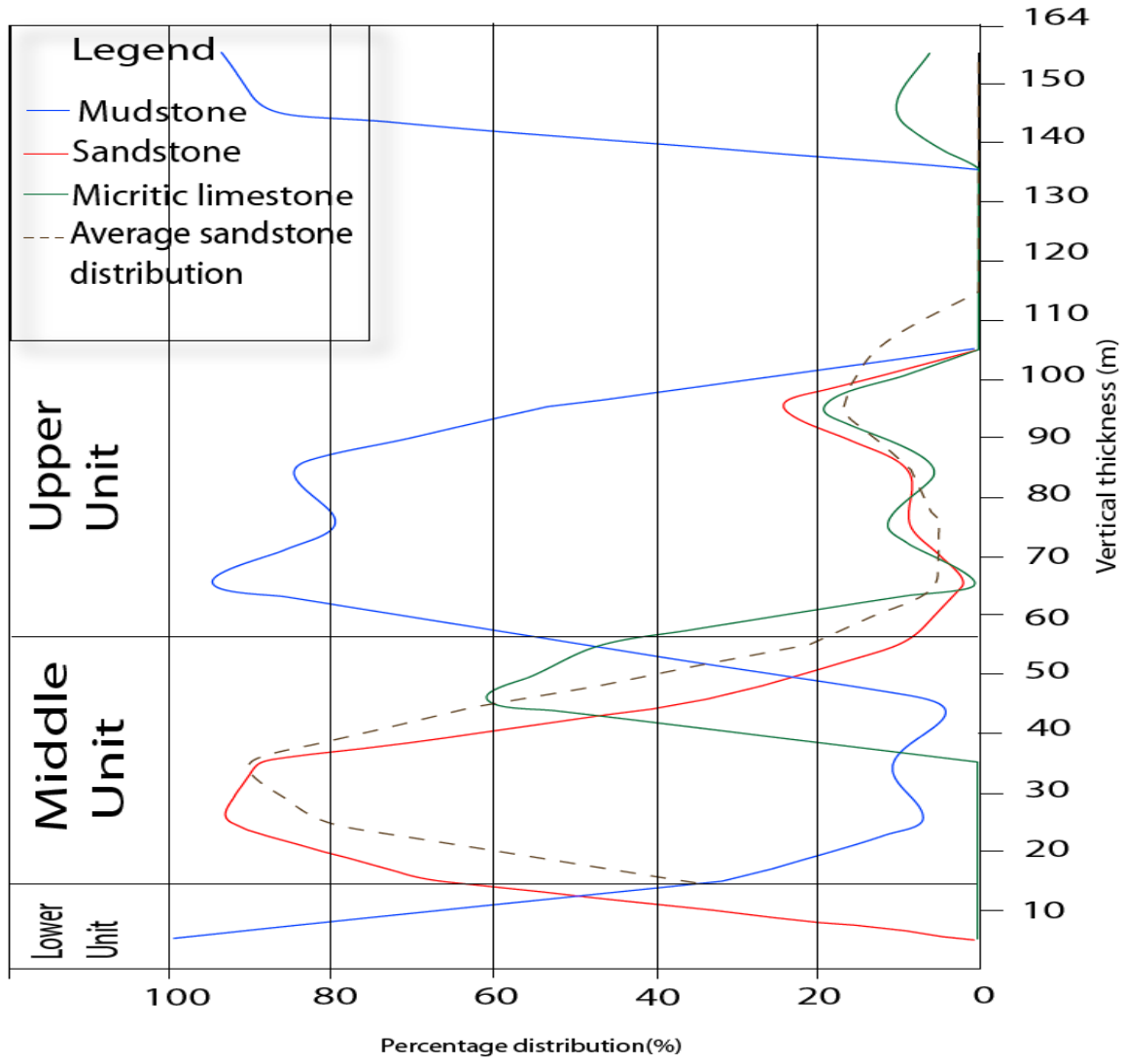

Figure 7. 1: Vertical facies distribution (in percent) and the three informal units.

Lithologies of the lower unit of the succession are always characterized by massive mudstone units with strong bioturbations and no fossils fragments. These mudstone beds have both sharp and gradational boundaries with the overlying middle unit. In sections 1 and 7 this unit is generally 5 to 12 meters thick.

The middle unit rocks are carbonate rich sandstones interbedded with both fissile and massive mudstones. The rocks contain variable amounts of nummulites; very rare plant fragments are also found locally. Individual sandstone beds show dominant fining upward trend but ungraded and reversely graded beds are also there. These beds have sharp (uneven) bases and are separated by massive mudstones or fissile mudstones. The sandstone beds of this unit show variable sedimentary structures. These include hummocky cross-stratification, cross-bedding, parallel lamination, wavy parallel-lamination, and ripple lamination.

Micritic limestone beds interbedded with siliciclastic sandstone beds marks the top part of the middle unit. The micritic limestone shows normal grading with vertically and laterally variable nummulite content. The low-angle cross-bedded siliciclastic sandstone is present at the top of the micritic limestone and marks the top most part of the middle unit. The sandstone facies generally thickens and becomes abundant up in the stratigraphic column of the middle unit.

Lithofacies of the upper unit are more variable in composition, consisting of massive mudstone (facies H), micritic limestone (facies F), structureless carbonate rich sandstone (facies E) and siltstone (facies G). Massive mudstone and micritic limestone are the dominant facies of this stratigraphic position where both are laterally extensive and contain abundant nummulites and all the bivalves recorded. These mudstone rich intervals range from 3 to 5 meters thick (on average) and locally consist of massive sandstone and siltstone beds.

The thick massive mudstone beds increase in abundance and thickness upward in the stratigraphic section/ position. These deposits have been mainly recognized in sections 7 and 9.

8. ARCHITECTURAL ELEMENTS

An architectural element can be defined as a "morphological subdivision of a particular depositional system characterized by a distinctive assemblage of facies, facies geometries, and depositional processes" (Walker, 1992). The stacking pattern of stratigraphic units at a regional scale is described by stratigraphic architecture whereas the stacking patterns of facies units within a depositional system at a local scale (e.g., architectural-element analysis) are described by facies architecture (Gani and Bhattacharya, 2007). The concept was originally developed for fluvial and eolian rocks (Jackson 1975; Allen, 1983). The architectural elements of fluvial (e.g., Miall, 1996) and deep marine (e.g., Mutti et al., 2003a) deposits have been studied far more than their deltaic and shallow marine counterparts. Greater facies architectural complexity and process variability are shown by deltaic depositional systems than fluvial and marine depositional systems. These are because deltas mark the crucial link between the latter two depositional systems (Gani and Bhattacharya, 2007). Architectural elements can vary in type from one system (e.g., deltaic) to another (e.g., fluvial) or within the same system in time and space, but there should be a finite number of architectural-element types in any given depositional system (Gani and Bhattacharya, 2007).

There are three main reasons that initiate the importance of studying / clarifying the architectural elements in shallow marine and deltaic systems. First, architectural elements link to specific morphometric features, such as bed waves, mouth bars, and channels, which typically scale to a specific aspect of flow conditions and are thus potentially useful in hydrodynamic analysis. Second, surface-bounded geobodies, and specifically architectural elements, are the building blocks routinely used in reservoir and aquifer characterization and fluid-flow modeling. Thirdly, surface-bounded, bed-scale architecture provides a fundamentally different view of how subsurface facies should be correlated versus the layer cake correlations that are typically presented in evaluation of many modern delta systems (Walker, 1992). Accurate linking of architectural elements of position in sequence and in sequence hierarchy allows for forward prediction of proportions of element types and preservation of these elements, thus allowing a greater degree of determinism in 3-D reservoir models (Flint and David, 2007).

8.1 Depositional architectural elements of the study area

A simple classification of the studied depositional architectural elements into three informal units has been proposed. These units are the lower-, middle- and upper- depositional architectural elements. These architectural elements have been distinguished by a variety of characteristics including preserved stratal architecture, net to gross ratio (N/G), type of lithofacies, vertical and lateral facies associations and wave/current influences. These architectural elements control the overall reservoir architecture of the study area.

8.1.1 Lower Unit Depositional Architecture (LUDA)

The lower unit architectural elements have been recorded in two logged sections (section 1 and section 7) and contain very fine sediments. This architectural element type consists entirely of massive mudstone (e.g., log section 1), or massive mudstone that shows a slight increase in silt content upwards (e.g., log section 7, Figure 8.1). Therefore, the lower 5-12 meters of the stratigraphic unit represent the least heterogeneous part of the study area. Some intervals show faint fissility but in almost all sections the deposit is strongly bioturbated, hence no sedimentary structures are preserved.

The upper boundary to middle unit 1 (MUDA1) and MUDA 3 are gradational and sharp (flat), respectively. Even though there is a lack of data in both directions due to vegetation cover, the deposit seems to have a fairly good lateral continuity. The log sections which contain LUDA show no sand and/ or wave/current influence.

LUDA elements were interpreted to be deposited from suspension in a very quiet environment. The absence of sand grains and wave/current influences may indicate that this element was deposited in a relatively deep water environment far from the coastline.

8.1.2 Middle Unit Depositional Architecture (MUDA)

The middle unit is considerably more sand-rich than either the lower or upper units. It is identified as the interval between the siliciclastic sandstone on the top and an easily recognizable mudstone deposits at the bottom. MUDA is between 12 to ~ 40 meters thick. The architectural elements in MUDA are characterized by relatively high sand : gross ratio (average 65 %). Mudstone deposits are less common (thinner) than in either the lower or upper units, but they have been recorded interbedded with the sandstone beds.

The facies assemblage of middle unit Depositional Architecture, in addition to wave and/ or current influence, has resulted in the identification of three different MUDA elements. These are MUDA1, MUDA2 and MUDA3.

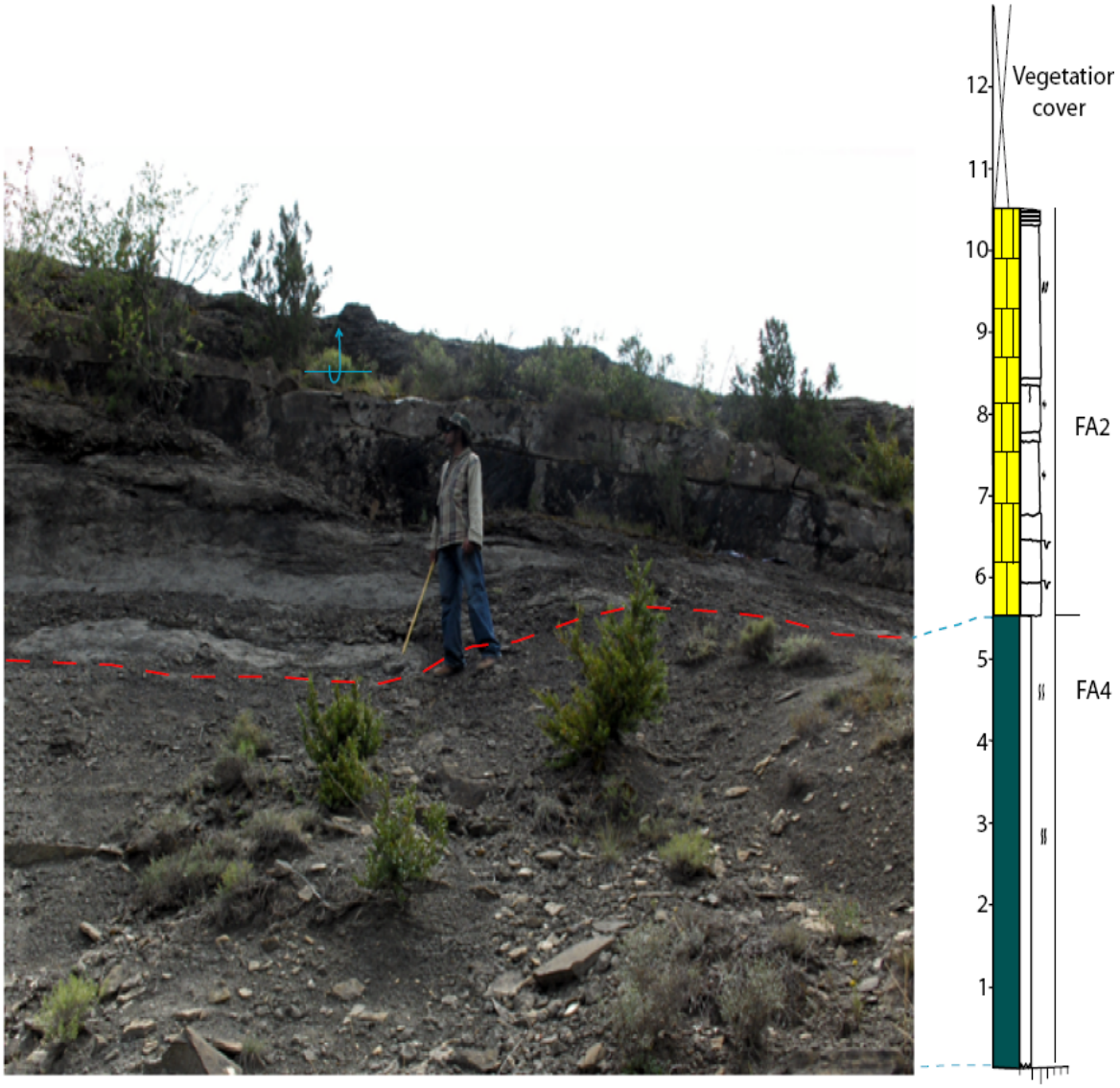

Figure 8.1: Outcrop photograph of log section 7 (overturned beds) in the northern part of the study area with the corresponding log section. The picture shows the sharp contact between the LUDA and the overlying MUDA3. The blue arrow on the picture shows the direction of the overturned beds. (Asfaw (1.78m) used for scale).

8.1.2.1 MUDA1

Amalgamated or interbedded elements are dominant in the well exposed road section outcrop (e.g., section 1). The architectural elements of MUDA1 consist of alternating carbonate rich sandstone and mudstone beds with micritic limestone on the top. Hummocky cross-stratification and massive sandstone beds are the dominant sedimentary structures recorded in the carbonate rich sandstone beds of MUDA1. Thinly hummocky cross-laminated carbonate rich sandstone beds showing few centimeters scale intercalations between fissile mudstones are restricted to MUDA1. The very fine grained carbonate rich sandstone coarsens upward to fine grain.

It shows a gradational lower contact with LUDA and an upper sharp contact with the overlying MUDA3. Laterally, some beds are consistent (up to 100 meters or more) and appear as tabular whereas other beds have wedge shape and thin in a preferred direction. Grain size, however, does not show any recognizable change in the lateral direction. This architectural element is ~41 meters thick (the interval from 12 to 53 meters of log section1, refer appendxe B) and contains upto five cycles of coarsening upward successions (Figure 8.2). Mudstone interbeds are mostly thin (except in some parts), in some cases absent, and as a result the beds appear as vertically interbedded/amalgamated. Therefore, MUDA1 shows relatively high sand: gross ratio, which varies from 60-70%. But for permeability distribution, this element represents heterogeneous three-dimensional bodies as there are interbedded hydraulically heterogenous lithofacies. The laterally continuous mudstones between sandstone units results in vertical compartmentalization of the possible reservoir unit.

Lack of sedimentary structures in some of the sandstone beds could be resulted from intense bioturbation, as described in facies description chapter (chapter 5). However, the dominance of hummocky cross-stratified beds shows that the beds have been deposited from storm activity in water depths between fairweather wave base and storm wave base. Amalgamated and laterally continuous (in outcrop scale) beds are interpreted to represent broad, sheet-like deposits emplaced by a relatively strong storm waves.

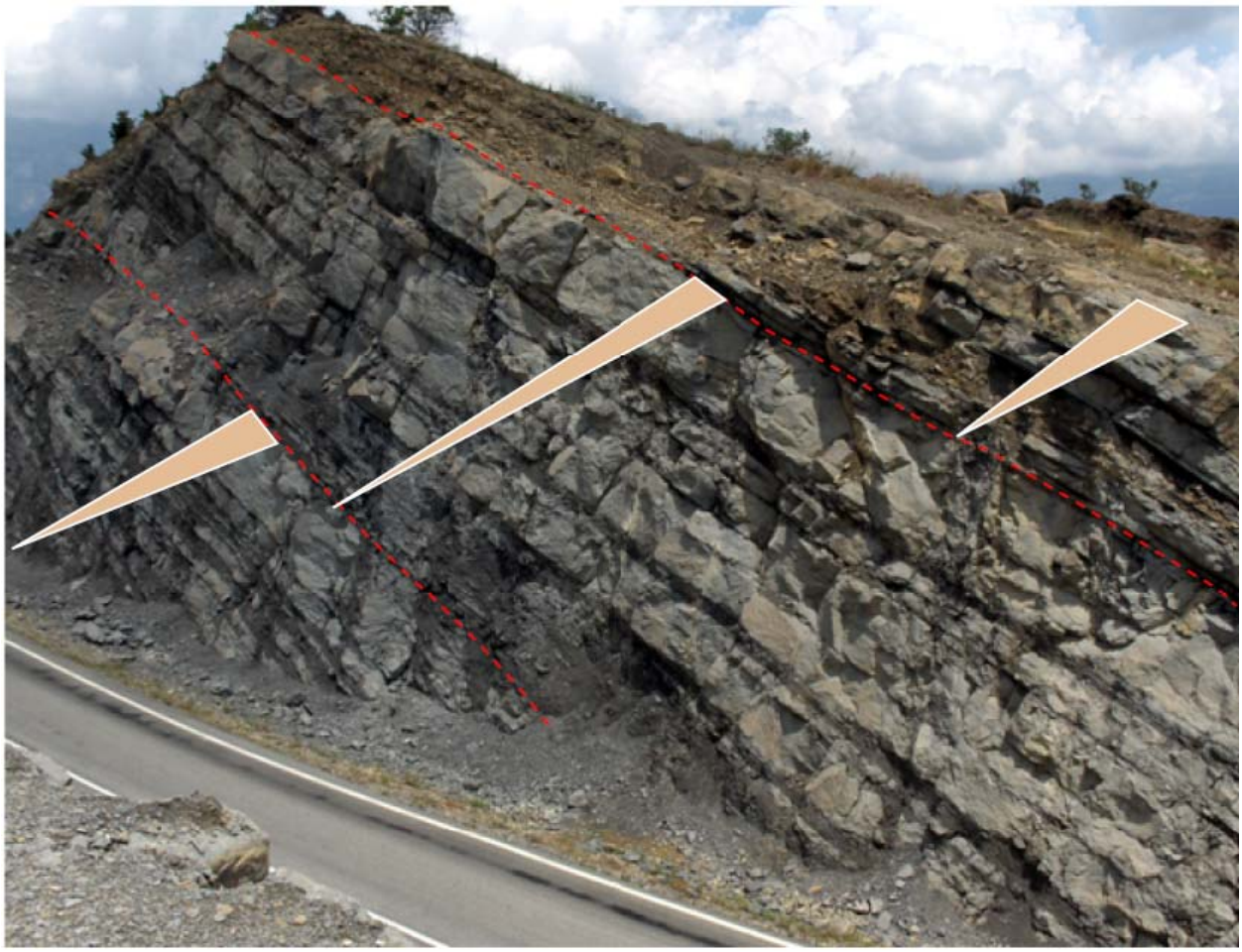

Figure 8.2: Outcrop photograph of part of MUDA1 element recorded in the road section (log section 1) showing an over all thickening upwards succession. Note also the three thickening upward trends.

8.1.2.2 MUDA2

This unit is located north of MUDA1 and is distinguished by the presence of all facies types except facies G and I. The lower boundary of this unit is difficult to trace over the entire outcrop but it is typically overlain by mudstone beds of MUDA3. MUDA2 comprises carbonate rich sandstone and micritic limestone and interbedded with mudstone intervals forming vertically thickening and coarsening packages up to 12 meters thick. The lateral extent seems to be proportional to the thickness: the thinnest element shows lateral pinch out. Sandstone-rich portions of packages have a wedge shape and shale-out in a preferred

direction; this resulted in less sandstone connectedness. The lower part of this unit is dominated by some 10 to 15 cm thick hummocky cross-stratified carbonate rich sandstone beds with interbedded massive (bioturbated) mudstone. These are followed by wavy parallel laminated, plane parallel (horizontal) laminated, cross-stratified and ripple laminated sandstone beds separated by structureless mudstones (facies H). The storm influence is prevalent in the lower part, but is significantly low or absent in the middle and upper part of MUDA2. It has an average sand : gross ratio of ~ 70 % and the ratio is observed to increase up the section.

Compared to MUDA1, the architectural elements in MUDA2 indicate the shallowing up of the water body along the vertical section. MUDA2 marks also the change in current or wave activity responsible for the deposition of MUDA1. The coarsening upward facies succession that could have been deposited during coastal progradation (Walker and Plint, 1992), and the sharp based sandstone beds with hummocky cross stratification and wave ripple lamination that correspond to storm beds (Dott and Bourgeois, 1982a), can be used to interprete this unit as a shoreface deposit.

8.1.2.3 MUDA3

MUDA3 has been documented in the northern most part of the study area (i.e., the overturned beds; Ako, 2008) and consist mostly of parallel laminated, wavy parallel laminated and cross-bedded carbonate rich sandstone beds. Hummocky cross-stratified beds are generally absent. The section is bounded above and below by mudstones of unit 1 and unit 3, respectively. These 28 meters thick MUDA3 consists mostly of very fine grained sandstone beds and exhibits a sharp basal bounding surface. Lateral continuity and connectivity of the sand beds are, however, difficult to evaluate as the deposits are covered by vegetation. However, locally, 80 – 100 m laterally continuous beds have been recorded.

Except in sections where the sand beds are separated by thin mudstones, MUDA3 shows a high degree of vertical stacking. This resulted in high sand : gross ratio, ~ 71 %. This might also suggest the presence of a high connectivity between the sand beds in 3D. Middle to upper shoreface depositional environment of these deposits are indicated by lack of HCS beds, and dominance of cross-beds, plane-parallel laminations and wavy beds.

8.1.3 Upper Unit Depositional Architecture (UUDA)

UUDA contains laterally extensive mudstone and micritic limestone beds with subordinate massive sandstone and siltstone beds. This unit marks the uppermost part of the stratigraphic succession and constitutes the largest portion of the studied section. For the most part it sharply overlies MUDA elements. The very few, thin sandstone beds recorded in the upper unit are laterally discontinuous and vertically separated from each other by thick mudstone and micritic limestone beds. It represents a small-scale three-dimensional sandstone bodies. Sand : gross ratio is estimated to be very low, usually < 5 %.

Lack of connectedness between the sandstone beds and the presence of thick mudstone beds suggest that this unit is considered as a poor reservoir. The unit is interpreted to be dominated by sediments deposited from suspension. The occurrence of micritic limestone, siltstone and sandstone beds suggests remobilization of relatively shallow water sediments, most probably by storm activity.

9. PETROGRAPHIC ANALYSIS

Petrographic analysis is used to describe the mineral content and textural relationships within a rock. Petrographic study, along with geochemical study, can be used to assess the provenance and tectonic setting of the area of interest.

9.1 Mineral Composition and Recognition of the studied thin-sections

Petrographic analysis of the studied ten thin-sections revealed that carbonate mud is the main component. Mainly quartz, and in lesser amounts feldspar (both plagioclase and microcline), mica, calcite, fossil fragments, organic matters and trace amounts of glauconite make up the framework. The framework grains are sub-angular to sub-rounded and usually floated in the carbonate dominated matrix.

Quartz

The quartz grains are identified by first order interference color (gray to pale yellow) in crossed polarized light (XPL) and no visible cleavage in plane polarized light (PPL). The quartz grains are mostly monocrystalline, while few of them are polycrystalline. There are also few strained quartz grains. The quartz grains may be with or without inclusion; the most common inclusion recognized is muscovite. Individual quartz grains are angular to sub-angular, and show mainly straight grain contacts, but sutured contacts have also been recognized.

The sutured grain boundaries and the internal strain are characteristic features of quartz from a metamorphic source; whereas the composite quartz with straighter crystal boundaries are from igneous sources (Adams et al., 1984).

Feldspar

Plagioclases, with a minor amount of potassium feldspar, represent the majority of feldspar components. Feldspars are identified in thin-sections by first order gray to very pale straw yellow interference colors, low relief, and albite (multiple) twins. On the other hand, microcline potassium feldspars, which occur only in a very small amount in some thin

sections, are identified by first order gray interference color, and 'basketweave' twinning (i.e. multiple twins crossing at almost right angles). In the studied thin sections, discrepancies in the amount of feldspars is expected as orientation has a strong effect on the appearance of a perthitic intergrowth when sliced and the relatively small fragments that are likely to be found in many siliciclastic rocks may be untypical of the original grain as a whole.

Optical or sub-optical intergrowths of albite and K-feldspar when the host material is potassium feldspars gives rise to what is generally known as perthite. These intergrowths have morphologies and chrystallographic characteristics that are distinctive of the igneous and metamorphic environments in which they grew and cooled to surface temperature (Parsons et al., 2005). Although the replacive phase is not always a pure albite, the replcements by Na-rich feldspar is called albitization (Lee and Parsons, 1997).

The cooling of igneous rocks and diagenesis are the causes of albitization; however, if it is encountered in clastic grains, it is not self-evident that it is a product of diagenesis (Parsons et al., 2005). Studies by Saigal et al. (1988) in offshore Norway showed that detrital grains of potassium feldspar have been albitized during burial diagenesis.

In carbonate rocks albite is more common than K-feldspar; whereas the reverse is true in sandstones (Kastner and Siever, 1979). The albitization of detrital feldspars is a wide-spread and important process which can significantly alter the original sandstone framework composition, form several products (e.g, illite, kaolinite, and calcite), and modify pore size and geometry. These changes can in turn influence reservoir properties (Saigal et al., 1988).

Mica

Mica grains were observed in all thin-sections examined, but the content being slightly higher in mudstones than in sandstones (Table 9.1 and Figure 9.5). It occurs both as biotite and muscovite. Biotite is identified by strong pleochroism in brown in PPL, reddish brown and green in XPL; and parallel extinction. Muscovite, on the other hand, is distinguished by second order interference colors in XPL; colorless to pale green color in PPL; and one excellent cleavage. In the studied thin-sections, muscovite appears to be more common than biotite. According to Adams et al. (1984) the abundance of muscovite, as compared to biotite, reflects its resistance to erosion.

The abundance of mica, in general, has been used to delineate the relative effectiveness of seafloor winnowing (Adegoke and Stanley, 1972). Mica contents of sediments can be used as one indicator of environmental energy level and depositional regime, as it is deposited with the finner clayey silts and fine sand in the deeper portion (Adegoke and Stanley, 1972).

Calcites

High order colors in XPL, colorless appearance in PPL, and rhombohedral cleavages are the characteristic features used in identifying calcites. Calcites have been observed filling the pore spaces between grains, microfractures, and the cavities left after the soft tissues of nummulites had been decayed.

Calcite cement is a common diagenetic feature in sandstone reservoirs. Pervasive pore-filling calcites can be found in spheroidal, elongate, tabular, or irregular forms (McBride, 1986). Calcite cemented sandstone can occur over a range of burial depths, depending on the supply of the cementing materials (Chang et al., 2007). Because concretions fill up the pore spaces as their volume expands the permeability and porosity distributions in sandstone reservoirs may be significantly affected (Hassouta et al., 1999).

Mud

Much of the finer grained sediment which appears brown or gray color in XPL and dominates the thin sections has been interpreted as mud. Mud is a mixture of silt and clay. Clay minerals are almost impossible to tell apart in thin sections. The mud is cabonate dominated and using the rock names of Folk's classification (1959), it can be named as micrite (carbonate mud). It consists of substantial amount of fossils (nummulites). Carbonate mud act as the main matrix material that support larger grains in the studied thin sections. Clays represent an end product of weathering and are abundant in a variety of sedimentary rocks and in soils (Perkins and Henke, 2000).

Nummulites

Nummulites, which are the largest and the best known foraminifera, are dominant in some of the studied thin sections. They are identified by their thick walls and their shape. Some of the nummulites are fragmented, most probably due to transportation. Some of the

nummulites comprise crystalline calcites that show abundant isochromes resulting from crystallization. Quartz grains also filled the space between the test walls.

Organic matter

Organic matter is identified by dark color in XPL and dark brown color in PPL. It has been identified in all thin-sections.

Accessary Minerals

Glauconite, dolomite and chert grains are included as accessary minerals and are present in minor or trace amounts.

Glauconite

Glauconite (K Mg (Fe, Al) $(SiO_3)_6$. $3H_2O$) is characterized by green or brownish-green color in PPL, and it is observed to occur as rounded pellets. Glauconite is formed under reducing conditions in sediments; exclusively it forms in marine environments, mainly in shallow waters (Adams et al., 1984). According to Fanning et al. (1989) the formation of glauconite (mica) is favoured by the chemistry of the sea water. It is preferentially deposited on the upper part of the continental shelf, with a slow deposition rate of precipitates of these products, in conditions under warm and shallow sea, 10-15^{0}C sea water temperature, 125-250 m of sea water depth, normal sea water salinity, and consumption of O_2 through bioactivity and internal pores of foraminiferal residues (McRae, 1972).

Dolomite

Dolomite (Ca Mg $(CO_3)_2$) occcurs only in few samples / thin sections, and it is identified by its extreme bireferengence, euhedral rhomb-shaped crystals (most of them show a brown rim/zone), and twinning characteristics under XPL. There is, however, a certain difficulty in clearly distinguishing dolomite from calcite as their optical properties are similar. Therefore, uncertainities exist in clearly identifying dolomite grains from calcites.

Dolomite is a major component of limestones, and is usually secondary, replacing pre-existing carbonate minerals (Adams et al., 1984).

Chert

Chert, which is a sedimentary clast, is recognized only in one sample. The disseminated chert was recognized by its gray to black speckled color in XPL.

Chert may represent either primary, where most of the silica is in the form of hard parts of siliceous organisms such as radiolars, diatoms, and some spongs, or secondary where it usually replaces limestone (Adams et al., 1984). Rogers and Longman (2001) suggested that the variations in sea-level have an importance in the cherts origin, particularly with respect to source and variety of organisms. They pointed out that at reservoir scale cherts appear to be independent of the frequency of sea-level changes.

Table 9.1 Pont counting results of ten samples

	Lower Unit	Middle Unit					Upper Unit				
Sample	A	B	L	E	M	N	S	H	T	Z	
No. of pts	470	540	503	469	524	460	449	540	544	576	
Facies	H	E	E	D	E	B	G	G	F	G	
Mono Q	24.40 %	26.80%	24.20%	31.30%	33.20%	40.60%	27.80%	12.20%	7.50%	12.30%	
Poly Q	0.00%	3.80%	0.30%	2.90%	8.30%	3.20%	0.60%	1.60%	0.0%	0.0%	
Felds.	0.40%	1.20%	0.10%	5.10%	1.90%	5.80%	3.10%	3.80%	0.10%	0.60%	
Mica	13.80%	6.60%	4.50%	5.50%	4.70%	5.20%	5.50%	12.70%	2.00%	15.40%	
Calc.	2.70%	3.10%	1.30%	3.10%	2.60%	3.20%	3.30%	1.40%	0.50%	0.50%	
Matrix	51.90%	51.60%	28.20%	39.60%	37.90%	25.20%	46.70%	51.8%	27.90%	55.70%	
Nummu.	0.0%	0.70%	40.30%	0.0%	4.70%	2.30%	5.50%	5.00%	61.20%	9.80%	
Org. Matt	6.30%	5.70%	0.50%	6.10%	4.30%	5.20%	7.10%	9.00%	0.50%	5.30%	
Glauc.	0.20%	0.0%	0.0%	0.40%	0.10%	0.20%	0.0%	1.10%	0.0%	0.0%	
Dolo.	0.0%	0.0%	0.0%	5.50%	1.50%	8.60%	0.0%	0.0%	0.0%	0.0%	
Misc.	0.0%	0.0%	0.0%	0.0%	0.0%	0.0%	0.0%	0.90%	0.0%	0.0%	

Mono Q.= Mono Quartz
Poly Q.= Ploy Quartz
Misc.=Miscellaneous
Glauc.= Glauconite
Felds.=Feldspar
Calc.= Calcium
Nummu.= Nummulites
Org.Matt=Organic Matter
Dolo.= Dolomite

9.2 Texture

Texture refers to the fabric of a rock- to its physical make-up as distinct from its mineral or chemical composition **(**Williams et al., 1955). Textural features have been used in the identification of mechanically deposited fragments and those minerals that have been chemically precipitated or recrystallized.

Sample B: this sample was taken from facies E, which is part of the middle unit. The sample is mainly dominated by carbonate mud (matrix), quartz, and mica. The carbonate dominated matrix represents the large percentage of the sediment, ~52% of the rock volume. Monocrystalline quartz which shows straight/undulose extinction dominates (~27% of whole rock volume) the quartz component of this sample. There is also some amount (4%) of polycrystalline quartz. Feldspar, organic matter, calcite and nummulites are present in minor amounts. The quartz grains are mostly angular; however sub-angular grains are also there and their grain size varies from coarse silt to very fine sand. The sample is poorly sorted.

Sample L: sample L represents facies E, and is recorded on the top part of the middle unit, log section 1. The nummulite content of this sample is ~40%, consequently as compared to sample B above; large increase in nummulites content has been observed. Besides nummulites, monocrystalline quartz, micritic (carbonate mud) matrix, mica and calcite occur in significant amounts (Figure 9.2). Very fine grained, sub-angular to angular quartz grains are separated by carbonate dominated matrix. The large variation of grain-size in this sample results in poor sorting. The porosity and permeability is, therefore, expected to be very low unless there are some preserved intrafossil pores that have been partly but not completely filled by calcite cement.

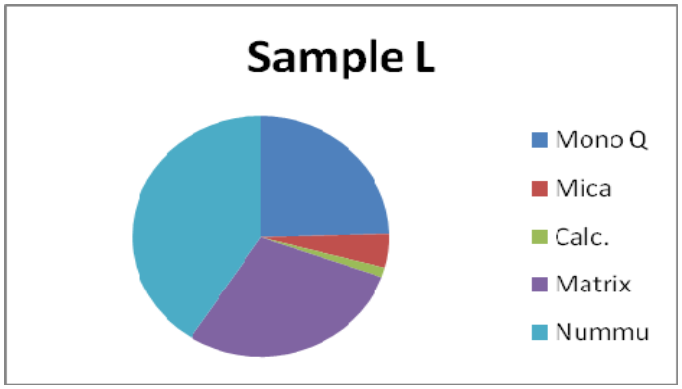

Figure 9.2: Pie-chart showing mean mineral compostion of sample L.

Sample M: this sample also represents facies E recorded in the middle unit. Monocrystalline and polycrystalline quartz grains represent ~33% and ~8%, respectively. The carbonate dominated matrix content of this thin-section is ~37%, a value higher than recorded in sample L**.** Glauconite, dolomite, chert, and feldspar occurs only in trace amounts. The quartz grains are angular to sub-angular; however, there are a higher proportion of angular grains. The grain size is mainly very fine sand but minor presences of coarse silt size grains have also been recognized. Calcite represents ~2.6%.

The presence of calcite and carbonate mud significantly reduces the connection between the sand grains, and thus the sample attains very low/negligible porosity.

Sample E: thin-section analysis of this sample, which represents facies D, showed that carbonate dominated matrix, quartz, feldspar, mica and calcite occur in significant amounts. No nummulites have been recognized, whereas organic matter present is ~6%. While dolomite predominates calcite, glauconite is a rare constituent. Very fine grained quartz grains are floating within the calcareous matrix and, based upon visual inspection, catagorised as subangular. Besides abundant carbonate mud presence, cementation of calcite reduces porosity.

Sample A: this sample represents facies H. High carbonate rich matrix, high mica content and very rare presence of feldspar characterized this sample (Figure 9.3). Medium silt sized quartz grains arranged to occupy smaller total volume. In this sample, where carbonate mud and calcite are important cements, porosity appears to be very low (negligible).

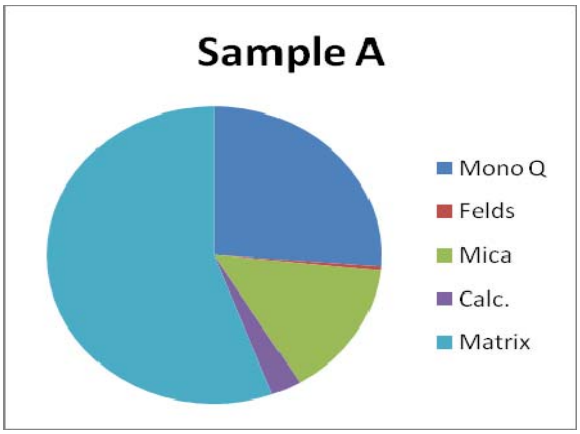

Figure 9.3: Pie-chart showing mean mineral composition of sample A.

Sample N: sample N represents facies B and contains a higher proportion of quartz (40.6%), carbonate rich matrix (25.20%), dolomite (8.6%), and feldspar (5.8%). Calcite and organic matter are also present in significant amounts. Both whole and fragments of nummulites occur. Texturally, the sample is characterized by poor sorting. Matrix and calcite fill the space between the quartz grains and results negligible porosity unless porosity is formed by secondary porosity forming events including calcite dissolution, leaching of feldspar and other unstable grains, and alteration of micas. Mainly coarse silt, but also very fine sand sized quartz grains have angular to sub-angular shape.

Sample H: this sample represents facies G and it is dominated by matrix, mica and organic matter. The highest amount of glauconites (~1%) has been recorded in this sample. The nummulites are almost always fragmented and show calcite crystals. The quartz grains have coarse silt size, and they are mostly sub rounded. This sample has negligible porosity.

Sample Z: compared to other samples, sample Z representing facies G contains the highest content of matrix material (~56%) and mica (~15%) (Figure 9.4a). The micas are mostly small in grain size. The quartz grains are totally monocrystalline and are medium silt in grain size. Sub-rounded grains dominate the sample although there are few sub-angular grains. Due to the dominance of matrix material no porosity is expected in the rock represented by this sample.

Sample T: sample T represents facies F, and it is located in the upper unit. It consists mainly of abundant nummulites (~61%), of which some of them have been recrystallized (Figure 9.4b). The central cavities of some nummulites have been filled with calcite/silica cement. It also consists of significant amount of carbonate mud with some quartz grains. The quartz grains are mainly sub rounded and have medium silt size. Feldspar and organic matter are almost absent. The rock of this sample has no porosity and, therefore, no permeability.

Sample S: this sample represents facies G, and was taken from the upper unit. The sample mainly consists of carbonate matrix (~47%) and quartz grains (~27%). It also consists of mica, nummulites and organic matters. The coarse silt size grains are sub-rounded and merely sub-angular. The sorting is poor.

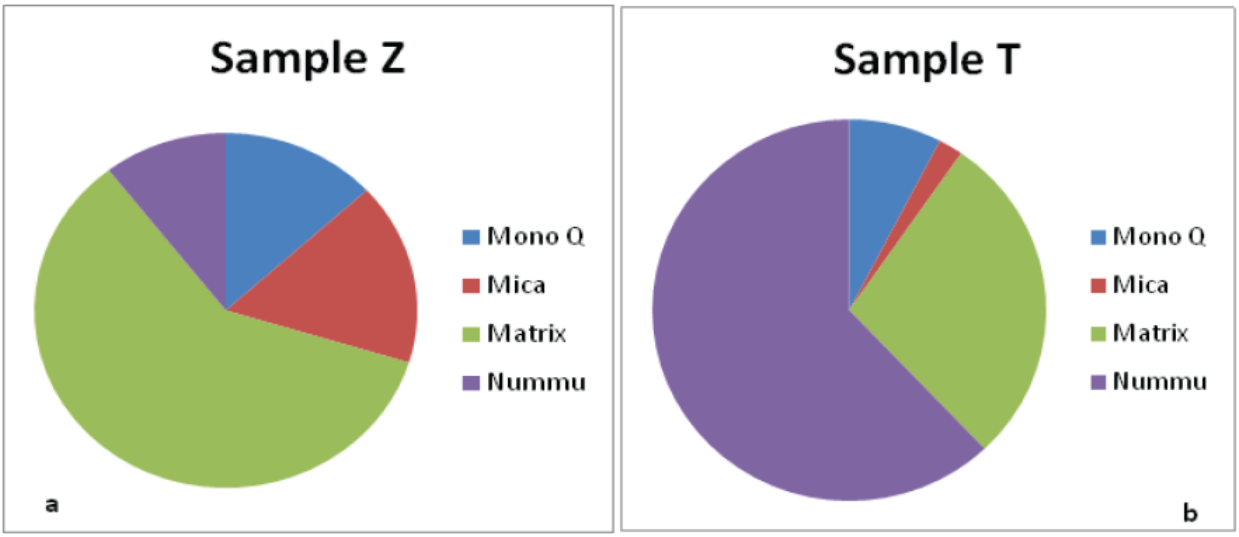

Figure 9.4: Pie chart showing the mean mineral compositions of sample Z (figure a) and sample T (figure b).

Figure 9.5, below, shows a vertical distribution of quartz, feldspar and mica. From the figure, it can be seen a general increase in quartz content up in the section up till the base of the upper unit. Feldspar content also increases slightly up the section through the middle unit. In the upper and lower units, a general decrease in both quartz and feldspar content has been observed. In the middle unit, mica content remains relatively constant but a relative increase in its content can be seen in both the lower and upper units.

Figure 9.6 shows selected pictures which have been taken during petrographic analysis. These pictures have selected to show different parameters of interest, such as mineralogy, matrix content, nummulite content, micro-fracture fillings, bioturbation, etc.

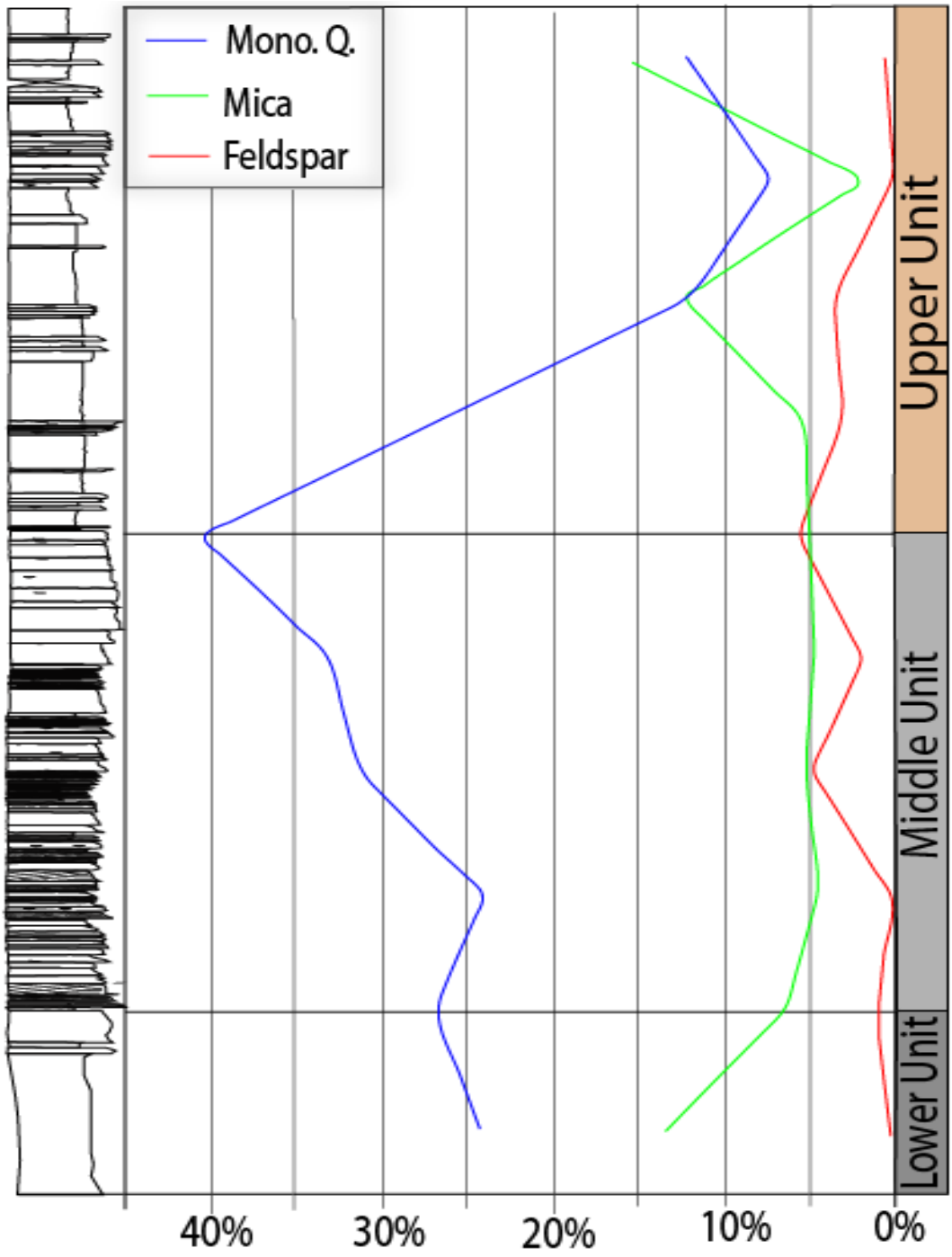

Figure 9.5: Graph showing the vertical distribution of mono quartz, mica and feldspar in percent. Note the increasing trend of both quartz and feldspar till the top part of the middle unit. The mica content remains relatively constant in the middle unit. While quartz and feldspar content decreases, a relatively higher content of mica can be observed in both lower and upper units.

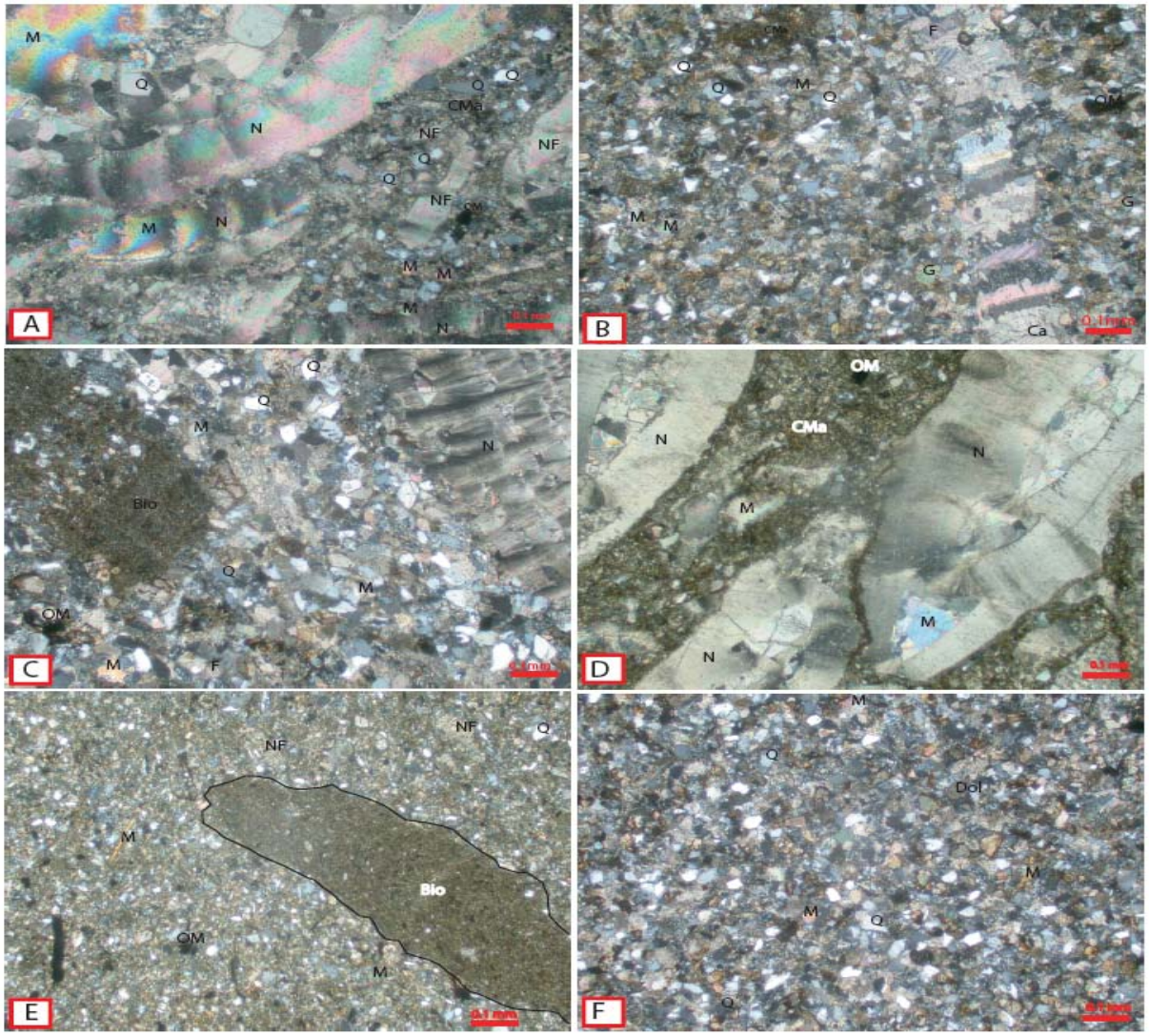

Figure 9.6: Thin-section photographs. A) Represents facies E and contains mainly nummulites and mica. B) Thin-section representing facies D. The picture shows a microfracture filled with calcite, quartz and feldspars. It also shows mica and organic matters. C) Thin-section picture representing facies E; shows quartz, mica and nummulites. D) Represents facies F and shows whole nummulite tests, carbonate dominated matrix and mineral fillings of the test. E) Represents facies G and shows carbonate rich matrix, very fine grained quartz and mica, nummulite fragments, and bioturbation. F) Represents facies B and shows quartz, mica, dolomite and organic matters. All pictures shown are taken in XPL and the scale bar is 0.1mm.

9.3 Provenance

Thin-section studies and their point counting under microscope show wide compositional variability. Quartz, carbonate mud (matrix), feldspar, mica, and nummulites are the main constituents.

Generally, sub-angular to angular quartz grains suggest a higher proportion of first-cycle grains with little transport history. But according to Williams et al. (1955) sub division of clastic deposits based on the roundness of their particles can not be applied to very fine grained deposits as small particles are not abraded and are invariably angular. In this context, it is a bit difficult to determine the distance the sediments of the study area had been transported before they deposited. But as suggested by Dabbagh and Roggers (1983) in other areas, the existence of high proportion of microcrystalline quartz grains may be attributed to the disaggregation of original polycrystalline quartz during high energy and/ or long distance transport from the source area. In the studied area monocrystalline quartz is more abundant than polycrystalline quartz grains. This can be explained, based on Dabbagh and Roggers (1983), by a relatively long transport distance from the source area.

It has been suggested by Nagtegaal and De Weerd (1985) in the Tremp-Ager Basin (South-central Pyrenees, Spain) that a relatively high content of quartz and feldspar grains in lower Eocene sandstones reflected a high input of detritus from the Upper Carboniferous granodiorites and the metamorphic complexes in the central part of the Axial Zone. In the studied thin sections, however, the recorded high abundance of monocrystalline quartz over polycrystalline quartz grains, the presence of feldspars, and the small content of strained quartz grains could give an idea that most of the siliciclastic materials were derived from igneous sources than metamorphic sources. The most likely igneous source that is found in the study area is the granite / granodiorite complexes that crop out in the Axial Zone. But the lack of granite/ granodiorite clasts in the studied outcrops and/or the very fine grain size texture of the identified quartz grains could give an idea that either there must have been a severe chemical weathering or a long transportation distance from the source area that caused the disintegration of granite clasts into quartz and feldspar grains. Both of the above mentioned reasons are likely to be the cause as the climatic condition of the Ainsa Basin during Eocene time were tropical to subtropical (Haseldonckx, 1972) that could cause severe chemical weathering (also proposed by Weltje et al., 1996) and also the Axial Zone was too

far (several tens of kilometers) from the site of deposition. Individual quartz grains that have been strained, and the observed suture contact between quartz grains gives an idea that some of the quartz grains were derived from metamorphic sources, as strained quartz is common in schists and gneisses (Williams et al., 1955) and suture contacts are typical of metamorphic rocks (Adams et al., 1984). Muscovite and biotite can be formed in felsic metamorphic or igneous rocks, and as recycled components in sedimentary rocks. Therefore, their presence may not give a clear idea of their provenance.

The high content of carbonates in the sediments indicates the presence of a large supply of bioclasts and a carbonate-rich source area in the eastern part of Ainsa Basin. Most of the carbonate grains were interpreted to be produced by nummulites (i.e., they are authochtonous). Depending on different factors (see section 10.3), nummulites can produce significant amount of carbonates. In the upper unit whole and/or fragmented nummulites, micritic limestones, and sand thought to have been deposited by marine processes (mainly storms) by erosion and/or truncation of previously deposited sediments in the shallower part. This may also possibly explain the high differences in nummulite concentration observed in some interbedded beds.

Some carbonate materials might have also been derived from the uplifted parts of the Southern Pyrenean Central Unit, which is located some 20 - 30 Kms away from the site of deposition (refer Figure 3.1, chapter 3). During thin section analysis, however, it was difficult to identify allochtonous carbonates; therefore uncertainities exist on the interpretation.

The above mentioned reasons are the possible causes that might have resulted in the formation of the mixed siliciclastic carbonate deposits that have been recorded in the studied area.

Based on textural and morphological features, calcite, which occurs in minor amounts, is interpreted to be present both as detrital grains between sand grains and as diagenetic cementation both in mudstone and carbonate rich sandstone.

Although less abundant, glauconite, which has fresh bright green color, is a typical sedimentary mineral formed by marine authogenesis (Williams et al., 1955). Its occurrence in brown color, apart from its well known green color, indicates that oxidation processes

have played an important role in oxidizing the ferric content of the glauconite. It could have formed on some parts of the sea floor where there was a very slow/none rate of sediment accumulation. The presence of glauconite might suggest higher concentrations of Si and Fe^{2+} than those usually occuring in surface sea water (Harder, 1980).

Cherts might have been formed from infilitrated silica containing brines that could have also resulted in minor dolomitization in the carbonate, as described by Siddiqui et al., (2006) for similar depostis. The source of silica is considered to have been derived from organisms, mainly from sponge spicules. Rogers and Longman (2001) suggested that the variations in sea-level have an importance in chert origin, particularly with respect to source and variety of organisms. They pointed out that at reservoir scale cherts appear to be independent of the frequency of sea-level changes.

Studies by Scholle (1978) on replacement and cementation minerals in carbonate rocks in other areas showed that the greater abundance of plagioclase relative to K-feldspar in host rocks could arise from the combination of preferential dissolution of K-feldspar in the more porous host rocks subsequent to concretion development and through preferential destruction of Ca-plagioclase by calcite replacement in the concretions. These two mechanisms could explain the reasons behind the common occurrence of feldspars, particularly plagioclase, in the study area.

9.4 Diagenesis, Porosity and Permeability

Mechanical and chemical compaction may significantly reduce the initial porosity in carbonate mud. Pore-spaces between grains (intergranular porosity) or porosity within grains, commonly fossils (intragranular porosity), can result in the origin of porosity in carbonate rocks (cf. Bjørlykke, 2007). All samples are rich in carbonate mud, i.e., they are matrix supported; therefore they are not expected to have got a good permeability. Depending on the grain size and lithology of the surrounding sediments, the porosity of nummulite tests can vary from zero to 50% (Racey, 2001), but fine grain materials can enter the test and significantly reduce the interparticle porosity. Aigner (1985) measured porosity as high as 72 % on larger foraminifers, whereas 40% porosity is common in Tunisian and Libyan accumulations (Racey, 2001). Based on this discussion, the nummulites of the study

area are expected to have a certain amount of porosity but the fine grain nature of the matrix and the observed calcite and quartz grains in the tests are expected to have a detrimental effect on the overall porosity anticipated.

Calcite cementation, representing an early diagenetic event, could have severely affected the primary porosity and permeability; but events like calcite dissolution, leaching of feldspar and/or alteration of mica could form secondary porosity. The porosity is further reduced by late stage diagenetic event, mainly by albitization. Some of the fractures observed in the studied outcrop and in thin sections (micro-fractures) have been filled with calcites. These can reduce the reservoir potential.

Finally, in all of the samples examined under microscope, no porosity was observed in thin sections. The primary porosity seems to have lost due to compaction or it might have been filled with carbonate cement. Thus, tectonic fracturing and dissolution of calcites and fossils may increase their porosity and particularly their permeability as it may not have a significant effect to the overall porosity.

10. DEPOSITIONAL ENVIRONMENT

10.1 Processes

Based on the identified sedimentary structures and facies, interpretation of physical processes has been done. The marine processes were dominated by waves and currents, but tidal influences have not been documented. In the studied succession there are deposits obviously influenced by currents brought about by waves and storms (e.g., facies D) and oceanic currents (facie A). There are also deposits which attest periods where bottom currents and wave activities were negligible and sediments settled out from suspension (e.g., facies H) or periods where no or very little siliciclastic sediment was put into the basin (this environment) (e.g., facies F).

The open marine (offshore) deposits do not show any wave and/or current influences, and they were mainly deposited from suspension fallout. Lack of fluvial, wave and current influences signify deposition far from the coastline where only very fine grained sediments could be transported through suspension and deposited by settling. The lack of sedimentary structures may also signify the predominance of biogenic activities (processes) in this part of the depositional environment.

Wave- and storm-generated processes are primarily the result of meteorological forces acting on the shallow parts of shelf and oceanic waters (Johnson and Baldwin, 1996).

Hummocky cross-stratification (HCS), wave ripples, plane parallel lamination (PPL), and cross-beds show dominance of wave and current influences during the deposition of the middle unit. There is an overall decrease in HCS towards north of the study area, whereas the dominance of PPL, wavy lamination, cross-bedding and wave ripples increase in the same direction.

The abundance of HCS could suggest deposition or reworking by storm activity (Walker, 1984; Duke et al., 1991), but based on recent works in other areas HCS dominated beds were found to be deposited by flood dominated deltaic systems (Mutti et al., 1996; Myrow & Southard, 1996). Thick and laterally extensive accumulations of parallel-sided graded beds commonly containing HCS have been documented in basin-margin shallow-marine and

shelfal successions of many foreland basins (Mutti et al., 2003b). According to the study, in such settings, sediment-water mixtures generated by fluvial floods enter sea waters as density-driven underflows, i.e. hyperpycnal flows. Much of the sediments carried by these flows can escape river mouths and be transported farther seaward. This increases the sediment flux to shelfal regions. Hummocky cross-stratified shelfal graded beds deposited by hyperpycnal flows that could escape river mouth regions have thus been termed 'flood-generated delta front sandstone lobes' (Mutti et al., 2003b). These deposits are thought to record the sandy depositional zones of a broad spectrum of relatively small, coarse-grained and high-gradient fluviodeltaic systems periodically dominated by catastrophic floods (Mutti et al., 2003b). Unlike the fluviodeltaic systems described by Mutti et al. (2003b) in many foreland basins, the carbonate dominated sediments of the study area are very fine to fine grained and are likely to be strongly influenced by storm activities than by processes of fluviodeltaic systems, as many storm deposits dominantly contain coarse silt to fine grain sediments (Duke et al., 1991) and the structure (HCS) is rarely observed in medium or coarse sandstone (Duke, 1984).

The structureless massive carbonate rich sandstone beds interbedded with HCS beds might have been deposited by storms and sedimentary structures destroyed later by intense bioturbation. Ghibaudo et al. (1974) (in Reading and Collinson, 1996) documented strongly bioturbated storm generated beds, showing only sporadically storm generated structures, in the Cretaceous Aren Sandstone of the Spanish Pyrenees. The interbedded fine grained sediments (mudstones) were deposited during the waning energy of storms or during times of fair-weather.

The occurrence of cross-beddding, plane-parallel lamination, undulating (wavy) lamination and current ripples might explain the shallowing up of the water body towards north of the study area. The influence of waves and storms also decreases up in the stratigraphic succession. In MUDA2 and MUDA3, parallel and lenticular very fine sand laminae and thin cross-laminated carbonate rich sands are intercalated with mudstones and reflect a combination of waves, sediment-laden current incursions and continued sedimentation from suspension.

The presence of micritic limestone on top of upward thickening succession marks a change in the depositional process. Carbonate sediments can be produced both organically and

inorganically with the organically controlled carbonate fraction as the dominant. Carbonate sediments consist of a skeletal component, at present time dominated by corals and algae, and a non-skeletal component of ooids, peloids, aggregates and clasts (Emery and Myres, 1996). The different factors which control carbonate production are discussed in section 10.3 and chapter 12. Carbonate sediments of the study area are interpreted to be produced mainly from nummulites, as these are the dominant benthic foraminiferids recorded. These carbonate accumulations might indicate a proximity to the coastline or deposition in shallow water. The upper mud dominated unit, deposited from suspension, are likely to record intermittent storm influences as there are preserved intercalated micritic limestone, sandstone and siltstone beds which could have been deposited by relatively strong storm events. The dominance of storm/wave dominated facies may suggest that fairweather tidal currents were absent or too weak to regularly rework the sea bed.

10.2 Paleocurrent Orientations

Paleocurrent structures and their orientation are fossilized indicators of the flow regime that permit interpretation of the transport system (Swift et al., 1987). In reconstructing flow directions the value of paleocurrent indicators has long been recognized, but little appreciated until Potter and Pottijohn (1977) made the tools of paleocurrent analysis widely available and formalized (Miao et al., 2007).

In the study of the transport direction of the study area, two main paleocurrent indicators have been used. These are cross-strata sets and flute casts. Cross bedding may be formed down to depths of 9 m, as shown by Howard and Reineck (1981) in the nearshore zone of the continental shelf of Ventura-port Hueneme area of California.

Paleocurrent directions measured from cross-strata sets up in the stratigraphic section of the middle unit have variable vector mean orientations. In section 7 (i.e. overturned beds), the orientation of the cross strata suggests a main NWN trending paleocurrent (Figure 10.1a); whereas in section 5 (i.e. the sanddunes) it suggests a NEN paleocurrent direction (Figure 10.1b). The rose diagrams from the cross-strata sets, thus, show a relative scattering. This variation in paleocurrent direction pattern may suggest transportation and deposition of sediments by flows that might have followed the local shape of the basin and / or local flow

directions. However, it must be emphasised that the number of measurements are too few for making any definite conclusion about paleocurrent directions.

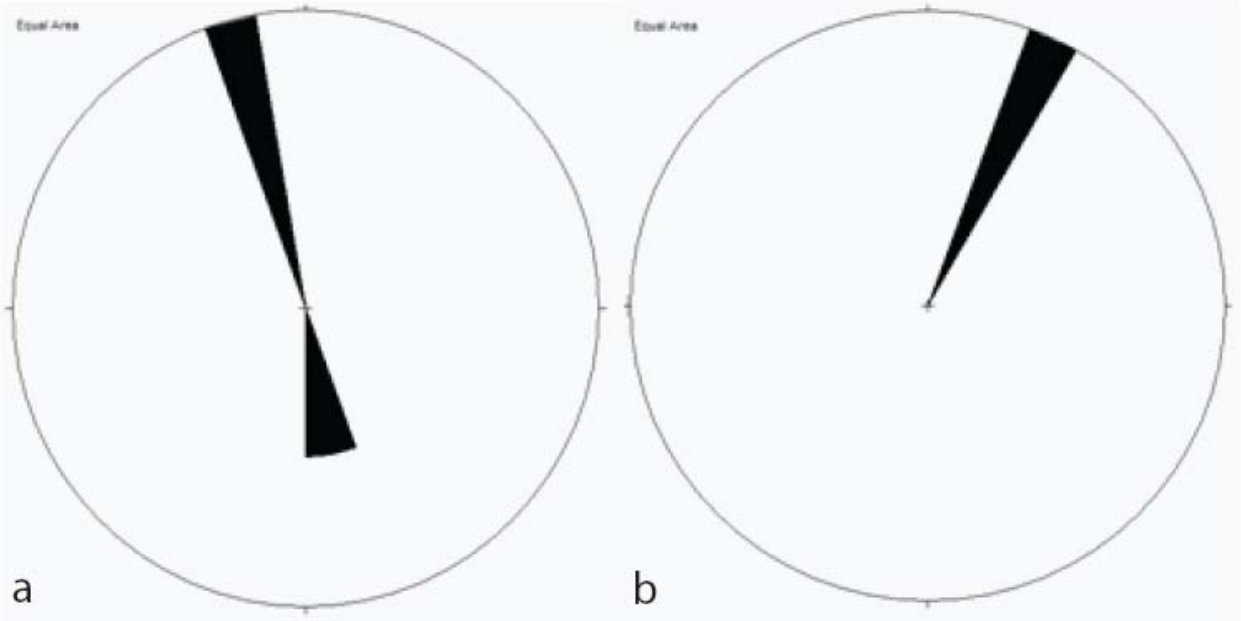

Figure 10.1: Rose diagrams showing paleocurrent directions measured from cross-beds in different parts of the study area. Figure (a) shows the paleocurrent direction measured in the overturned beds (Section 7) (N=4), whereas figure (b) shows the direction measured in section 5 (sand dunes) (N=1). Note that both diagrams show different paleocurrent directions.

Flute casts were recorded in the lower part of the middle unit (e.g. in sections 1 and 7). In section 1, it is observed to trend in various directions but the dominant ones are observed to trend NW and NE (N=6) (Figure 10.2a). The rose diagram of the flute casts measured in section 7 (Figure 10.2b) shows a variable paleocurrent direction, but it has a mean value of NW (N=2). The possible general shoreline direction determined from flute casts from section 1 and section 7 are thus WSW – ENE. Shore normal (Duke et al., 1991), paleocurrent direction indicators are likely to be formed in the lower shoreface beds and reflect the kind of fluid motion observed on modern lower shorefaces during storms (Swift et al., 1987). Shoreface studies by many researchers **(**e.g. Niedoroda et al., 1984; Swift et al., 1985) on the Atlantic shelf, for example, showed that during storms the capability of currents to transport sand had been observed to extend down across the lower shoreface and onto the inner shelf floor.

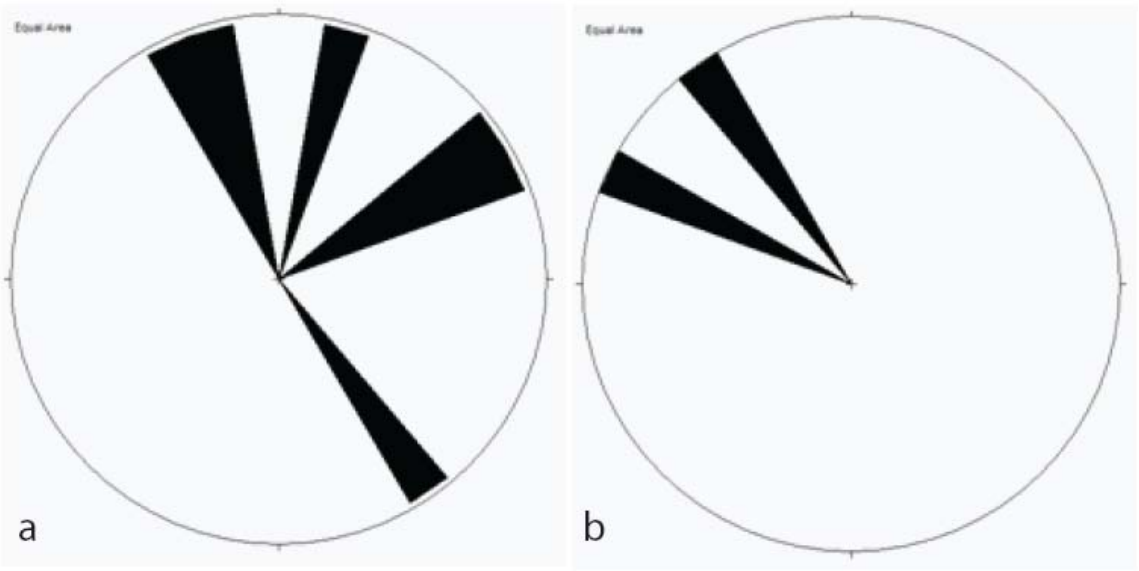

Figure 10.2: Rose diagrams showing paleocurrent directions measured from flute casts in different parts of the study area. Figure (a) shows the paleocurrent direction measured in section 1 (N=6); Figure (b) shows the direction measured in section 7 (overturned beds) (N=2).

Paleocurrent direction indicators measured in the studied outcrop are very small in number and, therefore, they can not represent the depositional direction of the whole succession. The shoreline orientation interpreted from flute casts does not show the same (similar) trend and therefore they are believed to represent local shoreline trends and not the regional trend of the depositional system. Had the orientations of current ripples been measured, it would have boosted / increased the reliablility of the paleocurrent direction measurement of the study area.

10.3 The ecology of nummulites

The fossil content of the Lower Eocene succession of the study area are dominated by larger foraminiferids (mainly nummulites) with minor consituents of bivalves and plant fragments. The nummulites have been recorded in almost all sections of the study area, but their concentration is observed to be variable. On the other hand, few bivalve fragments have only been recorded in the uppermost part.

Large benthic foraminiferids are important components of Tertiary (late Paleocene to mid-Oligocene) faunas in Tethyan regions and their occurrence in the oceans are encompassed by the 25 ^{o}C surface-water isotherms for the southern and northern summer (Murray, 1973). The data for their living occurrences, as summarised by Murray (1973), are presented below (Table 10.1).

Table 10.1 Summary of the data on modern living representative benthic foraminiferids (based on Wright and Murray, 1971; in Murray, 1973).

Genus \ Factor	Depth range (m)	Temperature (°C)	Salinity (‰)	Sea-grass	Seaweed	Other flora	Sediment	Coral reef	Energy conditions
Alveolinella									
Davies (1970)	0–6	18–26	39–50				√		high
Gypsina									
Logan (1969)	20–60					√			
Marginopora									
Davies (1970)	0–7.6	18–26		√					
Jell *et al.* (1965)					√				
Sorites									
Davies (1970)	0–7.6	18–26		√					
Blanc-Vernet (1969)	0–35	22–25*	>37*	√					
Peneroplis									
Murray (1970a)	0–7.5	24–27	40–53	√	√				
Davies (1970)	0–7.6	18–26		√					
Blanc-Vernet (1969)	0–35	22–25*	37*	√					
Jell *et al.* (1965)						√			
Spirolina									
Davies (1970)	0–7.6	18–26		√					
Blanc-Vernet (1969)	0–35	22–25*	>37*	√					
Amphistegina									
Blanc-Vernet (1969)	5–20	25*	>39*	√					
Seiglie (1970)	9.5–12.5	25–26	34–35				√	√	

* Indicates data from Sverdrup, Johnson and Fleming, 1942.

Nummulite accumulations commonly occur in platform- or shelf-margin settings and mid- to outer ramp settings, particularly in the circum-Mediterranean region, the Middle East, and the Indian Subcontinent (Figure 10.3) (Racey, 2001). They were restricted to warm (25^{0}), clear, shallow (< 120 m) waters within the euphotic zone (Reiss and Hottinger, 1984; Torricelli et al., 2006). Their restriction to the photic zone, where there is a good light penetration, is due to the fact that nummulites lived symbiotically with photosynthetic algae (Reiss and Hottinger, 1984), where algae produced oxygen and nutrients for the nummulite

host as a biproduct of photosynthesis, whereas nummulites provided shelter for the algae (Hallock, 1981a; Racey, 2001).

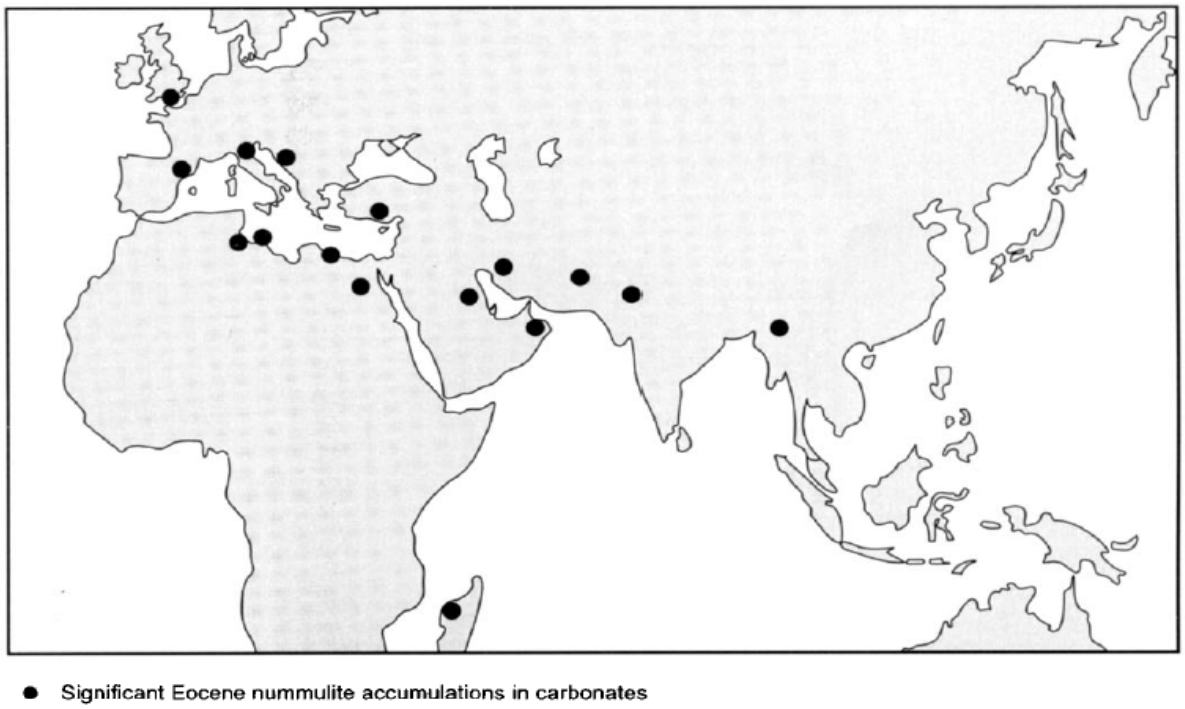

Figure 10.3: Geographical distribution of principal Eocene nummulite accumulations (taken from Racey, 2001). Note also the distinctive band of these facies around the margins of Tethys.

The distribution of modern large foraminifera is most importantly controlled by light intensity and water energy (Racey, 2001), but temperature and salinity are the most important gradients in the geographical distribution of large foraminifers (Hottinger, 1988). Both Pekar and Kominz (2001) and Racey (2001) showed that the distribution of benthic foraminifera is constrained by environmental conditions in which they live and not by water depths; however, environmental conditions such as substrate type, salinity, temperature, wave energy, turbidity, oxygenation, nutrients, etc are often depth dependent (Walton, 1964). The intensity of light and oscillatory water movements that is caused by waves decrease with depth (Reiss and Hottinger, 1984). According to Murray (1973) most genera of large foraminiferids always occur in regions of shallow water (maximum depth of 35 m). The type of symbiont and light penetration affect the water depth range of symbiont-bearing large foraminifera, therefore turbidity has a strong influence in determining the lower limit

of the photic zone (Reiss and Hottinger, 1984). Large foraminifers are found to live in the clear waters of the Indo-Pacific Ocean on both soft and hard sea bottom substrates between 0 and -140 m water depths (Romero et al., 2002); however, with increasing water turbidity the depth zone decreased without a significant change in the succession of communities along the depth gradient (Billmann et al., 1980).

The large, complex calcareous tests of large foraminifera are generally 2-5 mm in diameter but the largest variants, like nummulites, are more than 5 cm and they often live in association with coral reefs (Pekar and Kominz, 2001). According to Luterbacher (1984) nummulites smaller than 8 mm in diameter are common in almost all nearshore facies, whereas species larger than 8 mm are frequent in beach deposits and nearshore shoals.

Racey (2001) sugggested that the minor occurrence of associated micro- or macrofauna with nummulites can show the oligotropic nature of the environment in which they live and / or an environment with significant hydrodynamic sorting. Lithologies of the study area that are rich in large foraminifera (nummulites) are, therefore, interpreted to be deposited in oligotropic, calcium carbonate saturated environments. Such environments are characterisitic of tropical and subtropical seas where the input sediments are nutrient-deficit (Hallock, 1985). The climatic condition of the study area during lower Eocene time was tropical to seasonal sub-tropical (Haseldonckx, 1972), which was very conducive to the proliferation of large foraminifers (nummulites), according to the above discussions. In addition, the presence of storm beds manifests the existence of hydrodynamic reworking during deposition that might have made the existence of other faunas difficult.

Some nummulites of the study area (particularly in the upper part of the upper unit) resemble the allochtonous nummulite biofabrics described by Racey (2001), where allochtonous refers to nummulites that have been transported and hydraulically separated and / or broken by physical processes where winnowing and reworking would remove the finer material and cause fracturing of tests and thereby increasing the porosity and permeability of the sediment accumulations. But most of the nummulites in the middle unit and some part of the upper unit, on the other hand, resembled to have autochtonous biofabrics. According to Hallock (1981b) carbonate production by foraminifera often occur in higher energy environments

from which the tests are removed very soon after (sometimes before) the death of the foraminifera.

Detailed studies of large foraminiferal assemblage distribution with respect to ecological parameters and facies successions can give a good paleoenvironmental models for sedimentary successions containing these fossils (Bassi et al., 2007). Although variable distributions of nummulite content have been noted in the study area, the paleoenvironmental interpretations have got a limitation. This is mainly because nummulitids can live at different depths depending on different factors. According to Bassi et al., (2007) perforated hyaline foraminifera, for example, are dominant in the lower part of the photic zone. Studies by Hohenegger et al. (1999) in the western Pacific showed that large foraminifers were observed to inhibite sandy substrates in zones between fair-weather and storm-wave base where water motion was less intensive, whereas near and below the storm-wave base, fine sand substrates were inhibited by plate like nummulitids. Thus, with reference to these observations, one can suggest that the sediments and the recorded nummulites of the study area may have been deposited in the deeper part of the photic zone.

The other type of benthic skeletal fragments observed in trace/minor amounts in the studied section is bivalves. These fragments have been recorded in the upper most part of the studied section associated with FA4 where the majority of them occur in the mudstone beds (facies H). Its occurrence in trace amounts makes it difficult to use it for environmental interpretation.

10.4 Depositional environments of the study area

Depositional environments of the study area have been classified into three parts based on the already classified units, i.e., lower, middle and upper units (chapter 7). To have a better understanding of zonation of the shoreline profile, the following description is presented below based solely on the paper of Reading and Collinson (1996) and references therein.

10.4.1 Zonation of shoreline profile

In shoreline profiles, there are a number of zones (Figure 10.4) each with its characterisitc processes, morphology and facies (Bourgeois & Leithold, 1984). Depending on the emphasis of the study, i.e., process or morphology, the zones are differentiated primarily upon the position of storm and fairweather wave base, and on the mean high- and low-tide levels, and secondarily upon the nature of wave transformation.

The offshore-transition zone extends from mean storm wave base to mean fair weather wave base and is characterized by alternations of high and low energy conditions. The nearshore zone, on the other hand, extends from mean fairweather wave base to mean high water level. It comprises a shoreface, below mean low water level and a foreshore between mean low water and mean high water level.

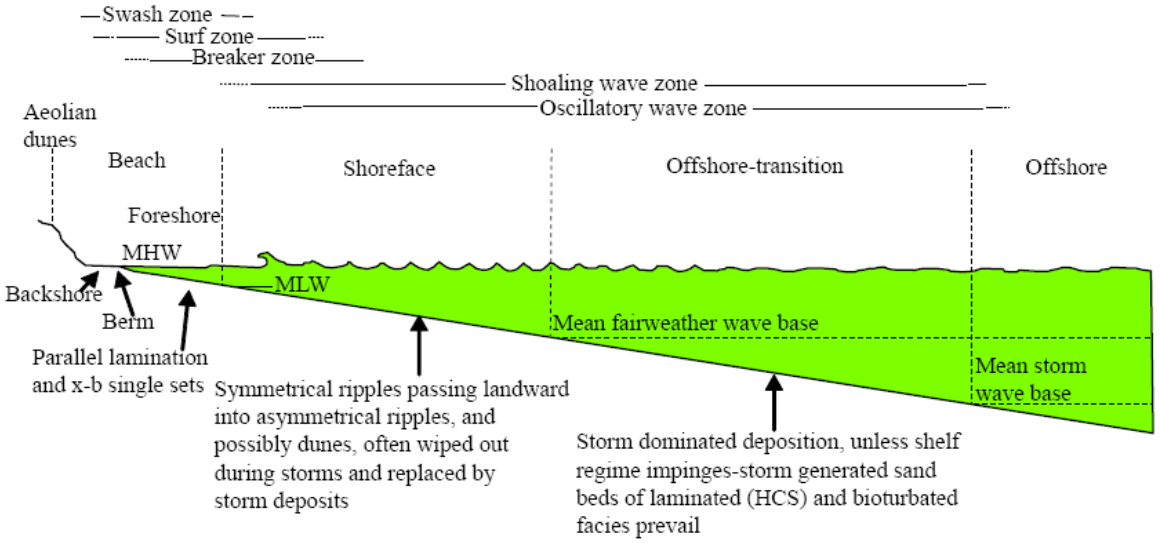

Figure 10.4: Generalized shoreline profile showing subenvironments, processes and facies (modified from Reading and Collinson, 1996).

According to Burchette and Wright (1993) (in Bensing et al., 2008) sedimentary features can be used to make divisions with respect to ramp position. The carbonate deposits of the study area have been interpreted to have been deposited in a gently sloping carbonate platform ramp; where a carbonate ramp is a low-angle seaward dipping surface, with no continuous elevated rim or clear break in slope and the sedimentation is dominated by basinal processes (Emery and Myers, 1996). The following three reasons are the main causes that helped in the interpretation of the studied platform into ramp. These are: the dominance of basinal processes (mainly waves and storms); the absence of slump/slide deposits which would otherwise occur in high angle platforms with steep slopes; and the presence of nummulites in most part of the middle and upper units that may suggest the absence of oceanic barrier along the ramp, which is typical of rimmed platforms. Although ramps are known from a wide variety of tectonic settings (Burchette and Wright, 1992), the largest develop along passive margins and in foreland basins where flexural subsidence dominates (Wright and Burchette, 1996). Based on the dominant processes, Wright and Burchette (1996) divided the ramp profile into three (Figure 10.5). These are: an inner ramp, located above the fairweather wave base where wave and current activities are almost continuous; the mid-ramp, a zone lies between fairweather wave base and storm wave base where storm processes are dominant; and the outer-ramp zone that extends from the normal storm wave base to the basin floor. Using this classification, the sediments of the study area have been classified into outer-, mid- and inner-ramps.

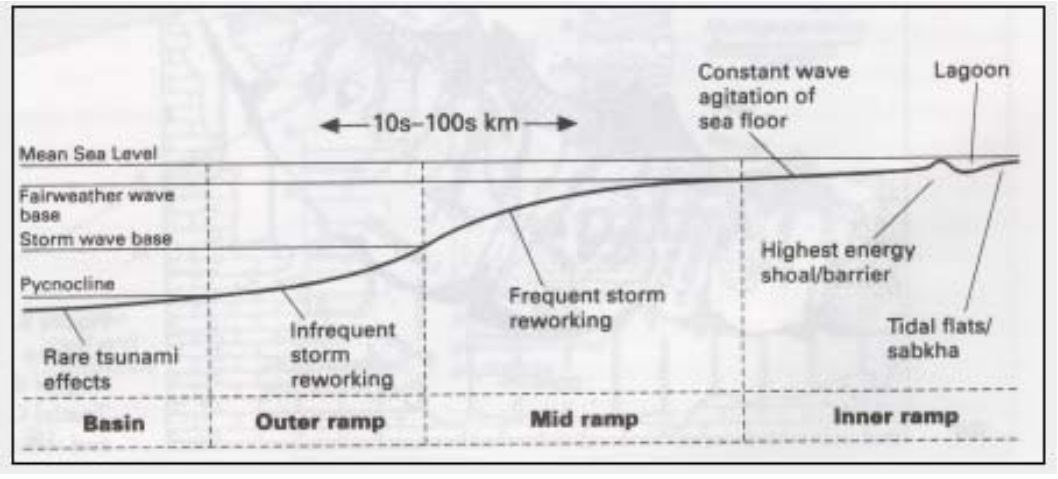

Figure 10.5: The main environmental subdivisions of a carbonate ramp (from Burchette and Wright, 1992; in Wright and Burchette, 1996).

10.4.2 Lower Unit depositional environment (LUDE)

Lithology and sedimentary structures of the lower unit depositional environment demonstrate that these mudstone deposits developed in relatively deep water, most probably below storm wave base, under quiet energy conditions. Absence of wave/current and storm influences and / or absence of slump/slide deposits could give an idea that the deposition occurred over a gently sloping deep water carbonate ramp, mainly in deep water outer ramp and basinal environment. The existence of dominant mudstone and very minor siltstone are indicative of deposition from suspension and reflects minor flactuations in sediment carried in buoyant plumes (plume shifting), or discharge flactuations. The bottom waters are likely to be aerobic, or most probably dysaerobic, as the laminae are strongly disturbed by bioturbation. The high degrees of bioturbation could also depict slow rates of sedimentation. Generally, description of the LUDE by means of physical characteristics is not straight forward but by comparing environments inferred from units above, this unit has been interpreted to be deposited in an open shelf/ outer ramp environment. This interpretation is also supported by the study of Flåt (2008) of strata belonging to the still deeper slope environment of the eastern part of the Ainsa Basin in this area.

10.4.3 Middle Unit depositional environment (MUDE)

The middle unit deposits could represent a relatively high energy environment, with strong reworking by storms, waves and currents. Unlike the lower unit, this unit consists of variable amounts of nummulites. Sedimentary structures like cross beds, wavy beds, and wave ripples are common. Amalgamated hummocky cross stratified sandstone beds also exist in this unit**.** This unit is interpreted to be deposited in positions ranging from mid- to inner-ramps. The slightly coarsening and thickening upwards beds show evidence of the increase in accommodation space. The depositional environment became quiter and the sediment input restricted/minimized up in the middle unit during the production of the carbonate sediments. Based on the dominant sedimentary structures recorded, the depositional environments of the middle unit have been further classified into three. These are MUDE1, MUDE2, and MUDE3.

10.4.3.1 MUDE1

This unit shows coarsening and thickening upward successions, which are believed to respresent mid-ramp rocks. These mid-ramp rocks were interpreted to be deposited in the offshore-transition zone. Even though most of them are thought to have been destroyed by bioturbation, the common occurrence of hummocky cross stratification is very helpful in the interpretation of the offshore-transition zone depositional environment, as storm activities are immense in this zone (Duke, 1990). But according to Jones and Desrochers (1992) storms can quickly and radically alter sediment distribution on any part of the platform that is above the storm wave base. The five cyclic motifs observed in this sub-unit demonstrate a shallowing up in each cycle and an overall shallowing of the basin during formation of the middle unit. The overall thickening upward trend gives an evidence of the buildup of a carbonate platform, which marks an increase in accommodation space. As can be seen in the figure below (Figure 10.6), individual thickening upward successions consist of mudstone beds in the lower part with an increase in sandstone content at the expense of mudstone in the upper part. This gives a general prograding pattern for each succession. The interbedded sandstone and mudstone beds reflect variation of deposition during storm- and fair- weather conditions.

10.4.3.2 MUDE2

This environment, representing the MUDA2, also shows an upward thickening trend which also heralds the shallowing up of the depositional environment. However, in the lower (middle) part of the unit a change in dominance of sedimentary structures from HCS to wave / current ripples, cross-beds, wavy bedding, parallel laminations, etc have been recognized, and this might mark the transition in environment of deposition between storm dominated and current dominated environments. Deposition by migrating small to medium wave ripples is though to have caused the formation of the observed wavy bedding pattern. This unit is interpreted to be deposited on the shoreface above wave base but below the beach (mid- to inner-ramp), as there are no structures that may indicate subaerial exposure. The fine-grained siliciclastic strata at the top of the middle unit are interpreted as foreshore deposit.

10.4.3.3 MUDE3

MUDE3 has much in common with the depositional environment described in MUDE2. However, unlike MUDE2, MUDE3 does not show any storm influences and it is dominated by unidirectional currents put up by waves. This marks the deposition of this unit in current-

dominated environment, most probably in shoreface / inner-ramp regime. This environment could be a relatively low-energy environment as the sediments are very fine to fine grained.

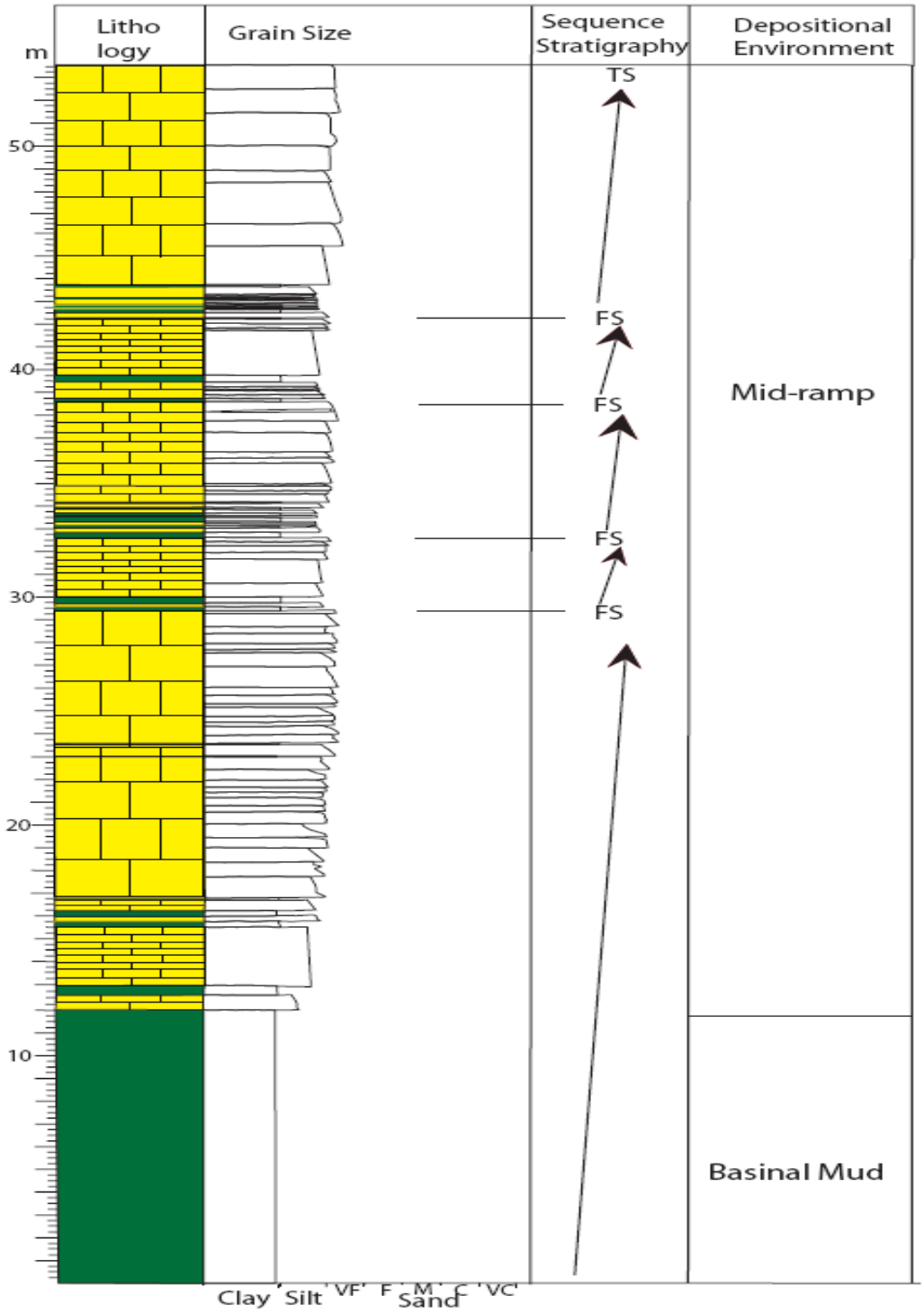

Figure 10.6: Depositional environments and sequence stratigraphic interpretation of part of the studied section (Section 1). Note the five upward shallowing successions. (Please refer appendix B for legends).

10.4.4 Upper Unit Depositional Environment (UUDE)

This unit is marked by absence of current influences or lack of shallow water sedimentary structures, dominance of mudstone and thin micritic limestone, and rare occurrence of sandstone, and siltstone beds. From petrographic analysis, it has been observed that the content and size of quartz grains decreases, whereas the micritic limestone gets higher nummulite (larger foraminifers) content. Based on these observations, deepening of the basin (depositional environment) is anticipated, as fine grained sediments can be transported a longer distance into the basin than coarser varieties. The intermittent occurrence of sandstone, micritic limestone, and siltstone in carbonate dominated mudstone background might envisage the environment of deposition below storm-wave base, where the fine grained material were settled out from suspension after major storm events. This environment could be an outer ramp, as carbonate mud is a significant part of surficial sediments only along the outer ramp (Dix et al., 2005). Deep water, gently dipping homoclinal platform depositional environment (setting) is also suggested for this unit due to the dominance of micritic limestone and mudstone and absence of interbedded resedimented deposits or slump/slide (Burchette and Wright, 1992). It is also believed that the depositional environment is located far from the site of coarse siliciclastic sedimentation and it might represent the distant ramp and beyond.

10.5 Discussion of depositional environment of the study area

In the studied outcrop, particularly in the middle unit, a systematic variation in depositional environment has been noticed. Entire sedimentary structure investigation of the study area showed the presence of a strong variation in dominant processes. In the northern part (overturned beds), for example, the dominant sedimentary structures recorded are wavy parallel beddings, cross-beds, etc; whereas in the southern part HCS beds that have been intensively bioturbated are dominant. Therefore, in the southern part the dominance of HCS beds suggest that the interpreted carbonate platform had experienced strong wave and storm influences. This might suggest the occurrence of this part of the platform on the updrift side of meteorological forces**.** The shift in sedimentary structures might also give an idea that the existence of a shift in depositional environment from inner- to mid-ramp or shoreface to

offshore-transitional zone, from north to south, respectively. Apart from sedimentary structures, northward shallowing of the basin can be inferred from the observed increase in vertical bioturbation trend in the middle unit in this direction, as shoreface deposits are heavily vertically bioturbated in the shoreface/foreshore environments (Pemberton et al., 1992). However, the shallowing up of the depositional environment, both vertically and laterally (northwards), have not been confirmed by other features like calcrete, or paleosols, or mudcracks. Glauconite presence may mark the slow rate of sediment deposition during deposition of the lower and upper units. The lithologies of the upper unit make it easier to understand the shallowing/coarsening up trend of the middle unit, which can give an indication of progradation of the platform.

Indicators of a shallow, wave agitated environment such as HCS and wave ripples (Dott and Bourgeois, 1982a) occur in the exposures of the middle unit. This might be similar to the fine to very fine grained sandstones interbedded with mud that have been reported from prograding lower shoreface-inner shelf environments of the Niger shelf (Allen, 1964); and on the delta – prodelta shelf of Book Cliffs, Utah (Swift et al., 1987) with their major differences with the studied succession being carbonate dominance of the studied deposits and their differences in response for changes in accommodation space / sea-level (chapter 11).

Based on the fossil content of nummulites it is difficult to determine the actual depth of the depositional environment, as different studies have shown the occurrence of large foraminifers at different depths depending on different factors (section 10.3). But the most likely nature of the depositional environment is its oligotropic nature and the existence of hydrodynamic reworking. These have been shown by the presence of minor varieties of faunas associated with nummulites and the existence of storm beds, respectively.

In some parts of the studied area, vegetation cover made it difficult to see the architecture of the deposits in 3D. Therefore, there is some uncertainity in the interpretation of the depositional environments. In addition, the depositional environment interpretation has been done based solely on sedimentary structures**.** According to Swift et al. (1987) primary sedimentary structures are responses to depositional agents rather than depositional environments, and that the behaviour, not the genesis, of the depositing medium is the critical aspect. The documented wave and current influences may not also reflect the

constructional processes as the plane view morphology of any given deposit reflects dominant surficial processes but not necessarily constructional processes (Geni and Bhattacharya, 2007). These might, therefore, describe the limitations of the depositional environment interpretation.

11. SEQUENCE STRATIGRAPHIC APPROACH

An attemp has been made to apply sequence stratigraphic approaches in the shallow marine deposits. According to Emery and Myers (1996) sequence stratigraphy is a tool to study the architecture of sedimentary successions. Sequence stratigraphy involves the analysis of repetitive genetically related depositional units bounded by unconformities and their correlative conformities (Mitchum et al., 1977, in Van Wagoner et al., 1988). Although the concepts were initially developed for eustacy-driven passive margin settings, the application of sequence stratigraphy to foreland basins has been attempted by various researchers (e.g. Dreyer and Fålt, 1993)**.** However, due to pronounced lateral variations in sedimentary architectures, the regional application of sequence stratigraphic models in structurally segmented foreland basins are difficult (Dreyer et al., 1999).

11.1 Key stratal surfaces

Sequence stratigraphic surfaces which have relevance for sequence stratigraphic interpretation of the studied successions are discussed below.

Flooding surface (FS): According to Van Wagoner et al. (1988) a flooding surface is defined as "a surface that separates younger from older strata, across which there is evidence of an abrupt increase in water depth." The flooding surface is used as the boundary of parasequences (Van Wagoner et al., 1988; 1990; Zecchin, 2007)

Transgressive surface (TS): is a surface that marks the boundary between prograding (regressive) and subsequent retrograding (transgressive) deposits (Posamentier and Vail, 1988). This change occurs when the rate of relative sea-level rise outpaces the sedimentation rate.

Maximum flooding surface (MFS): is a boundary between a transgressive unit, or retrogradational parasequence set, and an overlying regressive unit, or progradational parasequence (Van Wagoner et al., 1988; Embry 1995; Emery and Myres, 1996).

11.2 Carbonate vs siliciclastic sequence stratigraphy

Carbonate deposits and siliciclastic materials show quite astonishing differences in sequence stratigraphic approaches. Their first major difference is observed during lowstand systems. In siliciclastic systems, that is basins fed by terrigenous detritus, large volumes of sediments are transported into basins during lowstands; this is the reverse of what is actually happening in basins where sediments are produced by biogenically active carbonate systems. The other important difference is the stratigraphic and morphological response of basin succession to relative sea-level falls (lowstands). Unlike siliciclastic deposits which experiences physical erosion, carbonate strata will undergo chemical erosion during lowstands (Emery and Myers, 1996). Carbonates and siliciclastic materials also show major difference during transgressive systems tracts; while carbonate deposits aggrade, siliciclastic successions backstep (retrograde) during rapid sea-level rises. Backstepping is less common in organic carbonate systems, except where environmental deterioration occurs.

11.3 Sequence stratigraphic interpretation of the studied succession

It has been attempted to apply the above discussed bounding surfaces into sequence stratigraphic concepts of the study area.

The contact between lower- and middle- units has been well identified only in two sections. These are section 1 and section 7. The top contact of the lower unit in section 7 might mislead with a sequence boundary. Sarg (1988) suggested two major processes that can form a type I sequence boundary in carbonates. These are slope front erosion and seaward movement of regional fresh water meteoric lens. According to him slope front erosion results in substantial loss of platform/bank margin and upper slope material and results in downslope deposition of carbonate megabreccias by mass failure and by traction or density current transport and deposition of carbonate sand. Regional movement of freshwater lens in basinward direction is the second major process which would occur during the formation of a type I sequence boundary. According to Van Wagoner et al. (1988), during basinward shift in facies non marine or very shallow marine rocks, such as braided-stream or estuarine

sandstones above a sequence boundary, may directly overlie deeper marine rocks, such as lower shoreface sandstones or shelf mudstones. In the studied section neither evidence of subaerial exposure nor meggabreccias exist. There are also no braided-stream or estuarine sandstone deposits. In addition, in this part of the study area, the deposits are highly affected by tectonics, and thus they are overturned. Therefore, post- or syn-depositional tectonics might have played a role in creating the sharp contact by thrust movements. This interpretation is **s**upported by the lack of consistency of this sharp boundary at least on the study area scale, i.e., it was only observed on section 7. On the other hand, in section 1, this bounding surface appears to be sedimentologically gradational without any evidence of thrust movements at the boundary surfaces. Therefore, there are no enough evidences that help interprete the lower bounding surface as a sequence boundary. The lower and middle units are thus treated here as one parasequence set.

In the middle unit the coarsening-up successions have an aggradational to progradational pattern. In this unit, MUDA1, the five depositional units having textural and compositional properties revealing upward coarsening and shoaling (see figure 10.6) represent aggradational and basinward progradation of carbonate detritus. The units are bounded by thin mudstone beds representing flooding surfaces. These cyclic units are best exposed along the road section (section 1). The MUDA1 is thus interpreted to have been formed due to a large increase in carbonate production vs rate of creation of accommodation space. The flooding surfaces are thought to have been formed as response to events of rise in relative sea-level and transgression. Hence, the flooding surfaces are interpreted to form bounding surfaces of five parasequences in MUDA1. Across these flooding surfaces, changes in parasequence stacking pattern from landward- to basinward-steeping, which is suggested to be characteristic of 4^{th} order maximum flooding surfaces (MFS) (Dreyer and Fålt, 1993), have not been observed. The observed flooding surfaces, therefore, do not represent MFS's. Acording to Emery and Myres (1996) a maximum flooding surface may lie within an aggradational parasequence stack but passes into a shelfal and basinal condensed section in a distal direction. According to them the condensed section may be represented by a glauconitic horizon, chert band, etc., but these authors pointed out that not all condensed sections are indicative of maximum flooding surfaces. The glauconite and chert fragments observed during petrographic analysis of the thin sections/samples from the study area, however, seem to distribute randomly and therefore they are not good evidences to interpret

the horizons as MFSs. The flooding surfaces of MUDA1 may represent *abrupt* increase in water depth. The deepening events appear *not* to have been accompanied by any minor submarine erosion, which, according to Van Wagoner et al. (1988), may be a characteristic feature of marine flooding surfaces.

The typical motif of upward shallowing parasequences of MUDA1 is characteristic of a regressive cycle. According to Zecchin (2007) the formation of regressive cycles is favoured in middle to outer shelf settings characterized by a low gradient topography and a relatively low sediment supply during transgression phases compared to regressive ones.

In the case the lower boundary, discussed above, had been interpreted as a sequence boundary, the middle unit would have been interpreted as a lowstand prograding wedge, formed during a relatively accelerated rise in relative sea-level. Lowstand prograding wedges, according to Posamentier et al. (1988**),** are characterized by upward increase in parasequence thickness. This is actually not the case in the studied section. On the contary, the section shows a relatively upward thinning of parasequences, which is a characteristic feature of highstand prograding wedges **(**Posamentier et al. 1988). The highstand systems tract is bounded below by transgressive systems tract (TSS) (MFS) and above by a sequence boundary (SB). Highstand successions are formed during decelerating rate of relative sea-level rise that is supposed to result in initial aggradational and subsequent progradational architecture (Emery and Myres, 1996). A lower bounding MFS surface of the middle unit has not been identified. However, there is a possibility that a MFS might be located within the outer-ramp (offshore) deposits of the LU. Such a MFS is likley present below the recorded interval of this study and then within the very fine-grained offshore mudstone facies exposed farther to the west at the Nata River section (cf. Flåt 2008). .

The contact between the middle unit and the upper unit is identified at the base of fine grained siliciclastic sandstone facies. Based on the above discussion, this boundary may represent a candidate sequence boundary (CSB). This boundary might represent a basinward shift in facies from micritic limestone below the surface to siliciclastic sandstone dunes above it. However, no erosional features are associated with this boundary apart from abundant vertical bioturbations (particularly in the underlying micritic limestone). The siliciclastic bed appears to be laterally discontinuous, due most probably to post-depositional erosion. Therefore, in summary, based on the identified and inferred bounding surfaces and

its aggradational to progradational pattern, the middle unit is interpreted to represent a highstand systems tract.

According to Sarg (1988) highstand carbonate systems tracts, characterized by significant differences in micrite content and / or submarine cement at the platform, undergo two fundamentally different depositional histories. These are keep-up and catch-up carbonate systems. A keep-up carbonate systems tract shows a relatively rapid rate of accumulation and is able to keep up with rise in relative sea-level. At the platform margin, it is characterized by small amounts of early submarine cement and is generally dominated by grain-rich, mud-poor parasequences. A catch-up carbonate system, on the other hand, displays a relatively slow rate of accumulation, which may result from the maintenance of water conditions throughout most of the highstand that are not conducive to rapid carbonate production. It is characterized by extensive and early submarine cementation and it may contain abundant mud-rich parasequences. A catch-up system displays keep-up characteristics only during the latest portion of the highstand, when accommodation is reduced because of falling sea-level (Sarg, 1988). The sediments of the study area are rich in mud (micritic) and may fall into the catch-up carbonate systems of Sarg's (1988) subdivision.

Carbonate mud and micritic limestones identified in the upward thinning successions (upper unit) might have been the result of carbonate produced in the shallower part of a platform setting. This mostly occurred during relative highstands when sediment production is greatest compared to the rate of creation of accommodation space (relative sea-level). This phenomenon is commonly termed highstand shedding (Schlager et al., 1994; Emery and Myres, 1996; Wright and Burchette, 1996). According to Schlager et al. (1994), during the time of maximum carbonate production, shallow water carbonate materials will be transported to adjacent basinal environments that may accumulate as calciturbidites or settle out of suspension. Even though this is the case most of the time, Dix et al. (2005) suggested that not all highstand carbonate systems are associated with significant amounts of micritic mud in shallow-water environments, nor do they export large volumes of micrite to the peri-platform carbonate realm. Dix et al. (2005) suggested that some lowstand systems can produce and export significant volumes of carbonate mud that rival highstand systems.

Emery and Myres (1996) also agree with the ability of carbonate platforms to shed during transgression and sea-level falls. Sarg (1988) documented lowstand autochtonous wedges. But other factors being equal, a carbonate platform will shade much more sediments during highstands than lowstands (Emery and Myres, 1996). Emery and Myers (1996) suggested that the main reason for this to happen is that the slow rate of creation of accommodation space could result in the bypassing of over-produced carbonate on top of the platform. The type of platform determines this. In ramps, for example, the area of carbonate production may not be reduced significantly during lowstands; as a result a significant amount of carbonate can be sheded into the basin (Emery and Myres, 1996). As regard the carbonate platform of the study area, being interpreted as a ramp (refer section 10.1), the significance of lowstand shedding can not be ruled out.

The upper bounding surface of the upper unit has not been identified. The carbonate facies shows a thining and deepening upward trend, and attains a retrogradational pattern. Even though the upper bounding surface has not been identified, this unit may represent a transgressive succession, which is identified solely by the upward increase in mudstone thickness and/ or the upward decrease in frequency of micritic limestone, carbonate rich sandstone, and siltstone beds.

11.4 Limitations

The attempts of classifying the observed successions into sequence stratigraphic concepts have certain limitations**.** Except the road section, due to poor outcrop exposure, it was quite difficult to trace the bounding surfaces laterally; therefore, there is a big limitation on the interpretation of the bounding surfaces and thereby thorough application of sequence stratigraphic concepts. Using more detailed litho- and bio-facies analysis, good identification of the interpreted surfaces and their precise positioning needs to be further confirmed on a broader and regional scale. The lowstand prograding wedge and retrogradational pattern (transgressive systems tract) discussed in the middle unit, and inferred for the upper units, respectively, are based on thickness analysis trends (cf. Posamentier et al. 1988) which assume a constant parasequence frequency, which may not be a valid assumption in many cases.

12. CONTROLLING FACTORS

Following the application of sequence stratigraphic concepts on the studied seccessions, the possible controlling factors which were responsible both for the formation of the sequence boundaries and the architecture of the deposits are described below. Most emphasis has been given for the factors that affected the distribution of the benthic foraminifera, i.e. nummulites. In addition, other autogenic factors like the wave reworking and facies zone shifting**,** and allogenic factors like tectonics, eustacy and climate have been considered.

12.1 Autogenic factors/Processes

Autogenic processes refer to those processes which occur within the sedimentary system itself (i.e., intrabasinal) (e.g. Kim, 2006). The mechanisms of production of recorded biotas (mainly nummulites), wave reworking and storm scouring, and facies zone shifting are considered here to represent the autogenic processes/controls.

Most of the factors that might have affected nummulites production and distribution are discussed in section 10.3. However, some of them are more elaborated here.

The deposits of the middle unit are interpreted to have accumulated by *in situ* carbonate production of nummulites with some siliciclastic influences**.** According to Reading & Levell (1996) the most important controls on carbonate sediment production are temperature, salinity and light intensity: these determine the type and abundance of carbonate producing organisms, and whether or not carbonate is likely to be precipitated inorganically. Temperature is also an important factor for large benthic foraminifers as they normally are well developed in well-lit waters (Betzler et al., 1997).

High carbonate production is generally favoured by low/none siliciclastic input, as terrigeneous sediment input can inhibit carbonate production by decreasing light penetration and disrupting suspension feeding organisms (Hallock, 2001). Reid et al. (2007) also argued that the principal control for carbonate production is silciclastic sediment input; it has to be minimal for carbonate to accumulate. Being mixed siliciclastic carbonate deposits, the

carbonate rich sediments of the study area indicate the existence of terrigeneous siliciclastic sediment input which would have influenced carbonate producing organisms (nummulites). However, compared with the rate of carbonate production, the siliciclastic sediment input must have been minimal; that allowed the carbonate producing organisms to dominate the environment. According to Dreyer et al. (1999) during some intervals of the Ainsa Basin development clastic sediment supply was significantly reduced and allowed large-scale colonization of the shallow parts of the basin by carbonate-producing organisms.

The other important factor which influences carbonate production is nutrient content; it must be minimal **(**Reid et al., 2007)**.** Nummulites normally preferred nutrient deficit, oligotrophic environment (refer section 10.3). However, the presence of glauconite in the studied sections may envisage the presence of a relatively high content of nutrients, particularly in the form of iron. According to Odin and Matter (1981) glauconites are typically formed in "semi-confined micro-environments" irrespective of surrounding sea water. Therefore, their presence in the studied section may not necessarily indicate the presence of high iron and /or nutrients in the depositional environment. The nutrient deficit nature of the water can also be shown by the absence of abundant micro- and macro-faunas associated with nummulites, which otherwise would occur in nutrient rich waters (Hallock and Schlager, 1986). According to Hallock & Schlager (1986), for example, the presence of high input of nutrients, such as nitrates and phosphates, would stimulate the growth of planktons that would have reduced the water transparency. These would have limited the depth ranges of zooxanthellate corals and calcareous algaes and thereby reducing carbonate production.

Oceanographic controls such as wave reworking and storm scouring represent the other type of autogenic processes/controls which are expected to have had played a siginificant role. These autogenic control mechanisms were responsible for the fragmentation of the nummulite tests in the course of transportation from the shallower to the deeper part of the basin. The lateral discontinuity of most of the beds in the middle unit may indicate that the deposition was controlled by autogenic processes. According to Mack and James (1986) symmetrical cycles, particularly involving only two facies, could be originated from autogenic shifting of facies zones. They also pointed out that if the vertical change involved three or more facies, such as fossiliferous limestone – olive-grey shale – ripple laminated sandstone, or the asymmetric cycle, autogenic mechanisms are less likely, as the facies change may imply significant changes in sea level elevation and water depth.

Based on the above discussion, autogenic origin of the flooding surfaces (FS) recorded in the middle unit of the road section (section 1) seems acceptable as it involves two facies (mudstones and carbonate rich sandstones). But as we will see later in this chapter, these flooding surfaces can also be explained interms of allogenic processes mainly by tectonics and related sea-level flactuations.

12.2 Allogenic controls

Allogenic processes are external sedimentary processes (extrabasinal) (e.g. Kim, 2006). Among the allogenic mechanisms that can produce rhythmitic or cyclic sedimentation are tectonic uplift or basin subsidence, eustatic sea-level changes, and climatic flactuations (Mack and James, 1986). The fact that the Ainsa Basin is a foreland basin, the existence of allogenic variables, mainly tectonics, is inevitable. Puigdefabregas and Souquet (1986) suggested that the Southern Pyrenean Foreland Basin sedimentation was characterized by pronounced tectonic influence. Dreyer and Fålt (1993) on their studies of the Lower Eocene shallow marine Ametlla Formation, Spanish Pyrenees, suggested that a combination of episodic thrusting and high-frequency eustatic sea-level changes acted as controlling mechanisms and these factors might have caused frequent and irregularly spaced perturbations of the relative sea-level curve.

The flooding surfaces might reflect sea-level flactuations that were caused by alternating episodes of thrust-related deformation and relative tectonic quiescence, as discussed by Dreyer et al. (1999) for different deposits in the Ainsa Basin. The flooding surfaces might also be related to episodes of thrusting which resulted in subsidence that created the observed flooding surfaces (parasequence boundaries) and accommodation space for parasequence aggradation (Pickering and Corregidor, 2005). Carbonate production then exceeded the accommodation space created and caused progradation of the platform after every flooding event.

The development of Mediano Anticline during Lutetian (Pickering and Corregidor, 2005) and the Montsec Thrust, though it was not expressed on the surface during the Eocene (Nijman, 1998), were though to have had a significant influences. In addition, syn-sedimentary tectonism might have influenced the formation of the depositional architecture

and sequence boundaries, as there had been repeated episodes of thrusting during Middle to Late Eocene time all along the South Pyrenean Foreland Basin (Munoz et al., 1994).

Another allogenic variable which could have played a major role would be eustacy. A rise or fall in sea-level could have resulted landward or basinward shift in the shoreline (Emery and Myres, 1996). But as the shift in facies only involves two facies, using Mack's and James (1986) hypothesis discussed above, this is also a less likely mechanism to create the observed alternation in the middle unit. The global sea-level curve of Haq et al. (1987) shows five major to moderate sea-level falls between 53.3 and 47.2 Ma. One of these falls might have caused the erosion of the studied succession and deposition into the Ainsa Turbidite Complex.

Climate controls the factors that influence the rate of carbonate production and distribution such as water temperature, salinity and the wave energy of the environment (Wright and Burchette, 1996). Apart from the climate during Eocene in the Ainsa Basin was generally tropical and seasonal subtropical, not much is known about climatic variations that might have occurred during deposition of the studied units. Even though it is implicite that carbonate production is strongly influenced by climatic variation; refrain is preferred not to discuss/comment any further about the influence of this mechanism on the studied deposits. In general, in each of the parasequences identified in the middle unit, the increasing up trend of carbonate rich sandstone content was thought to have been controlled by a decrease in A/S-ratio.

Major sea-level rise must have occurred during the deposition of the upper unit that might have forced the shoreline to move landwards. This unit also involves three or more facies and it can best be described by allogenic variables, like eustacy and tectonics. Good lateral treceability of the micritic limestone (facies F) in the upper unit may also depict an allogenic nature of the controlling factor, as autogenically controlled deposits generally show poor traceability (Sami and Jack, 1994). In addition, the small value of sandstone-to-mud ratio suggests a large increase in the A/S-ratio. Although it seems clear that there was a rise in sea-level, caution must be excercised when interpreting which allogenic factor was more influential than the others.

12.3 Limitations

The study area represents the small part of the larger and structurally complex Ainsa Basin, which makes it difficult to pin point the dominant and critical tectonic events relevant to the studied section. Determining the actual controlling factor for the recorded flooding surfaces in the middle unit is very difficult as, independent of changes in the outside variables (mainly by low magnitude tectonics), this type of cycle could have also been resulted from lateral shifting of facies zones, i.e. autogenic (e.g. lobe-shifting) processes (Beerbower, 1964; in Mack and James, 1986). Determining which of these two factors exerted a dominant influence on the observed architecture is, therefore, difficult. According to Bridge (2003) it is commonly not possible to make a strict distinction between allo- or auto-genic influenced phenomena, because complicated interactions among these controls exist. Determination of a single dominant controlling factor for the studied sections is further hampered by some poor outcrop exposures, as most part of the outcrop is covered by vegetation and / or highly eroded, and therefore there was no good control in 3D.

13. RESERVOIR POTENTIAL

13.1 Nummulite accumulations as reservoirs

Nummulite accumulations have been recorded in different parts of the world along the Tethyan region, and many of them show evidences of significant physical reworking (Racey, 2001). To have better understanding of the reservoir potential of nummulite accumulations, some selected fields, based on the papers of Racey (2001) and references therein, are discussed below.

From central Tunisia to the Gulf of Gabes, the southern Tethys margin is covered by nummulite platform of Early Eocene age (Bishop, 1988, in Jorry et al., 2003) that generates significant amounts of sediments that are dominated by nummulites and silt-grade nummulithoclastic debris (Jorry et al., 2003). Nummulitic limestones have been documented to be good reservoirs. In Tunisia and Libya, for example, significant oil production comes from nummulite limestone reservoirs (Racey, 2001).

Even though the nummulite deposits in Oman are generally affected by diagenesis, the deposits have a porosity and permeability values that range between 0.7-14 % and 0.95 md, respectively (Racey, 2001). Along the north coast of Tunisia, on the other hand, there are shallow marine and lagoonal carbonates of Early Eocene age that contain nummulitic limestones (Racey, 2001). According to MacCaulay et al. (2001) (in Racey, 2001) Eocene nummulitic limestones in Hasdrubal field (Tunisia) has an average porosity and permeability of 10.5% and 0.5 md, respectively. In this limestone, almost all the nummulites are transported (i.e allochtonous), which is quite similar to the nummulites recorded in the upper unit of the study area. In Ashtart field, on the other hand, in the nummulitic packstones with subordinate wackstone and grainstone deposits, the primary intergranular porosity is significantly occluded by calcite cements (Hmidi and Sadras, 1991, in Racey, 2001). In this deposit the authors recorded a high interparticle porosity (on average 15%) but low permeability (average 6 md) within the nummulite tests. The authors also pointed out that in younger sequence accumulations (i.e. Middle-Late Eocene) than the above discussed nummulite accumulations, the deposits are found to be good reservoirs for gas condensates and oil (Hmidi and Sadras, 1991, in Racey, 2001). In Libya, the nummulite banks, which are

time equivalents of the nummulites discussed above in Tunisia, have an average porosity of 16% (El Ghoul, 1991, in Racey, 2001). In addition, nummulitic accumulations have been documented in Egypt, Italy, and in former Yugoslavia though not much is known about their reservoir potential (Racey, 2001).

13.2 Reservoir potential evaluation of the studied succcession

In considering the reservoir potential of the study area, the total stratigraphic column can be divided into the three units, based on the units which have been discussed in previous chapters. These are the lower unit; the upward coarsening and shoaling part (i.e. the middle unit), and the upward fining part that is incorporated into the upper unit.

The architectural elements of the lower unit are entirely dominated by massive mudstone, or massive mudstone that shows a slight increase in silt content upwards (section 8.1.1). No sand grains were documented in this unit, and therefore, the deposit attains relatively a homogeneous characteristic. Even though these fine grain deposits are expected to have had a good porosity during deposition, it is believed to have been lost during burial, mainly due to compaction. In addition, since the depostis are very fine grained (i.e. silt and clay), even if it can still have a certain porosity, the permeability is expected to be very low (i.e., it can act as ‘aquiclude’), as the pores would be too small to allow possible fluids to pass through them. Therefore, mudstone dominated deposits with some siltstone beds of the lower unit generally lack any reservoir potential, particularly for oil.

The upward coarsening successions of the middle unit contain interbeds of mudstone and carbonate rich sandstone which has variable stacking pattern, sand : gross ratio, etc. The grain size of the deposits varies from very fine to fine, with thin interbedded mudstone beds that separate the carbonate rich sandstone beds, which gives for the deposits a poor vertical connectedness. This could also create possible flow discontinuities among the different beds. The carbonate rich sandstone beds are also observed, in most cases, to pinch out laterally. This could also limit the lateral interconnection. Only in some sections, the beds appear to be amalgamated.

These upward coarsening and thickening successions of the middle unit also show variable sand : gross ratio across the study area (section 8.1.2). In the northern part of the study area, for example, the sand: gross ratio calculated is up to 71 %, whereas in the southern part it is 60-70%. These calculated values seem to be high (good values) and may seem to give high reservoir potential for the deposits, but keeping in mind the lack of connectedness in both lateral and vertical directions and their very fine grain size, the deposits alltogether are expected to have poor reservoir quality. The few beds that show moderate lateral continuity in this unit are also separated by thin mudstone beds. These beds could possibly create permeability barriers that would form a pronounced reservoir heterogeneity in the reservoir. The relatively coarsening upward trend and the increase in nummulite content in the upward direction of the middle unit may depict a relative improvement of the reservoir potential. Had there been a matured source rock below, the bouyancy forces could have caused the petroleum to migrate upwards with high efficiency without much secondary migration losses in such coarsening upward sandstones (Karlsen, 2007). However, during petrographic analysis it has been observed that the studied thin-sections were matrix dominated and possible porosities were not identified.

Facies of the upper unit, which attains retrogradational pattern, shows a very heterogeneous reservoir characteristic. As discussed in previous chapters, this unit is dominated by carbonate rich mudstone and micritic limestone, with some interbedded carbonate rich sandstone and siltstone beds, and significant nummulite content. The N/G ratio is very low (<5%). However, the existence of nummulites, based on the discussion on section 13.1, could boost up the reservoir potential. The nummulites identified in this part of the section are mostly fragmented, whereas the intact ones are filled with fine grained matrix materials, and minerals like feldspar, quartz, and calcite, which would have reduced the reservoir potential expected from the volume of nummulites alone. In comparing different units of the study area, unlike the lower and upper units, the middle unit deposits are expected to have a better reservoir potential.

Generally, from sedimentological (mainly from grain size) point of view, the mixed siliciclastic-carbonate deposits of the study area are interpreted to have poor reservoir potential. Very fine- to fine- grain size of the deposits, lack of good connectedness, filling of the nummulite tests by other minerals, could result in low reservoir potential. In addition, the initial porosity is expected to have been lost due to compaction and diagenetic effects (burial

cementation). On this study, the general influence of the biostratigraphy (mainly nummulites) on the porosity distribution is not known for sure but other studies in different parts of the Tethyan region (section 13.1) show that nummulite accumulations can form good reservoirs, both for oil and gas. In addition, in the overall evaluation of the reservoir potential of the study area, the effect of diagenesis, which could have further adversely affected the porosity and thus the reservoir potential of the deposits, have not been considered.

13.3 Analogue studies

Analogue studies have been used to understand facies types and their relationships, which is a key tool for better understanding of the subsurface reservoirs. From section 13.1 it has seen that nummulite accumulations can form potential reservoir rocks. Similar to the above discussed nummulite accumulations; the carbonate platform of the study area has a significant amount of nummulite accumulations, though the types of nummulite species have not been identified (note that till now a general name 'nummulite' has been used). The deposits also show significant physical reworking. Thus, to some extent, this study can be used as analogue study for other nummulitic limestones, or nummulite accumulations. But the study may not be presented as a good analogue to the above discussed fields due to the limited scale of the area which has been covered by this study, and the sealing potential of the interbedded mudstones are not known very well. In addition, the dominant fine grained matrix material of the study area could enter into the test via the surface pores of nummulites that could reduce the interparticle porosity significantly.

13.4 Shale as Gas reservoirs

Contrary to the conventional sandstone, conglomerate, or carbonate reservoirs, shale (mudstones) can be potential reservoirs for gas (e.g., Newark East field of Texas where gas is produced from Barnett Shale; Martineau, 2007). According to Martineau (2007) the Newark East field produced approximately 2.0 bcf / day (i.e., 2 billion cubic feet/day) in 2006. In considering the reservoir potential of the studied successions, with reference to the Newark East field, there is a possibility that the matrix dominated deposits can act as gas reservoir.

14. CONCLUSIONS

1) The shallow marine successions of the study area represent mixed siliciclastic-carbonate deposits that have an architectural pattern of shallowing upward, followed by a deepening upward pattern. The deposits have been accumulated on a carbonate platform. The carbonate platform has been interpreted as located within a land-attached ramp.

2) Nine facies, which have been grouped into four facies associations, have been identified. These facies have been classified based on their composition and dominant sedimentary structures which have been very helpful in interpretation of the depositional environment.

3) Petrographic analysis showed that most of the quartz grains were derived from igneous sources with minor amounts of metamorphic influences. The most likely igneous sources for the dominant quartz grains are the granites/granodiorites that cropped out in the axial zone of the Pyrenees. The carbonates originated mostly by *in situ* carbonate producing organisms, mainly by nummulites.

5) The depositional environment shows a systematic variation from relative shallow to deep parts of a paltform setting, towards the northern and the southern parts of the studied area, respectively. The presence of storm layers in the studied successions allowed estimation about palaeobathymetric depths of the depositional environments. The lower unit represents outer-ramp/ mostly basinal environments and shows no influences of oceanic currents; the middle unit sediments are mid- to inner-ramp environments which have been interpreted as deposited above the storm wave base but below the sea-level; and the upper unit represents an outer-ramp, i.e., below storm wave-base depositional environment. In addition, the signatures of oceanic currents on the deposits give an idea that they played a major role on reworking the sediments at shallower water level. Oceanically formed currents were also the main mechanisms that caused possible transportation of littoral and shallow marine deposits to a relatively deeper part.

6) In the overall coarsening and shallowing upward parasequence sets in the middle unit, minor flooding surfaces have been identified. In addition, a candidate sequence boundary at the top part of the middle unit has been proposed. These surfaces have been used to put the

studied successions into sequence stratigraphic concepts with the interpreted highstand systems tracts for the combined lower and middle units and transgressive systems tracts for the upper unit.

7) Both autogenic- and allogenic- controls are interpreted to have played a major role in controlling the *in situ* carbonate production and the observed architectural style and the sequence bounding surfaces. Variation in stratal architecture could be related to changing A/S ratio, which in turn could be related to base level flactuations.

8) Even though high sand : mud ratio have been recorded in the middle unit, the reservoir potential of the deposits generally seem to be poor as the most sand-rich units have poor connectedness, very fine grain size, and the interparticle porosity filled by other materials. These features are interpreted to give rise to poor connectivity between pore voids, and therefore, low permeability. These properties give alltogether poor reservoir characteristics for the deposits of the study area. In addition, mudstone beds may act as a barrier for fluid flow. These types of carbonate ramp deposits are likely to form low-permeability reservoir that might be more suited for gas production than oil production. The upper unit is very heterogeneous, and has not got any reservoir architecture/potential. This unit represents a higher A/S ratio conditions. On the contrary, the lower unit is relatively a homogeneous unit (mudstones with minor siltstones) which could also show a higher A/S ratio conditions.

15. REFERENCES

Adams, A. E., Mackenzie, W. S. and Guilford, C. (1984) *Atlas of sedimentary rocks under the microscope*. United States of America, Halsted Press, 104 pp.

Adegoke, O. S. and Stanley, D. J. (1972) Mica and shell as indicators or energy level depositional regime on the Nigerian Shelf. *Marine Geology*, **13**, M61.

Aigner, T. (1985) Biofabrics as dynamic indicators in nummulite accumulations. *Journal of Sedimenary Petrology*, **55**, 131-134.

Ako, O. G. (2008) *Structural development of the Ypressian-Lutetian sequences of the northeast central Ainsa Basin, Pyrenees.* Thesis (Master). Petroleum Geology and Geophysics, Department of Geosciences, University of Oslo

Allen, J. R. L. (1964) The Nigerian continental margin: bottom sediments, submarine morphology and geological evolution. *Marine Geology*, **1**, 289-232.

Allen, J. R. L. (1983) Studies in fluviatile sedimentation: bars, bar complexes annd sandstone sheets (low sinuosity braided streams) in the Brownstones (L. Devonian), Welsh Borders. *Sedimentary Geology*, **33**, 237-293.

Allen, P. A. and Leather, J. (2006) Post-Marinoan marine siliciclastic sedimentation: The Masirah Bay Formation, Neoproterozoic Huqf Supergroup of Oman. *Precambrian Research*, **144**, 167-198.

Anastasio, D. J. (1992) Structural evolution of the external sierra, Spanish Pyrenees. In: Mitra, S. and Fisher, G. W., (Eds) *The Structural Geology of Fold and Thrust Belts.* Johns Hopkins University press, 239 – 251.

Arbues, P., Corregidor, J. and Puigdefabregas, C. (1999) Anatomy and evolution of the tectonically – controlled Ainsa Slope System (Eocene, South – Pyrenean Foreland Basin, NE Spain). AAPG annual meeting, San Antonio, Texas.

Arbues, P., Munoz, J. A., Poblet, J., Puigdefabregas, C. and McClay, K. (1998) Significance of submarine truncation surfaces in the sedimentary infill of the Ainsa basin (Eocene of south-central Pyrenees, Spain) (abs.). *Abstracts of the 15th International Sedimentological Congress, Alacante, Spain*. Publicaciones de la Universidad de Alicante, 145-146.

Bassi, D., Hottinger, L. and Nebelsick, J. H. (2007) Larger foraminifera from the Upper Oligocene of the Venetian area, north-east Italy. *Palaeontology*, **50**, 845-868.

Bensing, J. P., James, N. P. and Beauchamp, B. (2008) Carbonate deposition during a Time of Mid-Latitude Ocean Cooling: early Permian Subtropical Sedimentation in the Sverdrup Basin, Arctic Canada. *Journal of Sedmentary Research*, **78**, 2-15.

Bentham, P., Burbank, D. W. and Puigdefabregas, C. (1992) Temporal and Spatial controls on the alluvial architecture of an axial drainage system: late Eocene Escanilla Formation, southern Pyrenean foreland basin, Spain. *Basin Research*, **4**, 335-352.

Betzler, C., Brachert, T.C. and Nebelsick, J. (1997) The warm temperature carbonate province: a review of the facies, zonations, and delineations. *Courier Forschungsinsitut Senckenberg*, **201**, 83-99.

Billmann, H., Hottinger, L. and Oesterle, H. (1980) Neogene to Recent rotaliid foraminifera from the Pacific Ocean; their canal system, their classification and their stratigraphic use. *Mém. Suisses Paléontol.*, **101**, 71–113.

Bjørlykke, K. (1989) *Sedimentary and Petrology Geology.* Berlin, Springer-Verlag, 363 pp.

Bjørlykke, K. (2007) *GEO 4250: Reservoir Geology, lecture notes*. Available at: blyant.uio.no. (Accessed: 20.04.08)

Bourgeois, J. (1980) A Transgressive Shelf Sequence exhibiting Stratification: the Cape Sebastian Sandstone (Upper cretaceous), Southwestern Oregon. *Journal of Sedmentary Research*, **50**, 681-702.

Bourgeois, J. and Leithold, E. L. (1984) Wave-worked conglomerates – depositional processes and criteria for recognition. In: Koster, E.H. and Steel, R.J. (Eds.) *Sedimentology of Gravels and Conglomerates. Mem. Can. Soc. Petrol. Geol.*, **10**, 331-343.

Brenchley, P. J. (1985) Storm influenced sandstone beds. *Modern Geology*, **9**, 369-396.

Brenchley, P. J., Pickerill, R. K. and Stromberg, S. G. (1993) The role of wave reworking on the architecture of storm sandstone facies, Bell Island Group (Lower Ordovician), eastern Newfoundland. *Sedimentology*, **40**, 359–382.

Bridge, J. S. (2003) *Rivers and Floodplains: Forms, Processes, and Sedimentary Record.* Oxford, U.K., Blackwell Science, 504 pp.

Burchette, T. P. and Wright, V. P. (1992) Carbonate ramp depositional systems. *Sedimentary Geology*, **79**, 3-57.

Camara, P. and Klimowitz, J. (1985) Interpretation geodinamica de la vertiente centro – occidental Surpirenaica (Cuenca de Jaca – Tremp). *Estudios Geologicos*, **41**, 391 – 404.

Chang, S. S., Shau, Y. H., Wang, M. K., Ku, C. T. and Chiang, P. N. (2007) Mineralogy and occurrence of glauconite in central Taiwan. *Applied Clay Science*, Articles in Press.

Chaudhuri, A. K. and Howard, J.D. (1985) Ramgundam Sandstone. A middle Proterozoic shoal-bar sequence. *Journal of Sedimentary Petrology*, ***55***, 392–397

Choukroune, P. (1969). Sur la presence, le style et l'hge des tectoniques superposees dans la Cretace nord pyrenean de la region de Lourdes (HautesPyrenees). *Bull. Bur. Rech. gdoL rain. Ft.* 2nd ser. **2**, 11-20.

Choukroune, P. and Seguret, M. (1973) Tectonics of the Pyrenees: role of compression and gravity. In: DeJong, K. A., and Scholten, R., (Eds.) *Gravity and Tectonics.* New York, John Wiley, 141 – 156.

Choukroune, P., Le Pichion, X., Seguret, M. and Sibuet, J. C (1973a) Bay of Biscay and Pyrenees. *Earth and Planetary Science Letter*, **18**, 109-118.

Choukroune, P., Seguret, M. and Galdeano, A. (1973b) Caracteristique et evolution structural des Pyrenees. *Bull. Soc. Geol. Fr.*, **7**, 601 – 611.

Collinson, J. D. (1969). The sedimentology of Grindslow Shales and the Kinderscout Grit: a deltaic complex in the Namurian of northern England. *Journal of Sedimentary Petrology*, **39**, 194-221.

Collinson, J. D. and Thompson, D. B. (1982) *Sedimentary Structures*. Great Britain, George Allen & Unwin Ltd, 194 pp.

Colquhoun, G. P. (1995) Siliciclastic sedimentation on a storm- and tide- influenced shelf and shoreline: the Early Devonian Roxburgh Formation, NE Lachlan Fold Belt, southeastern Australia. *Sedimentary Geology*, **97**, 69-98.

Coney, J. A., Munoz, J.A., McClay, K. R. and Evenchick, C. A. (1996) Syntectonic burial and post–tectonic exhumation of an active foreland thrust belt, southern Pyrenees, Spain. *Journal of the Geological Society, London,* **153**, 9-16.

Dabbagh, M. E. and Roggers, J. J. W. (1983) Depositional environments and tectonic significance of the Wajid Sandstone of southern Soudi Arabia. *Journal of African Earth Sciences*, **1**, 47-57.

Deramond, J., Graham, R. H., Hossack, J. R., Baby, P. and Crouzet, G. (1985) Nouveau modele de la chaine des Pyrenees. *Competes Rendes de l'Acadamie des Sciences*, *Paris*, **301**, 1212 – 1216.

Diegel, F. A. (1988) The Rome Formation decollement in the Mountain City window, Tennessee; a case for involvement of evaporites in the genesis of Max Meadows – type breccias. In: Mitra, G. and Wojtal, S. (Eds) *Geometries and mechanisms of Thrusting with Special Reference to the Applachians. Geological Society of America, special paper*, **222**, 137 – 164.

Dix, G. R., James, N. P., Kyser, T. K., Bone, Y. and Collins, L. B. (2005) Genesis and Dispersal of Carbonate Mud Relative to Late Quaternary Sea-Level Change Along a Distally – Steepened Carbonate Ramp (Northwestern Shelf, Western Australia). *Journal of Sedimentary Research,* **75**, 665-678.

Dott, R. H. and Bourgeois, J. (1982a) Hummocky stratification: significance of its variable bedding sequences, *Geological Society of America Bulletin,* **93**, 663–680.

Dott, R. H. and Bourgeois, J. (1982b) Cross-stratification, tropical hurricanes, and intense winter storms. *Sedimentology,* **32**, 167-194.

Dreyer, T. and Fålt, L. M. (1993) Facies analysis and high-resolution sequence stratigraphy of the Lower Eocene shallow marine Ametlla Formation, Spanish Pyrenees. *Sedimentology*, **40**, 667-697.

Dreyer, T., Corregidor, J., Arbues, P. and Puigdefabregas, C. (1999) Architecture of tectonically influenced Sobrarbe deltaic complex in the Ainsa Basin, northern Spain. *Sedimentary Geology*, **127**, 127-169.

Duke, W. L. (1985) Hummocky cross-stratification, tropical hurricanes, and intense winter storms. *Sedimentology*, **32**, 167- 194.

Duke, W. L. (1990) Geostrophic circulation or shallow marine turbidity currents? The dilemma of paleoflow patterns in storm influenced prograding shoreline systems. *Journal of sedimentary Petrology*, **60**, 870-883.

Duke, W. L. and Leckied, A. (1984) Origin of hummocky cross-stratification. Part 2. Paleohydraulic analysis indicates formation by orbital ripples within the wave-formed flat-bed field (abs.). *Can. Soc. Petrol. Geol., Shelf. Sands and Sandstones Symp.* Program and Abstracts, 32 pp.

Duke, W. L., Arnott, R. W. C. and Cheel, R. J. (1991) Shelf sandstones and cross-stratification: new insights on a stormy debate. *Geology*, **19**, 625-628.

ECORS Pyrenees Team (1988) Deep Refraction Seismic Survey across an entire orogenic belt, the ECORS Pyrenees profile. *Nature*, **31**, 508 – 511.

Ekdale, A. A., Bromley, R. G. and Pemberton S. G. (1984) Ichnology- the use of trace fossils in sedimentology and stratigraphy. *SEPM Short Course*, **15**, 317 pp.

Embry, A. F. (1995). Sequence boundaries and sequence hierarchies: problems and proposals. In: Steel, R.J., Felt, V.L., Johannessen, E.P. and Mathieu, C. (Eds.) *Sequence Stratigraphy on the Northwest European Margin. Norwegian Petroleum Society (NPF), Special Publication*, **5**, 1-11.

Emery, D. and Myers, K. J. (1996) *Sequence Stratigraphy*. Oxford, Blackwell, 297 pp.

Falivene, O., Arbues, P., Howell, J., Munoz, J. A., Fernandez, O. and Marzo, M. (2006) Hierarchical geocellular facies modelling of a turbidite reservoir analogue from the Eocene of the Ainsa basin, NE Spain. *Marine and Petroleum Geology*, **23**, 679-701.

Fanning, D. S., Keramidas, V. Z. and El-Desoky, M. A., (1989) Micas. In: Dixon, J.B. and Weed, S.B. (Eds.) *Minerals in Soil Environments* (2nd edn.). Soil Science Society of America, Madison, 634 pp.

Fernandez, O., Munoz, J. A., Arbues, P. and Falivene, O. (2005) 3D reconstruction of oblique fault and fold system and related growth strata: Ainsa Basin, Spanish Pyrenees. *AAPG Bull*., Digital, **89.**

Fernandez, O., Munoz, J. A., Arbues, P., Falivene, O. and Marzo, M. (2004) Three-dimensional reconstruction of geological surfaces: An example of growth strata and turbidite systems from the Ainsa basin (Pyrenees, Spain). *AAPG Bull*., **88**, 1049-1068.

Fitzgerald, P. G., Munoz, J. A. and Baldwin, S. L. (1999) Asymmetric exhumation across the Pyrenean Orogen; implications for the tectonic evolution of a collision orogen. *Earth and Planetary Science Letters*, **173**, 157-170.

Flåt, R. (2008) *Development and sedimentology of Lower Eocene deep-marine gravity flow deposits in the eastern part of the Ainsa Basin, Pyrenees, Spain***.** Thesis (Master). Petroleum Geology and Geophysics, Department of Geosciences, University of Oslo.

Flint, S. and David, H. (2007) Sequence Stratigraphic Organinsation of Architectural elements. *AAPG Bull*., Digital, **91**.

Folk, R. L. (1959) Practical Petrographic Classification of Limestones. *AAPG Bull.,* **43**, 1-38.

Gani, M. R. and Bhattacharya, J. P. (2007) Basic Building Blocks and Process Variability of a Cretaceous Delta: Internal Facies Architecture Reveals a More Dynamic Interaction of River, Wave, and Tide Processes Than Is Indicated by External Shape. *Journal of Sedimentary Research*, **77**, 284-302

Garrido-Megios, A. (1973) *Estudio geologicio y relacion enter tectonica y sedimentacion del secundario y Tarciario de la vertiente meridional pirenaica en su zona central (provincias de Husca y Lerida).* Thesis (PhD). Universidad de Granada, Granada, 395 pp.

Gibbons, W. and Morena, T. (Eds.) (2002) *The Geology of Spain*. Geological Society, London.

Google Earth ™ (2008). (Accessed: 20.05.2008)

Grelaud, S., Malo, M., Verges, J. and Taberner, C. (2003) Structure of the Bóixols - Sant Corneli anticline (SE Pyrenees): Fractures and Fluid Flow. *AAPG Bull.*, **87**, No. 13 (Supplement).

Gressly, A. (1883) Observations geologiques sure le Jura Soleurois. *Neue Denkschr. Allg. Schweiz, Ges. ges. Naturw.*, **2**, 1-112.

Grimaud, S., Boillot, G., Collette, B. J., Maufferet, A., Miles, P. R. and Roberts, D. G. (1982) Western extension of the Iberian – European plate boundary during the early Cenozoic (Pyrenean) convergence: a new model. *Marine Geology*, **45**, 63 – 77.

Hallock, P. (1981a) Algal symbiosis: a mathematical analysis. *Marine Biology*, **62**, 249–255.

Hallock, P. (1981b) Production of carbonate sediments by selected large benthic foraminifera on two pacific coral reefs. *Journal of Sedimentary Petrology*, **51**, 467-474.

Hallock, P. (1985) Why are larger Foraminifera large?. *Paleobiology*, **11**, 195–208.

Hallock, P. (2001) Coral reefs, carbonate sediments, nutrients, and global change. In: Stanley, G.D.Jr. (Ed.) *The history and Sedimentology of Ancient Reef Systems*. New York, Kluwer Academic/Plenum, 387-427.

Hallock, P. and Schlager, W. (1986) Nutrient excess and the demise of coral reefs and carbonate platforms. *Palaios*, **1**, 389–398.

Haq, B. U., Hardenbol, J. and Vail, P. R. (1987) Chronology of flactuating sea levels since the Triassic. *Science*, **235**, 1156-1167.

Harder, H. (1980) Synthesis of glauconite at surface temperatures. *Clays and Clay Minerals*, **28**, 217–222.

Haseldonckx, P. (1972) The presence of Nypa palms in Europe: a solved problem. *Geologie en Mijnbouw*, **51**, 645-650.

Hassouta, L., Buatier, M. D., Potdevin, J. L. and Liewig, N. (1999) Clay diagenesis in the sandstone reservoir of the Ellon Field (Alwyn, North Sea). *Clays and Clay Minerals*, **47**, 269-285.

Hohenegger, J., Yordanova, E., Nakano, Y. and Tatzreiter, F. (1999) Habitats of larger foraminifera on the upper reef slope of Sesoko Island, Okinawa, Japan. *Marine Micropaleontology*, **26**, 109-168.

Holl, J. E. and Anastasio, D. J. (1993) Paleomagnetically derived folding rates, Southern Pyrenees, Spain. *Geology*, **13**, 271-274.

Holl, J. E. and Anastasio, D. J. (1995) Cleavage development within a foreland fold and thrust belt, Southern Pyrenees, Spain. *Journal of Structural Geology*, **17**, 357-369.

Hottinger, L. (1988) Significance of diversity in shallow benthic foraminifera. Atti del Quarto Simposio di Ecologia e Peleoecologia delle Comunità Bentoniche, Museo Regionale di Scienze Naturali, Torino, 35–51.

Howard, J. D. and Reineck, H. E. (1981) Depositional Facies of High-Energy Beach-to-Offshore Sequence: Comparison with Low-Energy Sequences. *AAPG Bull.*, **65**, 807-830.

Jackson, R. G. II, (1975) Hierarchical attributes and a unifying model of bed forms composed of cohesionless material and produced by shearing flow. *Geological Society of America Bull.*, **86**, 1523-1233.

Johnson, H. D. and Baldwin, C. T. (1996) Shallow Clastic Seas. In: Reading, H.G. (Ed.) *Sedimentary Environments: Processes, Facies and Stratigraphy* (3rd edn.). Oxford, Blackwell, 232-280.

Jones, B. and Desrochers, A. (1992) Shallow Platform Carbonates. In: Walker, R.G. and James, N.P. (Eds.) *Facies Models: Response to Sealevel change*. Geological Association of Canada, St. John's, Newfoundland, 277-301.

Jorry, S., Davaud, E. and Caline, B. (2003) Controls on the distribution of nummulite facies: a case study from the Late Ypressian El Garia formation (Kersa Plateau, Central Tunisia). *Journal of Petroleum Geology*, **26**, 283-306.

Karlsen, D. A. (2007) *Geo4211: Petroleum System analysis, lecture notes.* University of Oslo.

Kastner, M. and Siever, R. (1979) Low temperature feldspars in sedimentary rocks. *American Journal of Science*, **279**, 435-479.

Kim, W. (2006) Shoreline response to autogenic processes of sediment storage and release in the fluvial system. *Journal of Geophysical Research*, **111**, F04013.

Lee, M. R. and Parsons, I. (1997) Dislocation formation and albitization in alkali feldspars from the Shap granite. *American Mineralogist*, **82**, 557–570.

Luterbacher, H. (1984) Paleoecology of foraminifera in the Paleogene of the southern Pyrenees. *Benthos'83, 2nd Int. Symp. Benthic Foraminifera, Pau, France*, 389-392.

Mack, G. H. and James, W. C. (1986) Cyclic sedimentation in mixed siliciclastic-carbonate Abo-Hueco transitional zone (Lower Permean), southwestern New Mexico. *Journal of Sedmentary Petrology*, **56**, 635-647.

Martineau, D. F. (2007) History of the Newark East field and the Barnett Shale as gas reservoirs. *AAPG Bull.*, **91**, 399-403.

McBride, E. F. (1986) Diagenesis of the Mexon Sandstone (Early Cretaceous) Marathon region, Texas, a diagenetic quartzarenite. In: *SEPM Midyear Meeting*, **3**, 73 pp.

McRae, S. C. (1972) Glauconite. *Earth-Science Review,* **8**, 397–440.

Miall, A. D. (1996) *The Geology of Fluvial Deposits: Sedimentary Facies, Basin Analysis, and Petroleum Geology*. Berlin, Springer-Verlag, 582 pp.

Miao, X., Lu, H., Li, Z. and Cao, G. (2007) Paleocurrent and fabric analyses of the imbricated fluvial gravel deposits in Huangshui Valley, the northeastern Tibetan Plateau, China. *Geomorphology*, article in Press.

Middleton, G. V. (1973) Johannes Walther's law of correlation of facies. *Bull. Geol. Soc. Am.*, 84, 979-988.

Middleton, G. V. (1978) Facies. In: Fairbridge, R.W. and Bourgeois, J. (Eds.) *Encyclopedia of Sedimentology.* Dowden, Hutchinson and Ross, Stroudsburg, 323–325.

Millington, J. J. and Clark, J. D. (1995) The Charo/Arro canyon-mouth sheet system, south-central Pyrenees, Spain: A structurally influenced zone of sediment dispersal. *Journal of Sedimentary Research*, **65**, 443-454.

Mukhopadhyay, J. and Chaudhuri, A. K. (2003) Shallow to deep-water deposition in a Cratonic basin: an example from the Proterozoic Penganga Group, Pranhita–Godavari Valley, India. *Journal of Asian Earth Science*, **21**, 613-622.

Munoz, J. A. (1985) *Estructura al pina I Herciniana a la vora Sud de la zona axial del pirineu Oriental*. Thesis (PhD). Barcelona, 305 pp.

Munoz, J. A. (1992) Evolution of a continental collision belt: ECORS – Pyrenean crustal balanced section. In: McClay, K.R. (Ed.) *Thrust Tectonics*. New York, Chapman and Hall, 235 – 246.

Munoz, J. A., Coney, P. J., McClay, K. R. and Evenchick, C. A. (1997) Reply to discussion on syntectonic burial and post – tectonic exhumation of the southern Pyrenees foreland fold – thrust belt. *Journal of Geological Society, London*, **154**, 361 – 365.

Munoz, J. A., McClay, K. and Poblet, J. (1994) Synchronous extension and contraction in frontal thrust sheets of the Spanish Pyrenees. *Geology*, **22**, 921-924.

Murray, J. W. (1973) *Distribution and Ecology of Living Benthic foraminiferids*. Charles Street, London, Rechard Clay.

Mutti, E., Roberto, T., Pierre, M. M. and Gustavo, B. (2007) Deep-Water Turbidites and Their Equally Important Shallower Water cousins. *AAPG Bull*., Digital, **91**.

Mutti, E., Seguret, M. and Sgavetti, M. (1988) Sedimentation and Deformation in the Tertiary Sequences of the Southern Pyrenees. *AAPG, Mediteranean Basins Conference. Nice*, 126 pp.

Mutti, E., Steffens, G. S., Primez, C. and Orlando, M. (Eds.) (2003a) Turbidites: Models and Problems. *Marine and Petroleum Geology, Special Publication*, **20**, 523-933.

Mutti, E., Tinterri, R., Benevelli, G., Di Biase, D. and Cavanna, G. (2003b) Deltaic, mixed and turbidite sedimentation of ancient foreland basins. *Marine and Petroleum Geology*, **20**, 733-755.

Mutti, M., Bernoulli, D., Eberli, G. P. and Vecsei, A. (1996) Depositional geometries and facies associations in an Upper Cretaceous prograding carbonate platform margin (Orfento supersequence, Maiella, Italy). *Journal of Sedimentary Geology*, **66**, 749-765.

Myrow, P. M. and Southard, J. B. (1996) Tempestite deposition. *Journal of Sedimentary Research*, **66**, 875-887.

Nagtegaal, P.J.C. and De Weerd, J.T. (1985) Provenance of Cambro-Ordovician to Ologocene sandstones in the Southern Pyrenees, Spain. *Geological en Mijnbouw*, **40**, 25-40.

Nagy, J. (2007) *GEO 4220: Trace fossil facies. Sedimentary environments and biostratigraphy, lecture notes*. Available at: blyant.uio.no. (Accessed: 30.03.2008).

Niedoroda, A. W. Swift, D. J. P., Hopkins, T. S. and Ma, C. M. (1984) Shoreface morhphodynamics on wave dominated coasts. *Sedimentary Geology*, **60**, 331-354.

Nijman, W. (1998) Cyclicity and basin axis shift in a piggyback basin: towards modelling of the Eocene Tremp-Ager Basin, South Pyrenees, Spain. *Geological Society, London, Special Publication*, **134**, 135-162.

Nijman, W. and Nio, S. D. (1975) The Eocene Montanana delta (Tremp-Graus Basin, provinces of Lerida and Huesca, southren Pyrenees, Spain). In: *The Sedimentary Evolution of the Paleogene South Pyrenean Basin: 9th Sedimentological Conference, Nice, Franc*e. Excursion Guidebook, **19**, 56 pp.

Nijman, W. and Van Oosterhout, C. W. M. (1994) *Quantitative model study of the nappe-top basin, the Eocene Tremp-Ager Basin, S. Pyrenees, Spain, phase I: data base (second extended version).* Vol. I: Utrecht University, Institute of Earth Sciences, Department of Geology, 20 p. (Unpublished).

Odin, G. S. and Matter, A. (1981) De glauconarium origine: *Sedimentology*, **28**, 611-641.

Olivet, J. L. (1996) La cinematique de la plaque. *Bulletin des Centres de Recherches Exploration-Production Elf-Aquitaine*, **20**, 131-195.

Ori, G. G. and Friend, P. F. (1984) Sedimentary basins formed and carried piggyback on active thrust sheets. *Geology*, **12**, 475-478.

Parsons, I., Thompson, P., Lee, M. R. and Cayzer, N. (2005) Alkali Feldspar Microtextures as Provenance Indicators in Siliciclastic Rocks and Their Role in Feldspar Dissolution During Transport and Diagenesis. *Journal of Sedimentary Research,* **75**, 921-942.

Pekar, S. F. and Kominz, M. A. (2001) Two-Dimensional Paleoslope Modeling: A New Method for Estimating Water Depths of Benthic Foraminiferal Biofacies and Paleoshelf Margins. *Journal of Sedimentary Research*, **71**, 608-620.

Pemberton, S. G., MacEachern, J.A. and Frey, R. W. (1992) Trace Fossil Facies Models. Environmental and Allostratigraphic Significance. In: Walker, R. G. and James, N. P. (Eds.) *Facies Models: Response to Sealevel change*. Geological Association of Canada, St. John's, Newfoundland, 47-72.

Perkins, D. and Henke, K. (2000) *MINERALS IN THIN SECTION*. New Jersey, Prentice-Hall, 125 pp.

Pickering, K.J. and Corregidor, L. (2005) Mass-Transport Complexes (MTCs) and Tectonic Control on Basin-Floor Submarine Fans, Middle Eocene, South Spanish Pyrenees. *Journal of Sedimentary Research*, **75**, 761-783.

Poblet, J., McClay, K., Storti, F. and Munoz, J. A. (1997) Geometries of syntectonic sediments associated with single-layer detachment folds. *Journal of Structural Geology*, **19**, 369-381.

Pomar, L., Gili, E., Obrador, A. and ward, A. C. (2005) Facies architecture and high – resolution sequence stratigraphy of an upper Cretaceous platform margin succession, southern central Pyreneees, Spain. *Sedimentary Geology*, **175**, 339 – 365.

Posamentier, H.W. and Vail, P.R. (1988) Eustatic controls on clastic deposition, II: sequence and systems tracts model. In: Wilgus, C.K., Hastings, B.S., Kandall, C.G.S.C., Posamentier, H.W., Ross, C.A. and Van wagoner, J.C. (Eds.) *Sea Level Changes: An Integrated approach. SEPM Special Publication*, **42**, 125-154.

Potter, E., Maynard, J.B. and Pryor, W.A. (1980) *Sedimentology of Shale*. New York, Springer- Verlag, 303 pp.

Potter, P., and Pettijohn, F. (1977) *Paleocurrents and Basin Analysis*. New York, Springer-Verlag.

Puigdefabregas, C. and Souquet, P. (1986) Tecto–Sedimentary Cycles and Depositional Sequences of the Mesozoic and Tertiary from the Pyrenees. *Tectonophysics*, **129**, 173 – 203.

Puigdefabregas, C., Munoz, J. A. and Marzo, M. (1986) Thrust belt development in the eastern Pyrenees and related depositional sequences in the southern foreland basin. *International Association of Sedimentologists, Special Publication,* **8**.

Puigdefabregas, C., Munoz, J. A. and Verges, J. (1992) Thrusting and foreland basin evolution in the Southern Pyrenees. In: McClay, K. (Ed) *Thrust Tectonics*. London, Chapman and Hall, 247 – 254.

Racey, A. (2001) A review of Eocene nummulite accumulations: Structure, formation and reservoir potential. *Journal of Petroleum Geology*, **24**, 79-100.

Reading, H. G. and Collinson, J. D. (1996) Clastic coasts. In: Reading, H.G. (Ed.) *Sedimentary Environments: Processes, Facies and Stratigraphy* (3rd edn.). Oxford, Blackwell, 154-231.

Reading, H. G. and Levell, B. K. (1996) Controls on the sedimentary record. In: Reading, H.G. (Ed.) *Sedimentary Environments: Processes, Facies and Stratigraphy* (3rd edn.). Oxford, Blackwell, 5-35.

Reid, C. M., James N. P., Beauchamp, B. and Kyser T. K. (2007) Faunal turnover and changing oceanography**:** Late Palaeozoic warm-to-cool water carbonates, Sverdrup Basin, Canadian Arctic Archipelago. *Palaeogeography, Palaeoclimatology, Palaeoecology*, **249**, 128-159.

Reineck, H. E. and Singh, I. B. (1980) *Depositional Sedimentary Environments With Reference to Terrigenous Clastics* (2nd edn.). New York, Spring-Verlag, 551 pp.

Reiss, Z. and Hottinger, L. (1984) *The Gulf of Aqaba. Ecological Micropalaeontology*. Berlin, Springer-Verlag, 354 pp.

Remacha, E., Fernandez, L. P., Maestro, E., Oms, O., Estrada, R. and Teixelle, A. (1998) The upper Hecho Group and their vertical evolution to deltas (Eocene, south-central Pyrenees). In: Hevia, A. M. and Soria, A. R. (Eds.) *Field Trip GuideBook of the 15th International Sedimentological Congress, Alicante*, 3-25.

Rogers, J. P. and Longman, M. W. (2001) An introduction to chert reservoirs in North America. *AAPG Bull.*, **85**, 1-5.

Romero, J., Caus, E. and Rosell, J. (2002) A model for the paleoenvironmental distribution of larger foraminifera based on late Middle Eocene deposits on the margin of the South Pyrenean basin (NE Spain). *Palaeogeography, Palaeoclimatology, Palaeoecology*, **179**, 43-56.

Saigal, G. C., Morad, S., Bjørlykke, K., Egeberg, P. K. and Aagaard, P. (1988) Diagenetic Albitization of Detrital K-feldspar in Jurassic, Lower Cretaceous,and Tertiary Clastic Reservoir Rocks from Offshore Norway, I. Texture and Origin. *Journal of Sedimentary Petrology*, **58**, 1003-1013.

Sami, T. T. and James, N. P. (1994) Peritidal carbonate platform growth and cyclicity in an Early Proterozoic foreland basin, Upper Pethei Group, Northwest Canada. *Journal of Sedimentary Research*, **64**, 111-131.

Sarg, J. F. (1988) Carbonate Sequence Stratigraphy. In: Wilgus, C.K., Hastings, B.S., Kandall, C.G.S.C., Posamentier, H.W., Ross, C.A. and Van wagoner, J.C. (Eds.) *Sea Level Changes: An Integrated approach. SEPM Special Publication*, **42**, 155-181

Saylor, B. Z. (2003) Sequence Stratigraphy and carbonate-siliciclastic Mixing in a Terminal Proterozoic Foreland Basin, Urusis Formation, Nama Group, Namibia. *Journal of Sedimentary Research*, **73**, 264-279.

Schlager, W., Reijmer, J. J. G. and Droxler, A. (1994) Highstand shedding of carbonate platforms. *Journal of Sedimentary Research*, **64**, 270-281.

Scholle, P. (1978) A Color Illustrated Guide to Carbonate Rock Constituents, Textures, Cements and Porosities. *AAPG*, **M27**, 241.

Seguret, M. (1972) Etude technique des nappes et series decollees de la partie central du varsant su des Pyrenees, caractere synsedimentaire role de la compression et de la gravite. Publications de L'universite des sciences et techniques du languedoc (USTELA), Montpellier – Serie Geol. Struct., **2**, 155 pp.

Sepkoski, J. J., Bambach, R. K. and Droser, M. L. (1991) Secular changes in Phanerozoic event bedding and biological overprint. In: Einsele, G., Ricken, W. and Seilacher, A. (Eds.) *Cycles and Events in Stratigraphy*. Berlin, Springer-Verlag, 298-312.

Siddiqui, A., Saner, S. and Abdulghani, W. M. (2006) Silica Occurrences in the Upper Jurassic Arab Carbonate Reservoirs, Soudi Arabia. *AAPG Bull.*, Digital, **90**.

Simo, A. and Puigdefabregas, C. (1985) Transition from shelf to basin on active slope, Upper Cretaceous, southern Pyrenees. In: Mila, M. D. and Rosell, J. E. (Eds.) *6th European Regional Meeting International association of Sedimentologists, Lerida, Spain*. Excursion Guidebook, 63-108.

Swift, D. J. P., Huddelson, P. M., Brenner, R. L. and Thompson, P. (1987) Shelf construction in a foreland basin: storm beds, shelf sandstones, and shelf slope depositional sequences in the Upper Cretaceous Mesaverde Group, Book Cliffs, Utah. *Sedimentology*, **34**, 423-457.

Swift, D. J. P., Niedoroda, A. W., Vincent, C. E. and Hopkins, T. S. (1985) Barrier island evolution, Middle Atlantic Shelf, U. S. A. Part I: Shoreface Dynamics. *Marine Geology*, **63**, 331-361.

Torricelli, S., Knezaurek, G. and Biffi, U. (2006) Sequence biostratigraphy and paleoenvironmental reconstruction in the Early Eocene Figols Group of the Tremp–Graus Basin (south-central Pyrenees, Spain). *Palaeogeography, Palaeoclimatology, Palaeoecology*, **232**, 1-35.

Uba, E. C., Huebeck, C. and Hulka, C. (2005) Facies analysis and basin architecture of the Neogene Subandean synorogenic wedge, Southern Bolivia. *Sedimentary Geology*, **180**, 91-123.

Van Wagoner, J. C., Posamentier, H. W., Mitchum, R. M., Vail, P. R., Sarg, J. F., Loutit, T. S. and Hardenbol, J. (1988) An overview of the fundamentals of sequence stratigraphy and key definitions. In: Wilgus, C.K., Hastings, B.S., Kandall, C.G.S.C., Posamentier, H.W., Ross, C.A. and Van wagoner, J.C. (Eds.) *Sea Level Changes: An Integrated approach. SEPM Special Publication*, **42**, 39-45.

Van Wagoner, J.C., Mitchum, R.M., Campion, K.M. and Rahmanian, V.D. (1990) *Siliciclastic Sequence Stratigraphy in Well Logs, Cores, and Outcrops: Concepts for High-Resolution Correlation of Time and Facies*. AAPG Methods in Exploration Series, No. 7, 1-55.

Verges, J., Marzo, M., Santaeularia, T., Serra – Kiel, J., Burbank, D.W., Munoz, J. A. and Gimenez – Montsant, J. (1998) Quantified vertical motions and tectonic evolution of the SE Pyrenean foreland basin. In: Mascle, A., Puigdefabregas, C., Luterbacher, H. P., and Fernandez, M. (Eds.) *Cenozoic Foreland Basins of Western Europe*. *Geological Society of London, Special Publication*, **134**, 107 – 134.

Walker, G. R. (1992) Facies, Facies Models and Modern Stratigaphic Concepts. In: Walker, G.R. and James, P.N. (Eds.) *Facies Models: Response to Sealevel change*. Geological Association of Canada, St. John's, Newfoundland, 1-14.

Walker, G. R. and Plint, G. A. (1992) Wave- and Storm-Dominated Shallow Marine Systems. In: Walker, G, R., and James P. N. (Eds.) *Facies Models: Response to Sealevel change*. Geological Association of Canada, St. John's, Newfoundland, 219- 238.

Walker, R. G. (1984) Shelf and shallow marine sands. In: R. G. Walker (Ed.) *Facies Models* (2nd edn.). *Geosci. Can., Repr. Ser*., **1**, 141-170.

Walton, W. R. (1964) Recent foraminiferal ecology and paleoecology. In: Imbrie, J. and Newell, N., (Eds.) *Approaches to Paleoecology*: New York, John Wiley, 151-237.

Weltje, G. S., Van Ansenwoude, K. J. and De Boer, P. L. (1996) High-Frequency Detrital Signals in Eocene Fan-Delta Sandstones of Mixed Parentage (South- Central Pyrenees, Spain): A Reconstruction of Chemical Weathering in Transit. *Journal of Sedimentary Research*, **66**, 119-131.

Williams, H., Turner, F. J. and Gilbert, C. M. (1955) *PETROGRAPHY: An Introduction to the Study of Rocks in Thin Sections*. San Francisco, Freeman and Company, 406 pp.

Wright, V. P. and Burchette, T. P. (1996) Shallow water carbonate envirnments. In: Reading, H.G. (Ed.) *Sedimentary Environments: Processes, Facies and Stratigraphy* (3rd edn.). Oxford, Blackwell, 235-394.

Zecchin, M. (2007) The architectural variability of small-scale cycles in shelf and rampclastic systems: The controlling factors. *Earth Science Reviews*, **84**, 21-55.

Ziegler, P. A. (1988) *Evolution of the Arctic-North Atlantic and the Western Tethys. AAPG*, **M43,** 1-206.

16. APPENDIXES

Appendix A: Log positions and correlations

Appendix B: Sedimentological logs

APPENDIX A

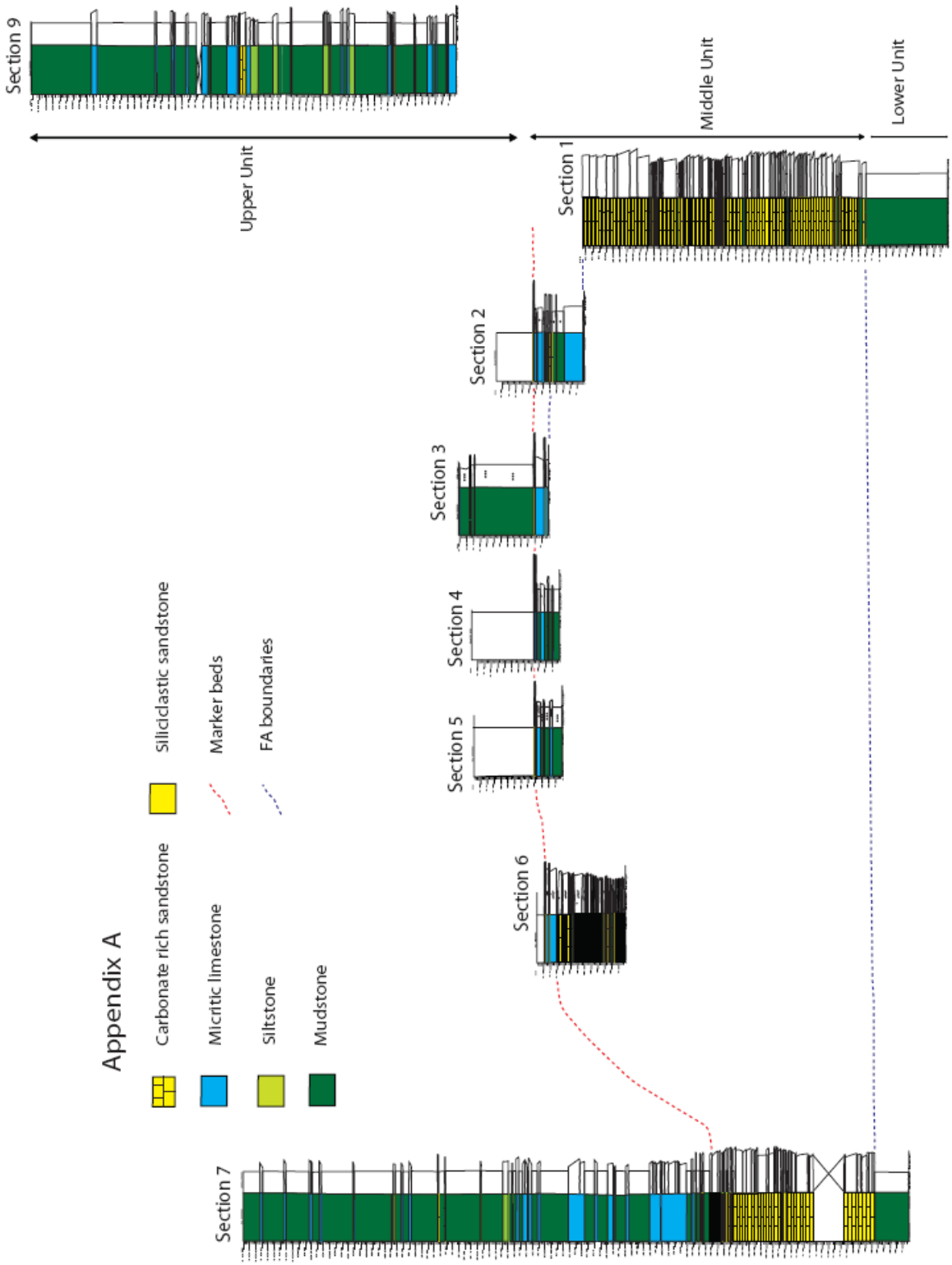
Section 9
Upper Unit
Middle Unit
Lower Unit
Section 1
Section 2
Section 3
Section 4
Section 5
Section 6
Section 7
Appendix A
Carbonate rich sandstone
Micritic limestone
Siltstone
Mudstone
Siliciclastic sandstone
Marker beds
FA boundaries

APPENDIX B

LEGEND FOR SEDIMENTARY LOGS

- Symmetrical ripples 

- Asymmetrical ripples 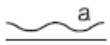

- Parallel lamination 
- Wavey (undulating) beds 
- Cross bedding - tabular 
- Cross bedding - low angle 
- Hummocky cross-stratification 
- Flute cast 
- Plant fragments 
- Bivalve 
- Nummulites
  - < 20% 
  - > 20% 
- Bioturbation (general)
  - slight
  - intense 
- Siliciclastic sandstone 
- Carbonate rich sandstone 
- Micritic limestone 
- Siltstone 
- Mudstone 

FRAMEWORK / STRATIGRAPHIC LOGS

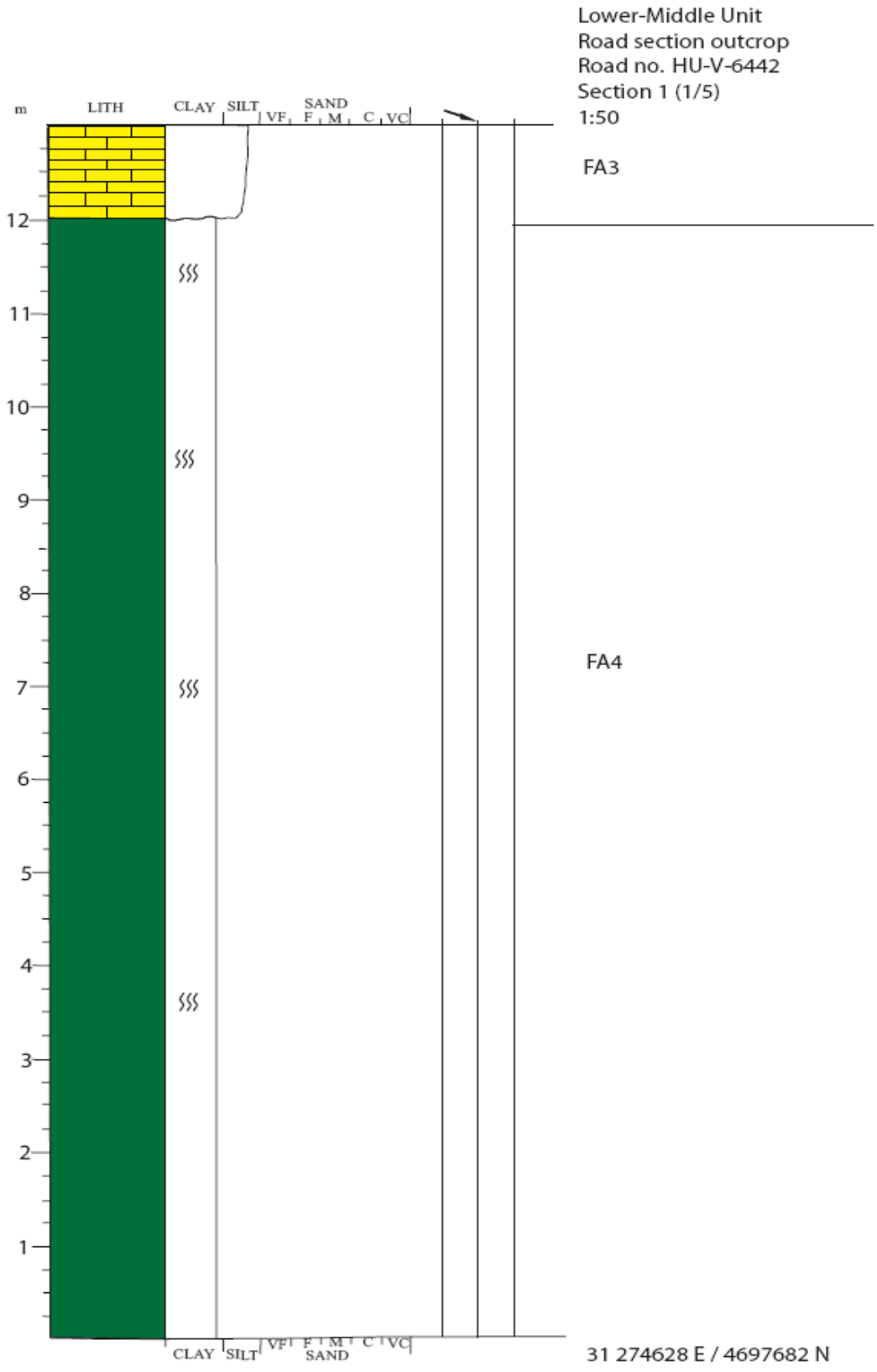

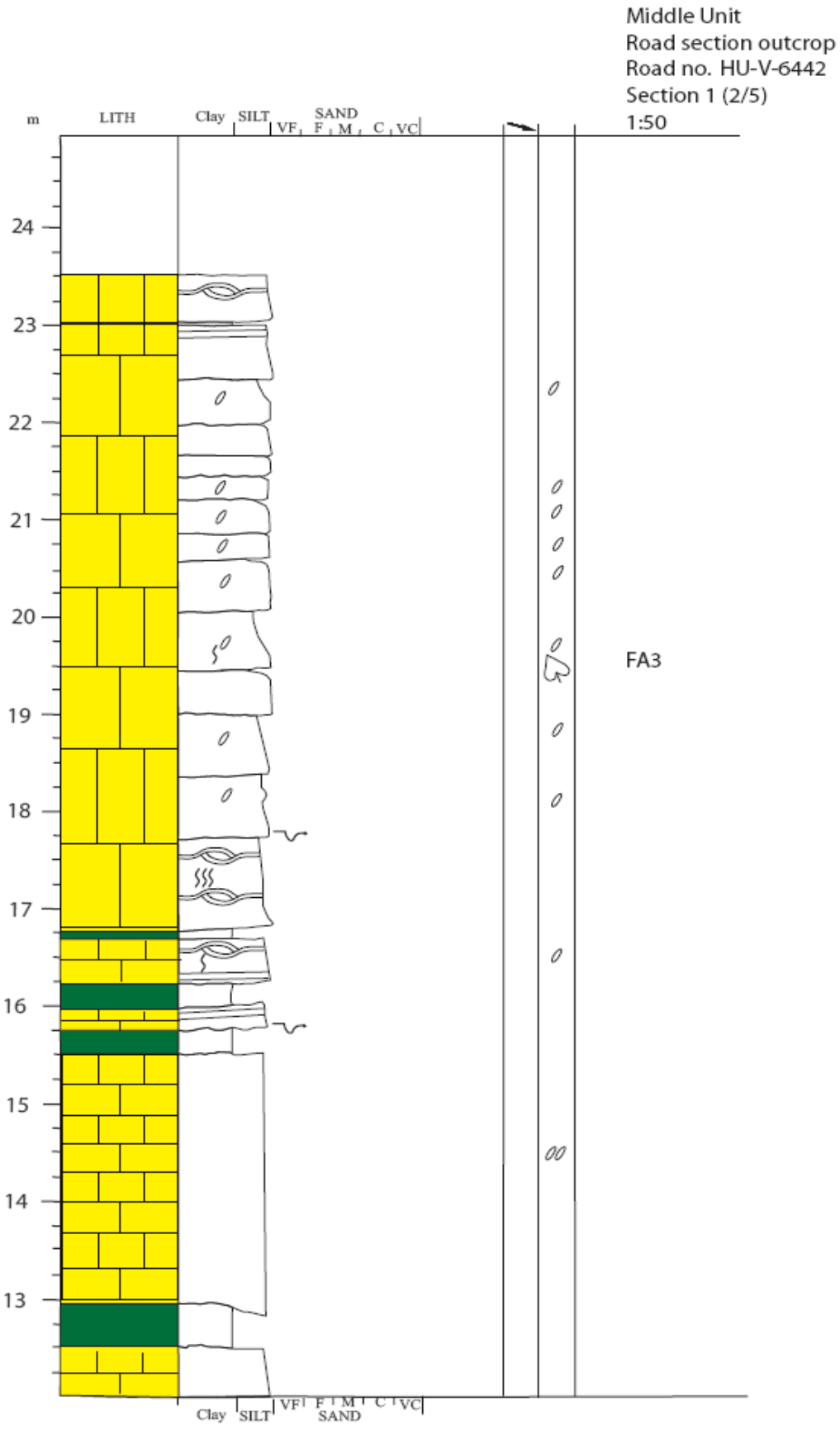
Middle Unit
Road section outcrop
Road no. HU-V-6442
Section 1 (2/5)
1:50
m
LITH
Clay
SILT
SAND
VF
F
M
C
VC
24
23
22
21
20
19
18
17
16
15
14
13
FA3

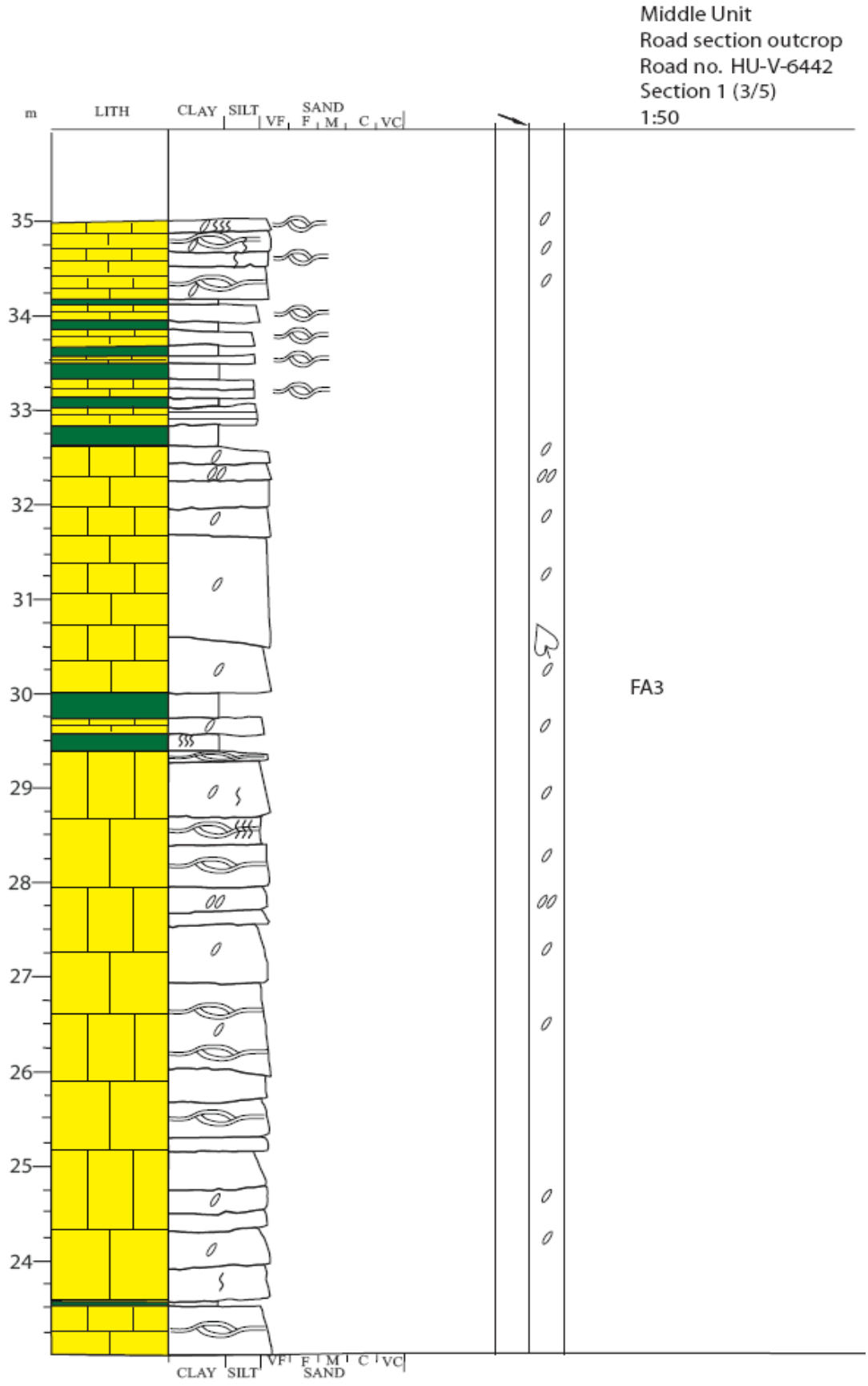
Middle Unit
Road section outcrop
Road no. HU-V-6442
Section 1 (3/5)
1:50
m
LITH
CLAY
SILT
VF
SAND
F
M
C
VC
35
34
33
32
31
30
29
28
27
26
25
24
FA3

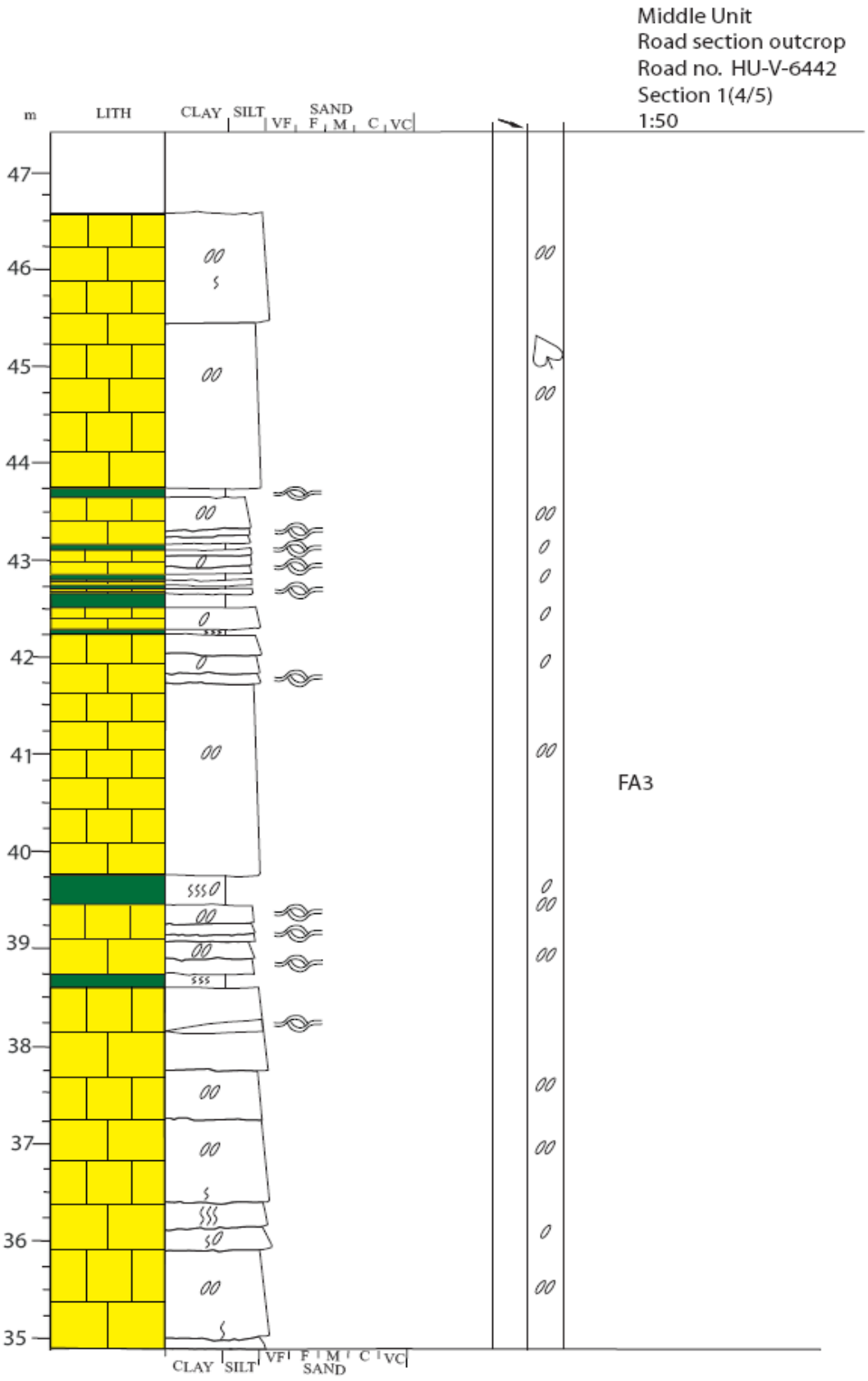
Middle Unit
Road section outcrop
Road no. HU-V-6442
Section 1(4/5)
1:50
m
LITH
CLAY
SILT
SAND
VF
F
M
C
VC
47
46
45
44
43
42
41
40
39
38
37
36
35
FA3

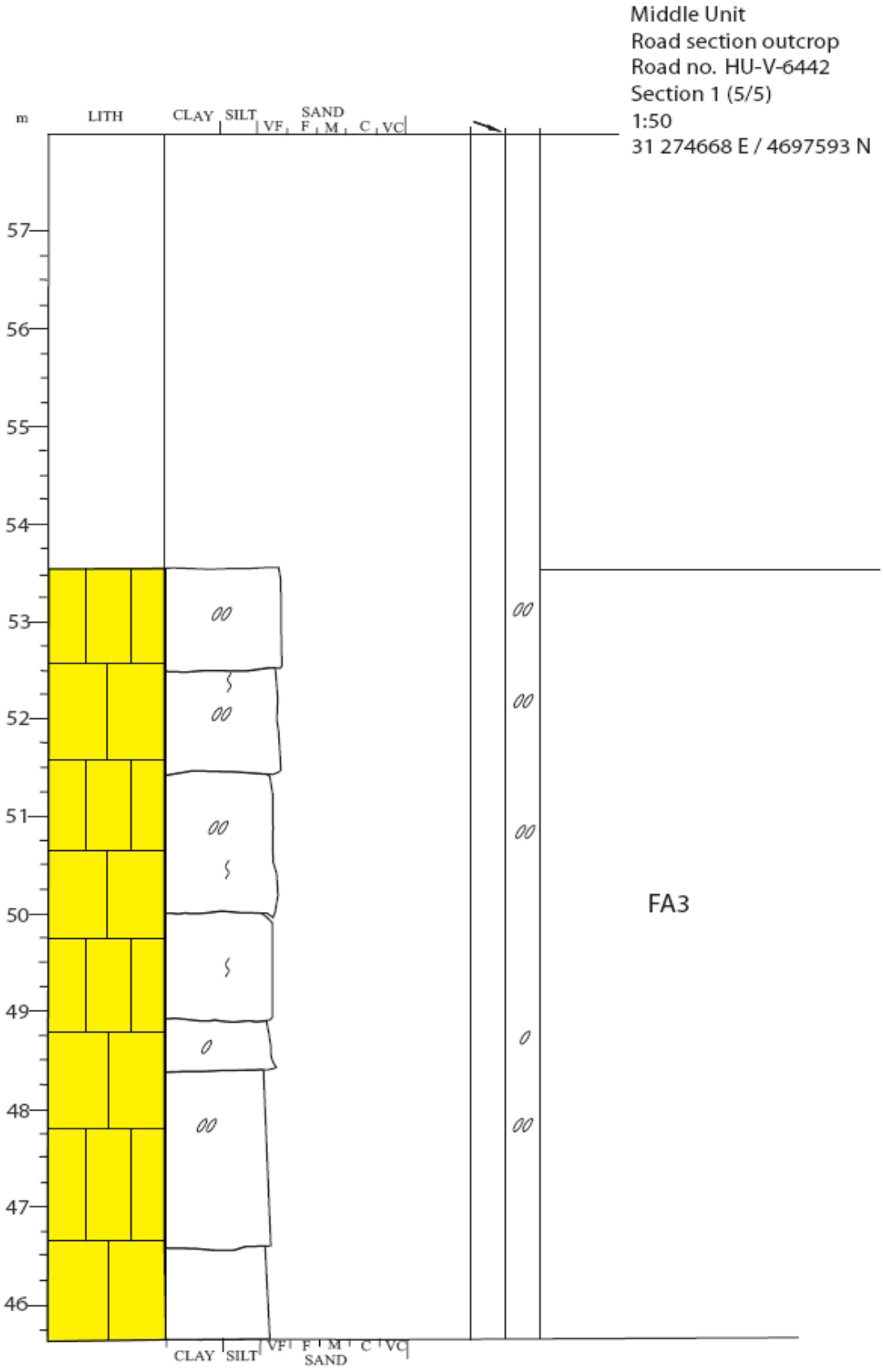
Middle Unit
Road section outcrop
Road no. HU-V-6442
Section 1 (5/5)
1:50
31 274668 E / 4697593 N
m
LITH
CLAY
SILT
SAND
VF
F
M
C
VC
57
56
55
54
53
52
51
50
49
48
47
46
FA3

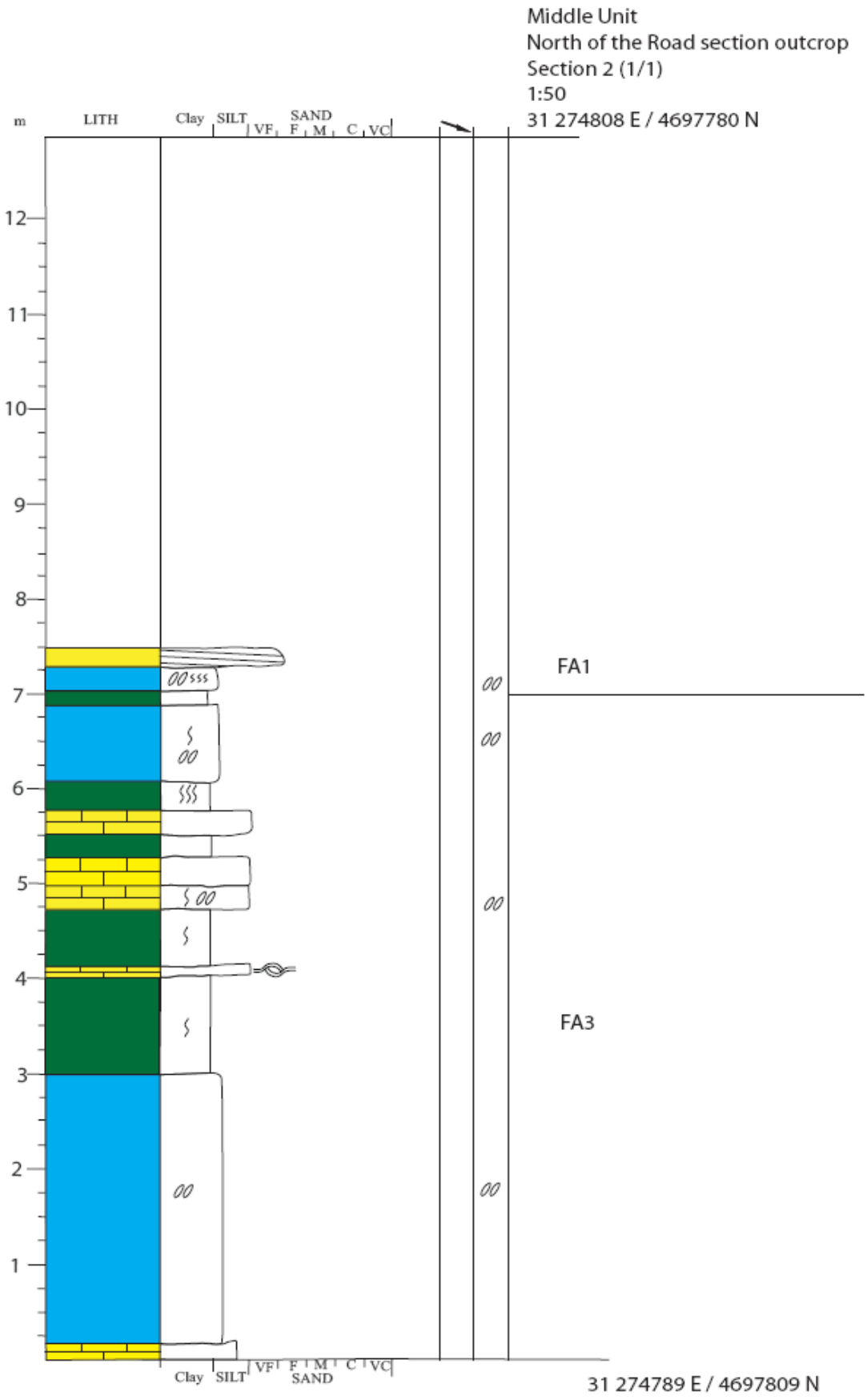
Middle Unit
North of the Road section outcrop
Section 2 (1/1)
1:50
31 274808 E / 4697780 N
m
LITH
Clay
SILT
SAND
VF
F
M
C
VC
12
11
10
9
8
7
6
5
4
3
2
1
FA1
FA3
31 274789 E / 4697809 N

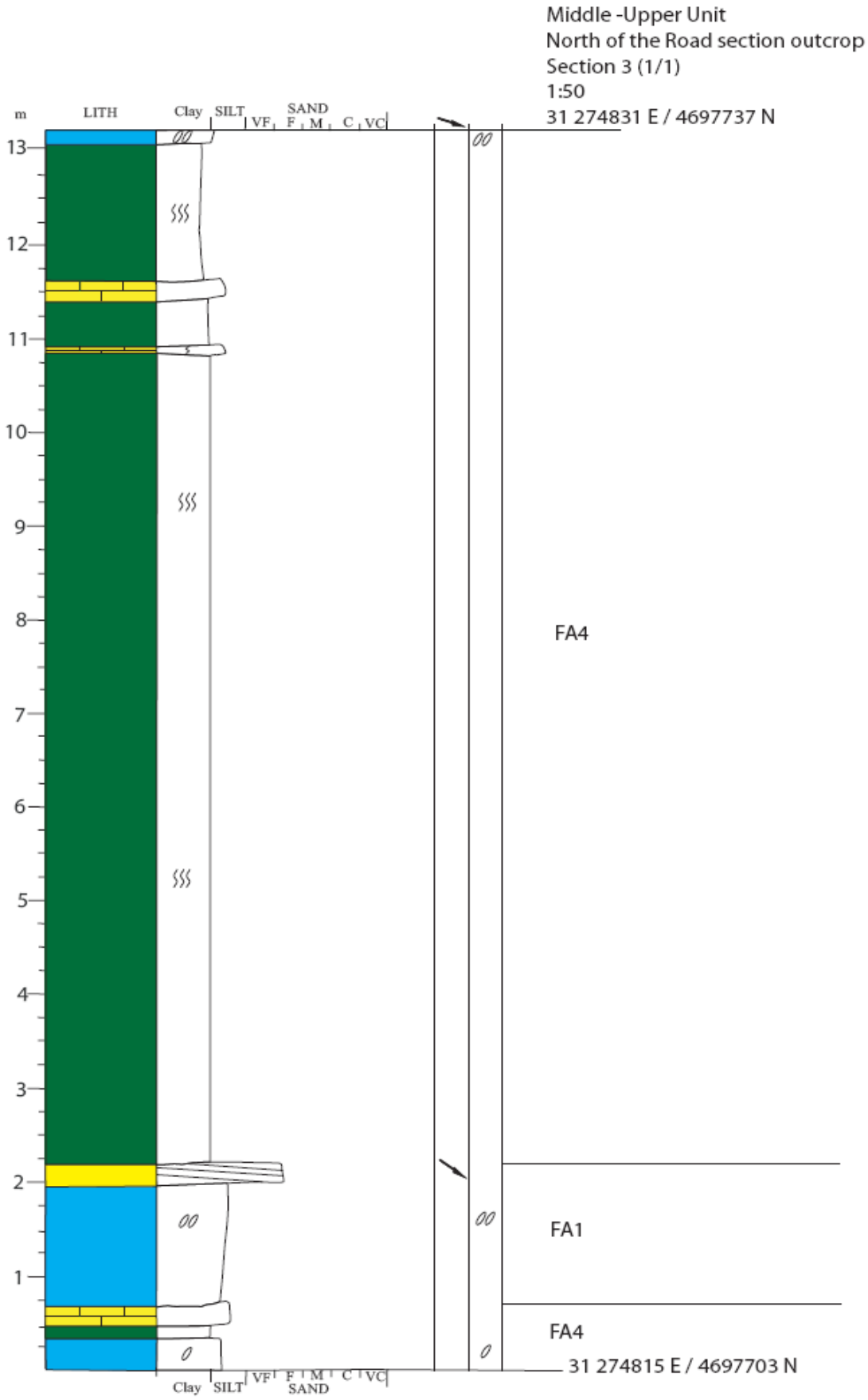
Middle -Upper Unit
North of the Road section outcrop
Section 3 (1/1)
1:50
31 274831 E / 4697737 N
m
LITH
Clay
SILT
SAND
VF
F
M
C
VC
13
12
11
10
9
8
7
6
5
4
3
2
1
FA4
FA1
FA4
31 274815 E / 4697703 N

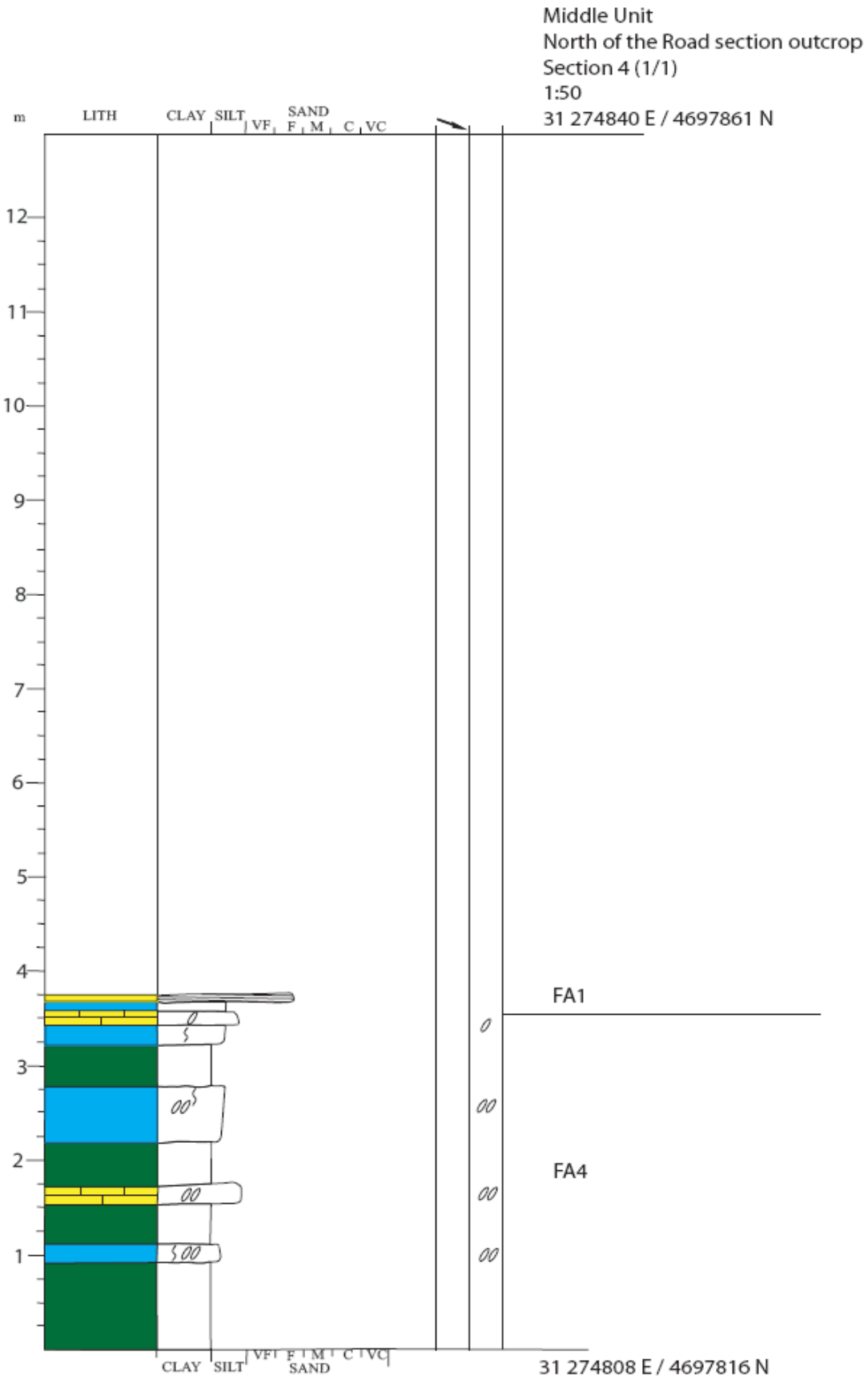
Middle Unit
North of the Road section outcrop
Section 4 (1/1)
1:50
31 274840 E / 4697861 N
m
LITH
CLAY
SILT
SAND
VF
F
M
C
VC
12
11
10
9
8
7
6
5
4
3
2
1
FA1
FA4
CLAY
SILT
SAND
31 274808 E / 4697816 N

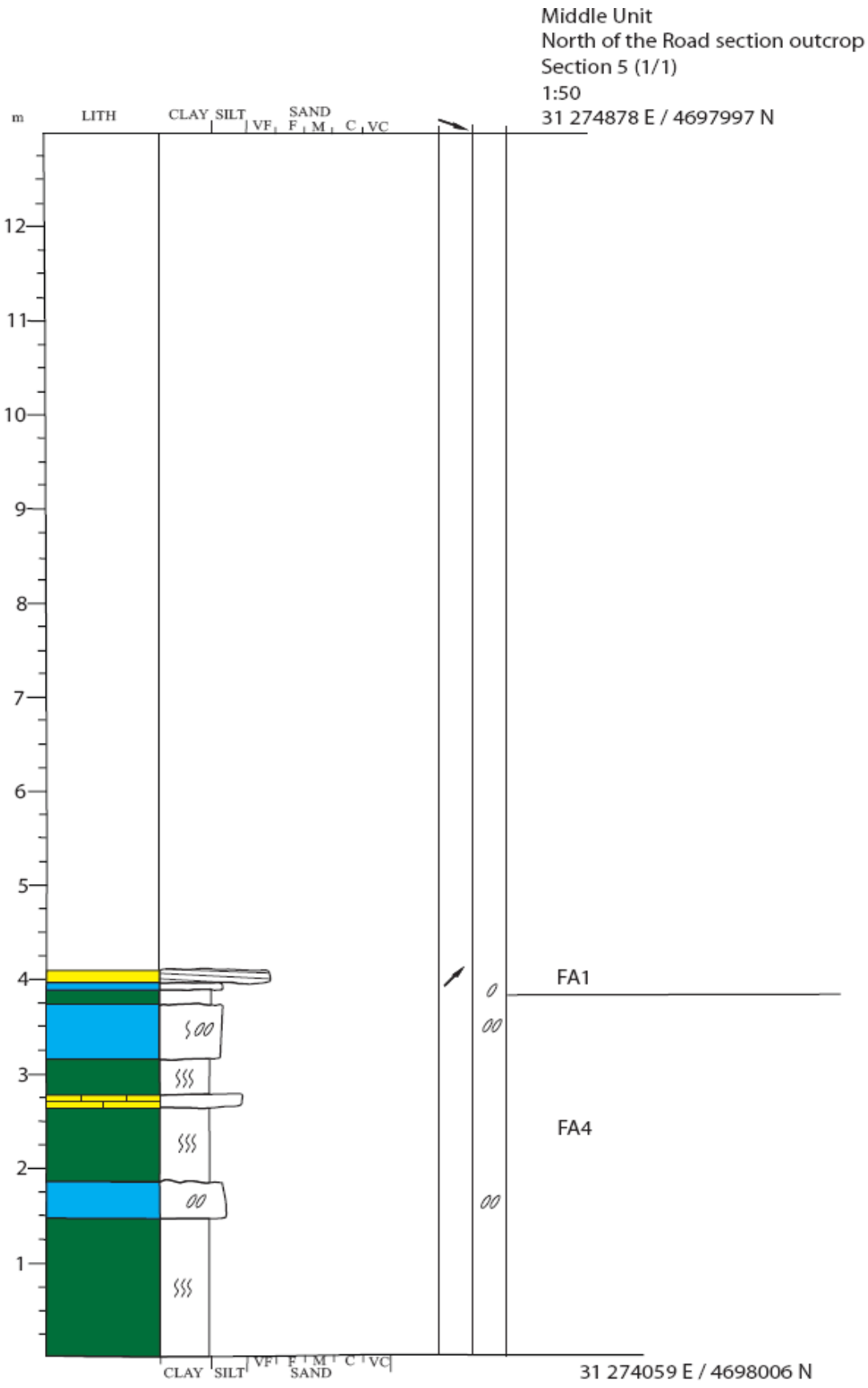
Middle Unit
North of the Road section outcrop
Section 5 (1/1)
1:50
31 274878 E / 4697997 N
m
LITH
CLAY SILT
SAND
VF F M C VC
12
11
10
9
8
7
6
5
4
3
2
1
FA1
FA4
CLAY SILT
SAND
VF F M C VC
31 274059 E / 4698006 N

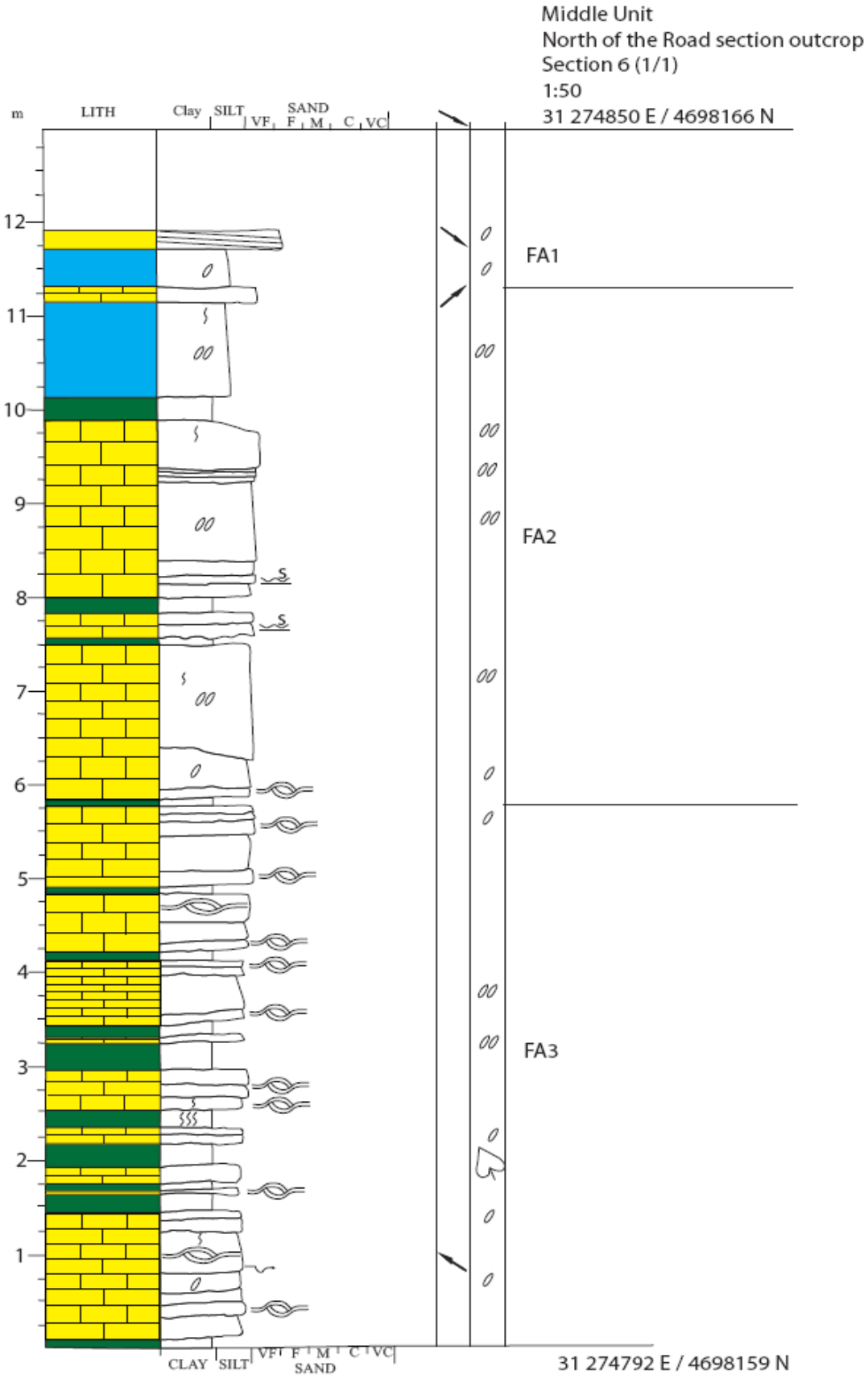
Middle Unit
North of the Road section outcrop
Section 6 (1/1)
1:50
31 274850 E / 4698166 N
m
LITH
Clay
SILT
SAND
VF
F
M
C
VC
12
11
10
9
8
7
6
5
4
3
2
1
FA1
FA2
FA3
CLAY
SILT
SAND
31 274792 E / 4698159 N

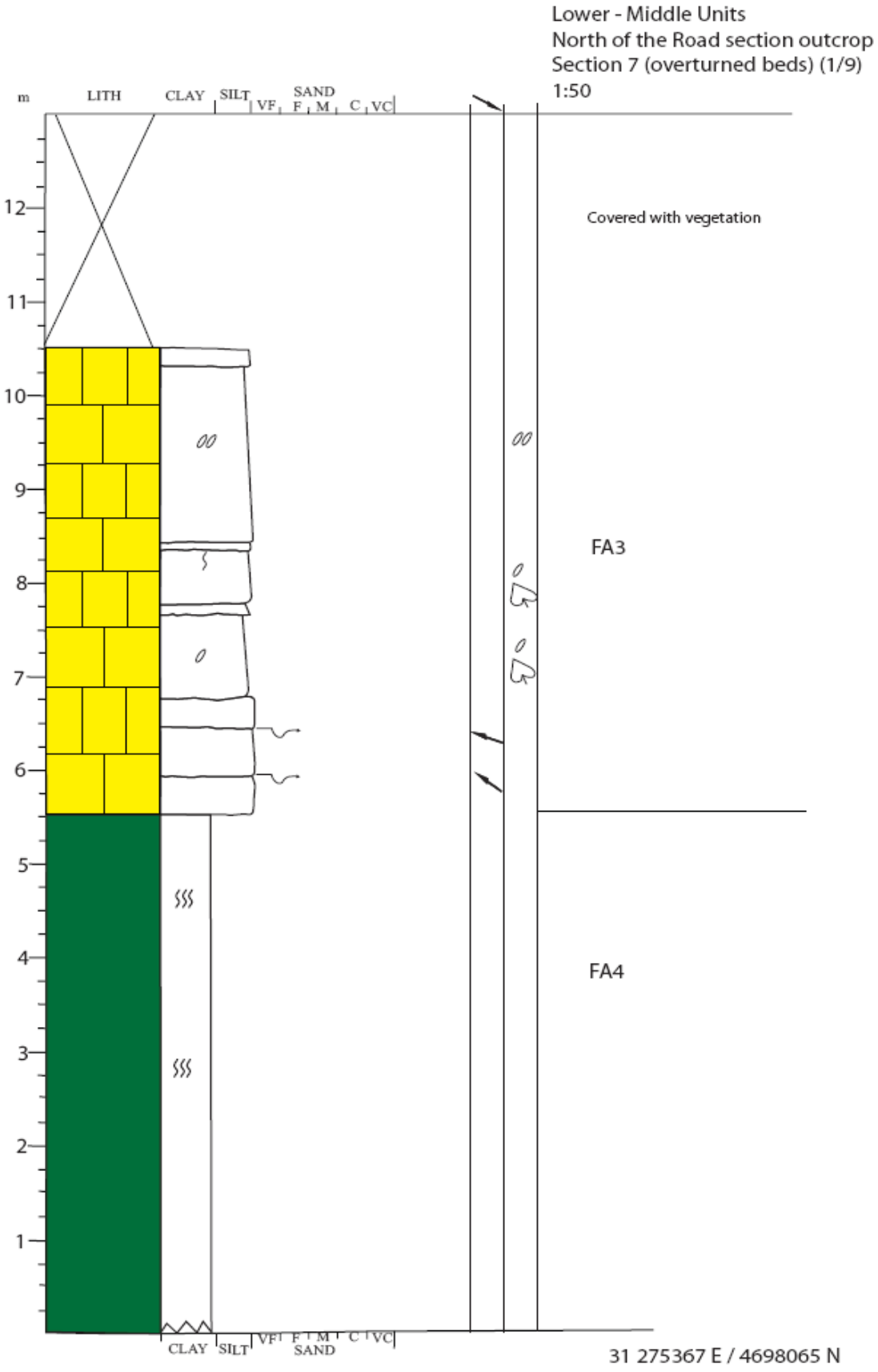
Lower - Middle Units
North of the Road section outcrop
Section 7 (overturned beds) (1/9)
1:50
m
LITH
CLAY
SILT
SAND
VF
F
M
C
VC
12
11
10
9
8
7
6
5
4
3
2
1
Covered with vegetation
FA3
FA4
31 275367 E / 4698065 N

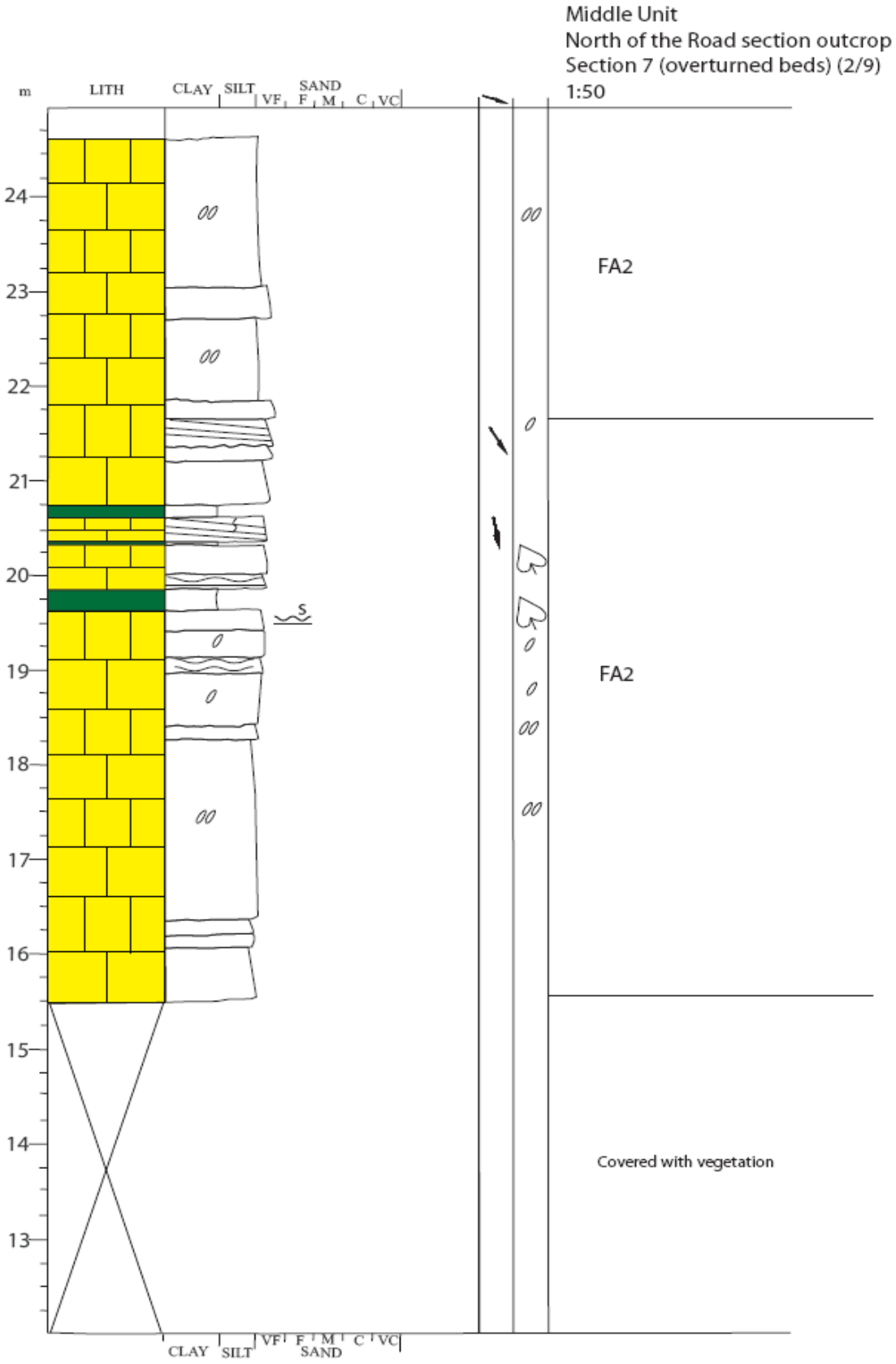
Middle Unit
North of the Road section outcrop
Section 7 (overturned beds) (2/9)
1:50
m
LITH
CLAY
SILT
VF
SAND
F
M
C
VC
24
23
22
21
20
19
18
17
16
15
14
13
FA2
FA2
Covered with vegetation

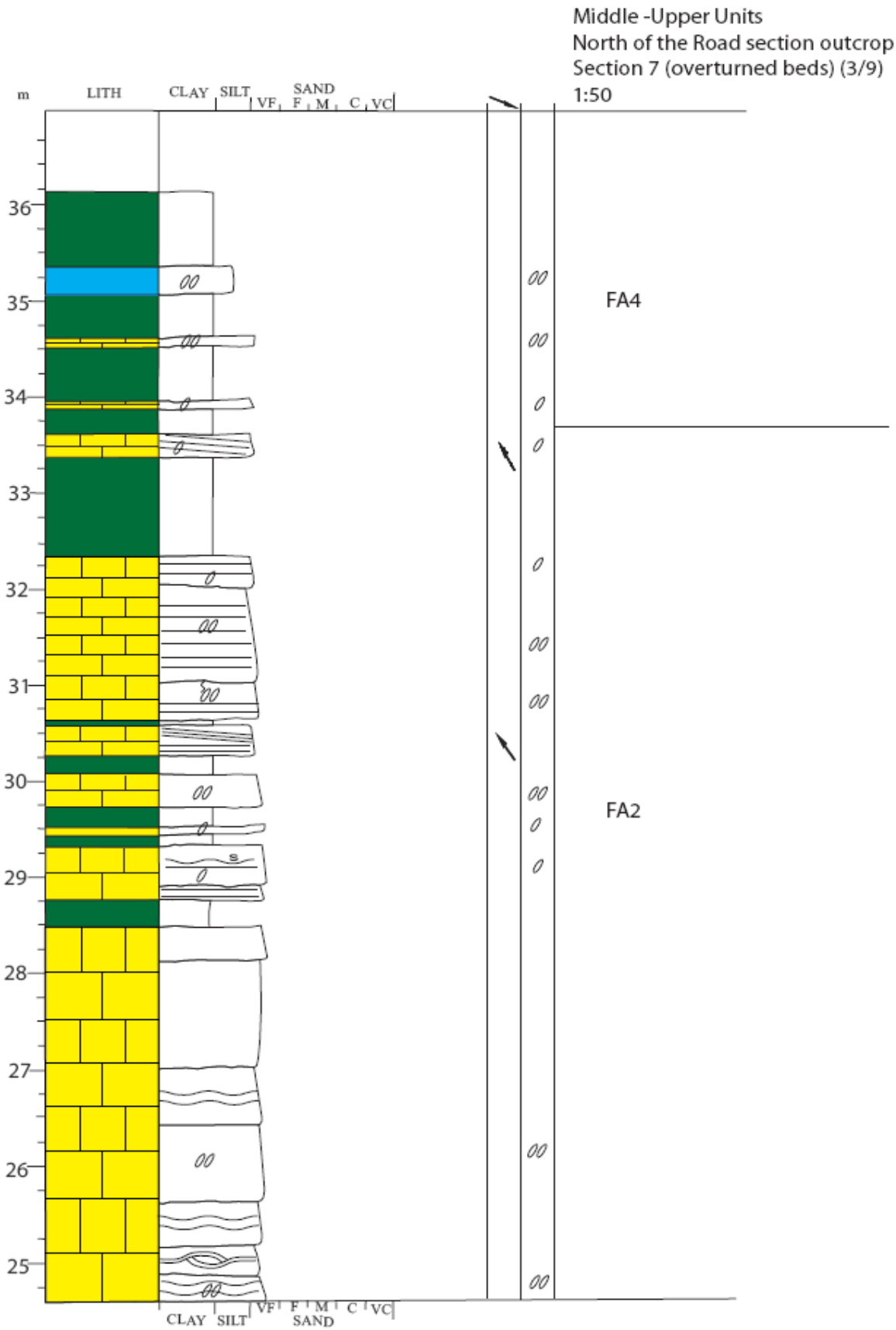
Middle -Upper Units
North of the Road section outcrop
Section 7 (overturned beds) (3/9)
1:50
m
LITH
CLAY
SILT
SAND
VF
F
M
C
VC
36
35
34
33
32
31
30
29
28
27
26
25
FA4
FA2

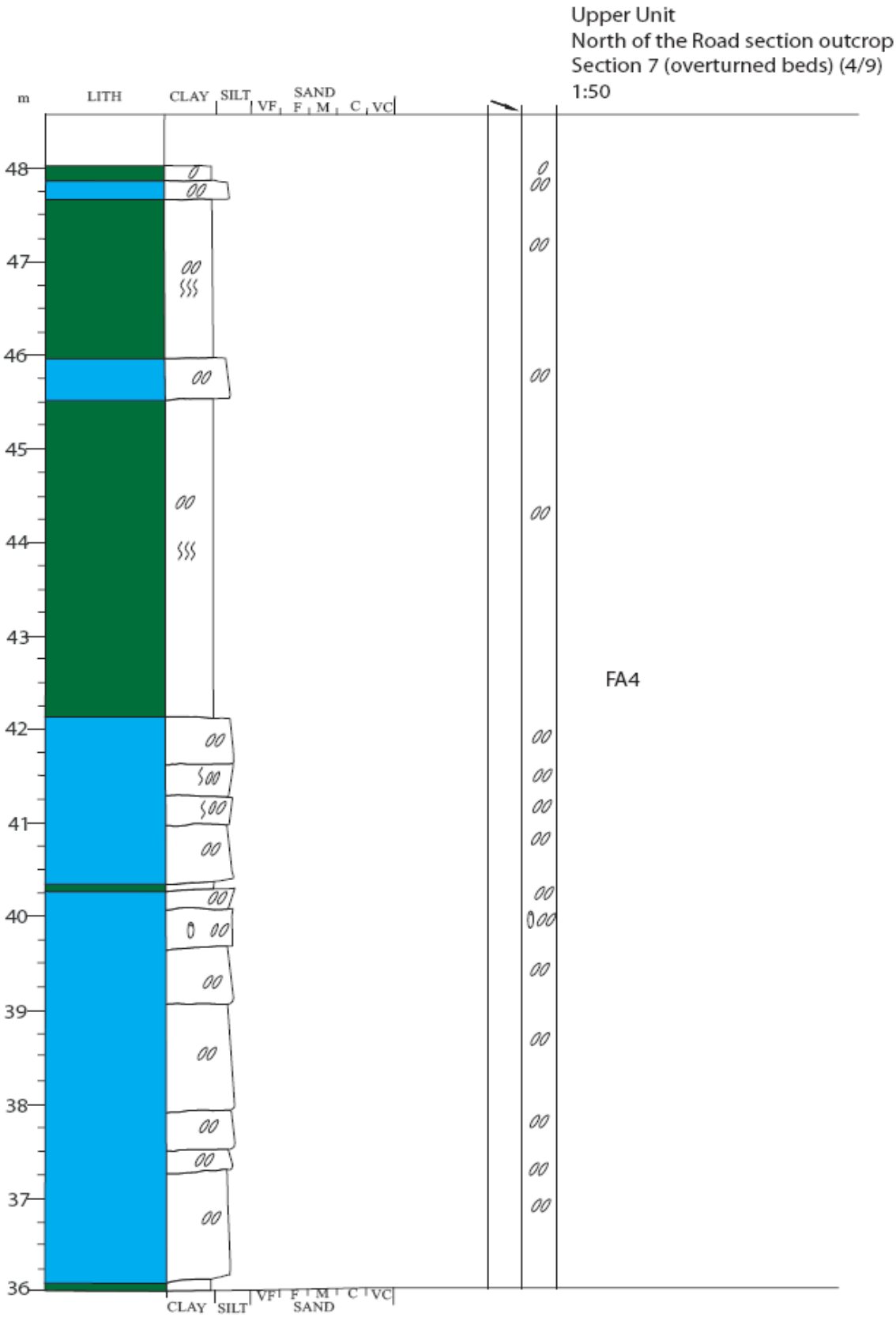
Upper Unit
North of the Road section outcrop
Section 7 (overturned beds) (4/9)
1:50
m
LITH
CLAY
SILT
SAND
VF
F
M
C
VC
48
47
46
45
44
43
42
41
40
39
38
37
36
FA4

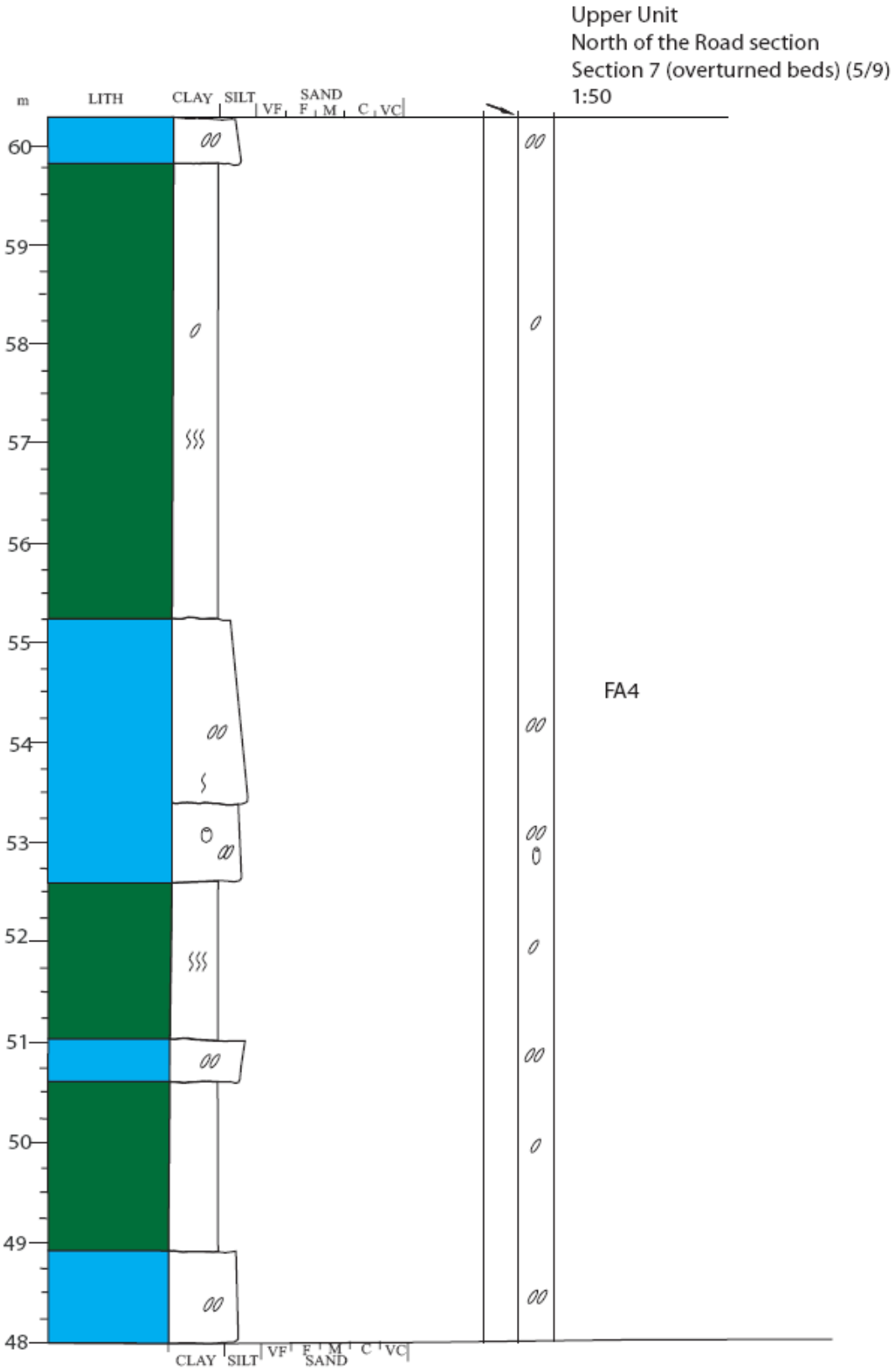
Upper Unit
North of the Road section
Section 7 (overturned beds) (5/9)
1:50
m
LITH
CLAY
SILT
SAND
VF
F
M
C
VC
60
59
58
57
56
55
54
53
52
51
50
49
48
FA4

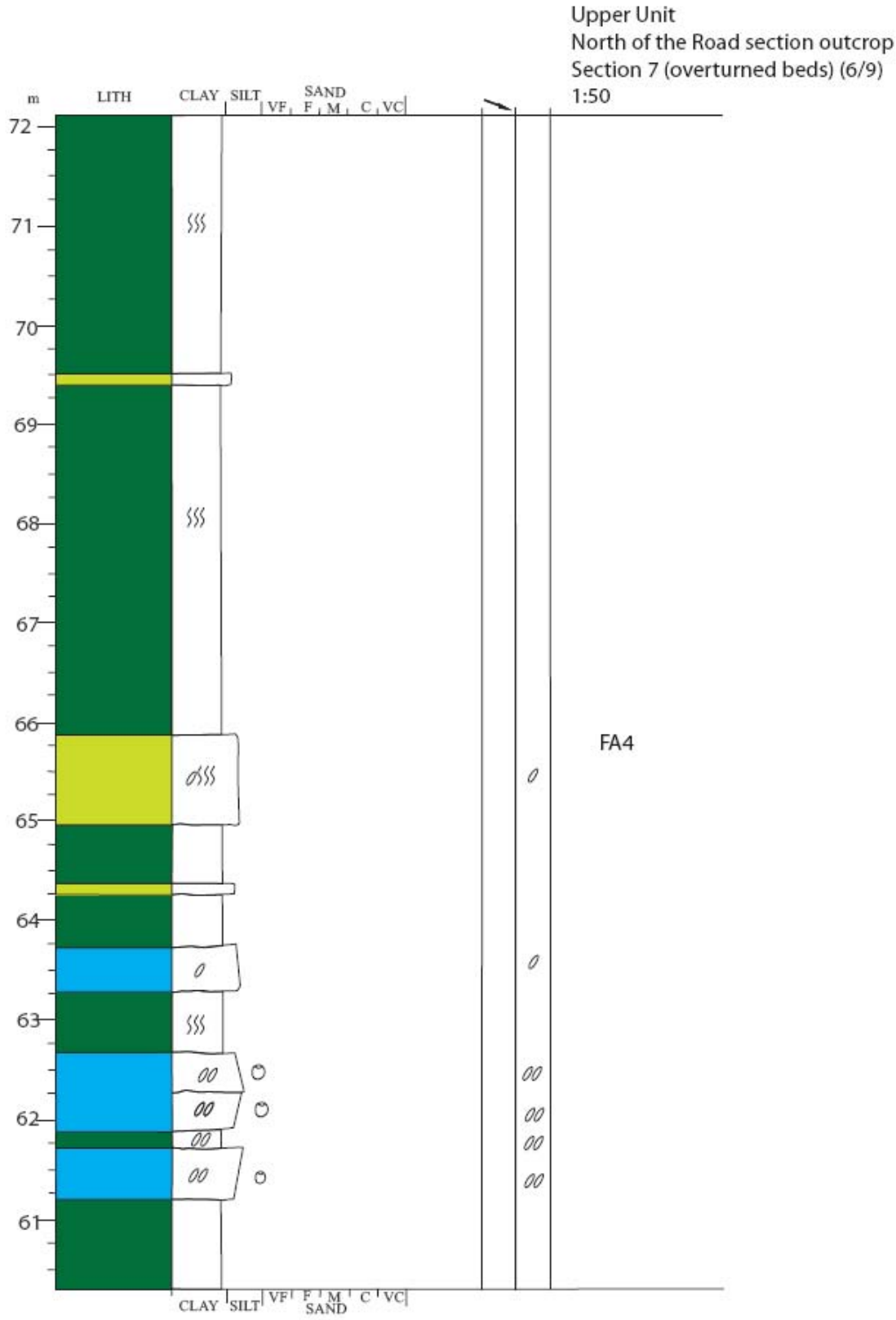
Upper Unit
North of the Road section outcrop
Section 7 (overturned beds) (6/9)
1:50
m
LITH
CLAY
SILT
SAND
VF
F
M
C
VC
72
71
70
69
68
67
66
65
64
63
62
61
FA4

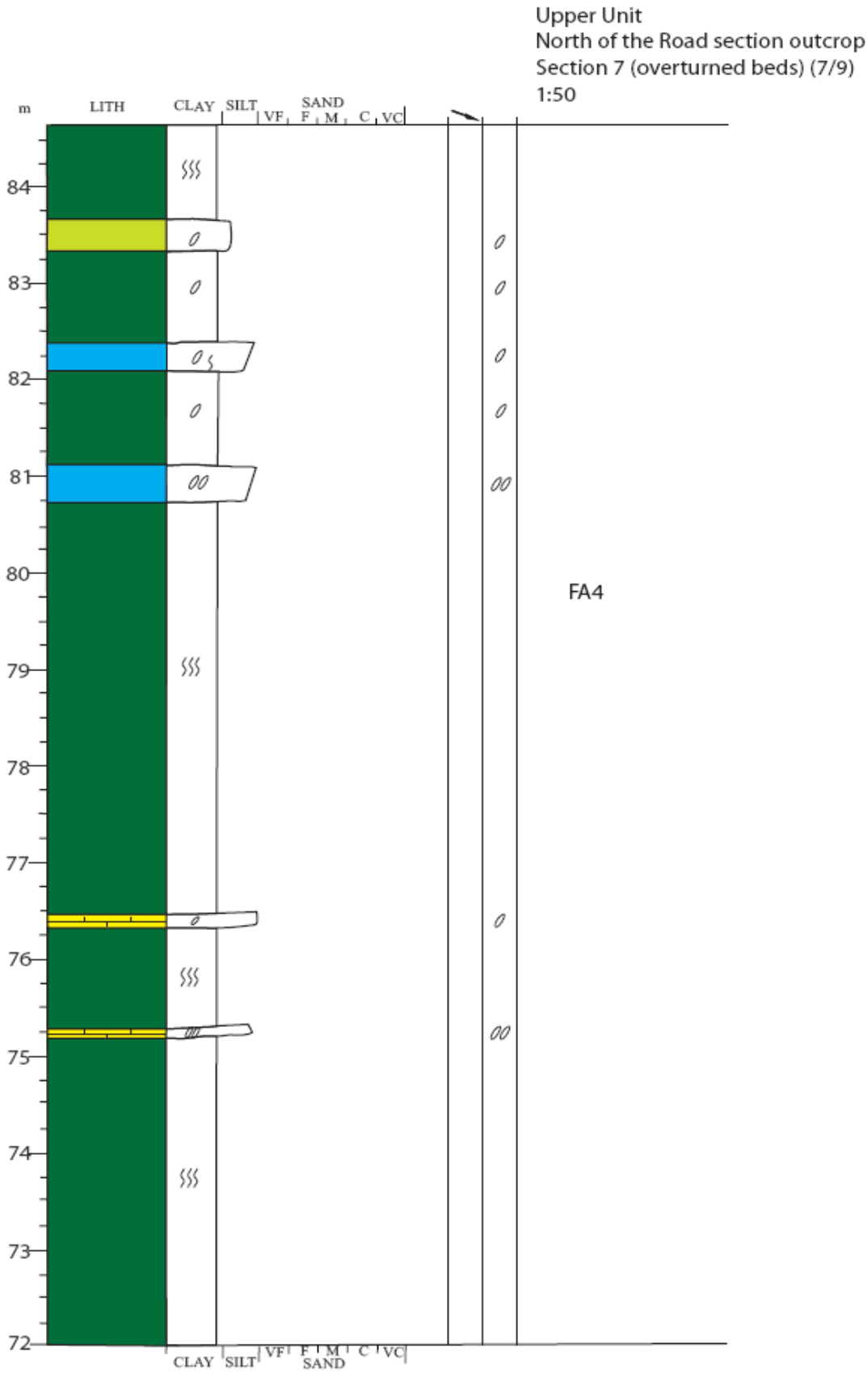
Upper Unit
North of the Road section outcrop
Section 7 (overturned beds) (7/9)
1:50
m
LITH
CLAY
SILT
SAND
VF
F
M
C
VC
84
83
82
81
80
79
78
77
76
75
74
73
72
FA4

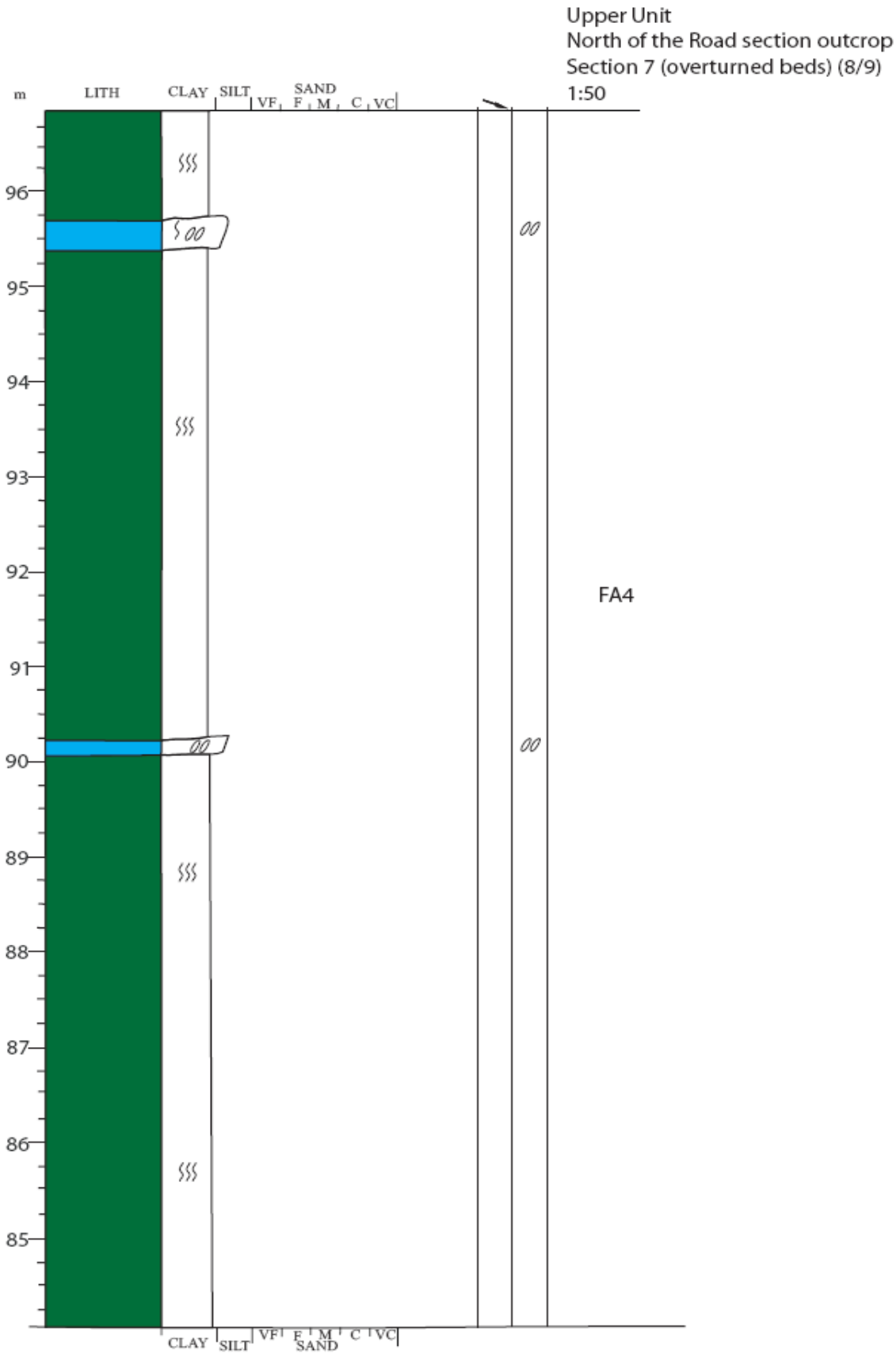
Upper Unit
North of the Road section outcrop
Section 7 (overturned beds) (8/9)
1:50
m
LITH
CLAY
SILT
SAND
VF
F
M
C
VC
96
95
94
93
92
91
90
89
88
87
86
85
FA4

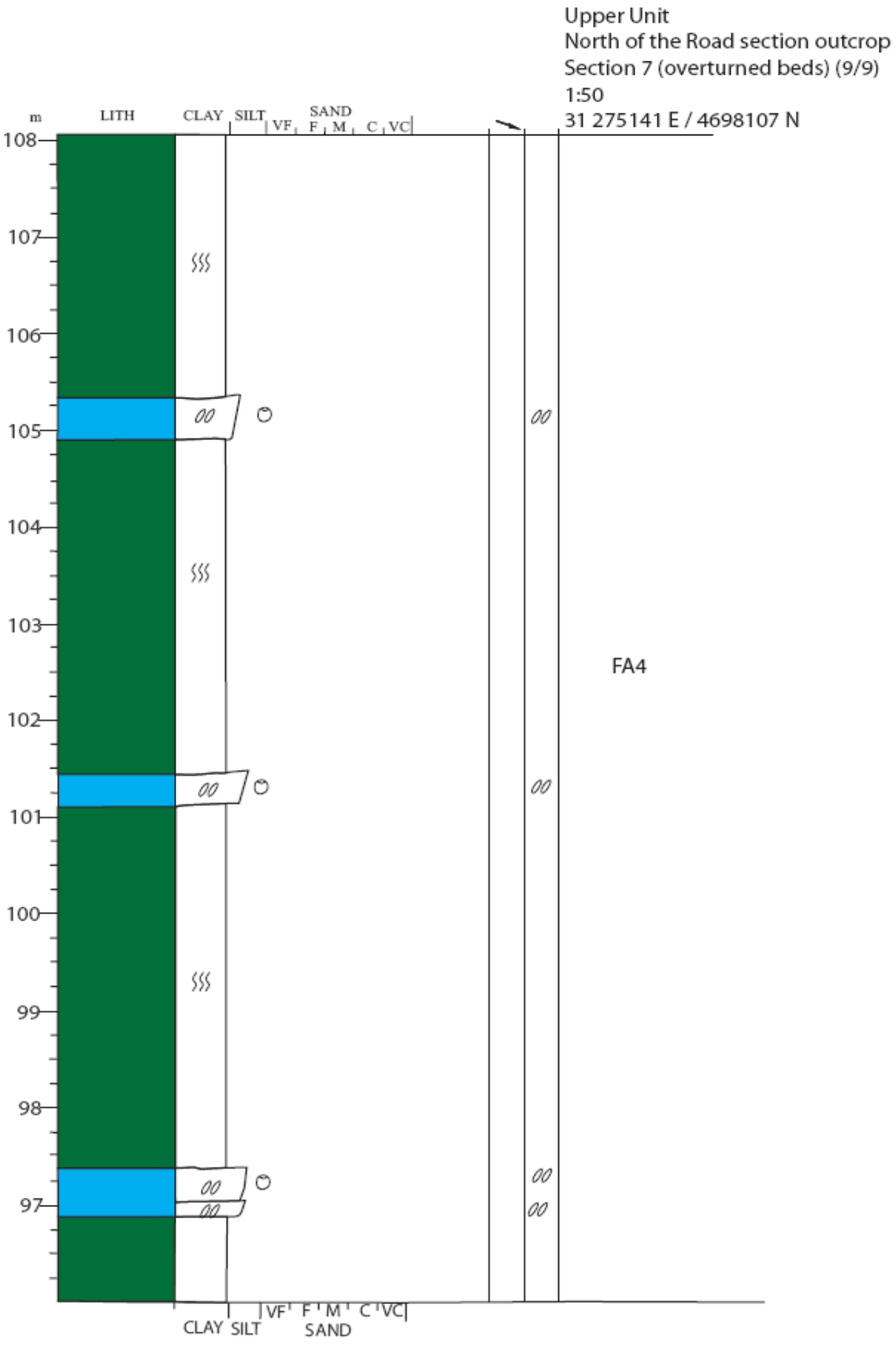
Upper Unit
North of the Road section outcrop
Section 7 (overturned beds) (9/9)
1:50
31 275141 E / 4698107 N
m
LITH
CLAY
SILT
SAND
VF
F
M
C
VC
108
107
106
105
104
103
102
101
100
99
98
97
FA4
CLAY
SILT
SAND

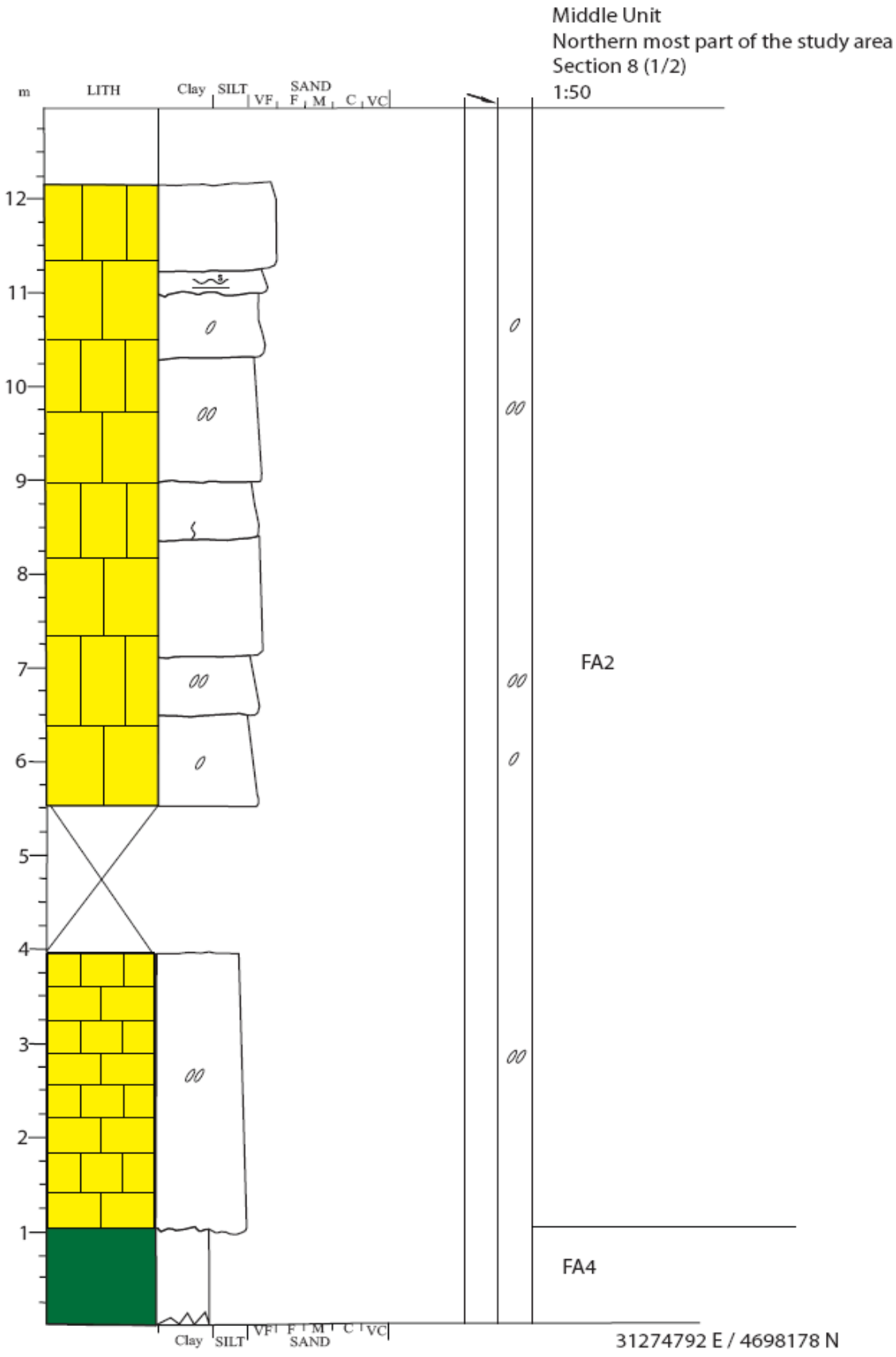
Middle Unit
Northern most part of the study area
Section 8 (1/2)
1:50
m
LITH
Clay
SILT
SAND
VF
F
M
C
VC
12
11
10
9
8
7
6
5
4
3
2
1
FA2
FA4
31274792 E / 4698178 N

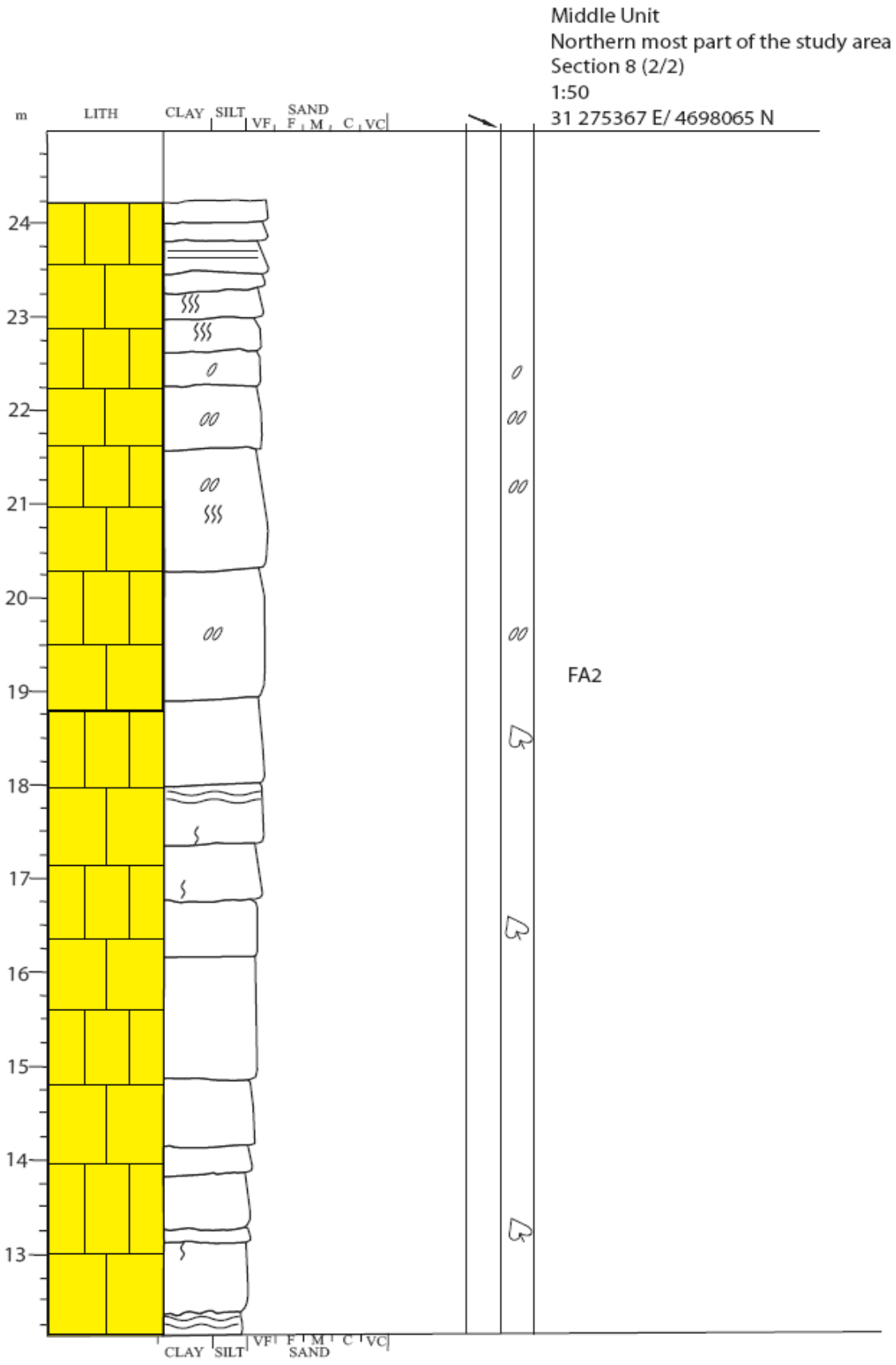
Middle Unit
Northern most part of the study area
Section 8 (2/2)
1:50
31 275367 E/ 4698065 N
m
LITH
CLAY
SILT
SAND
VF
F
M
C
VC
24
23
22
21
20
19
18
17
16
15
14
13
FA2

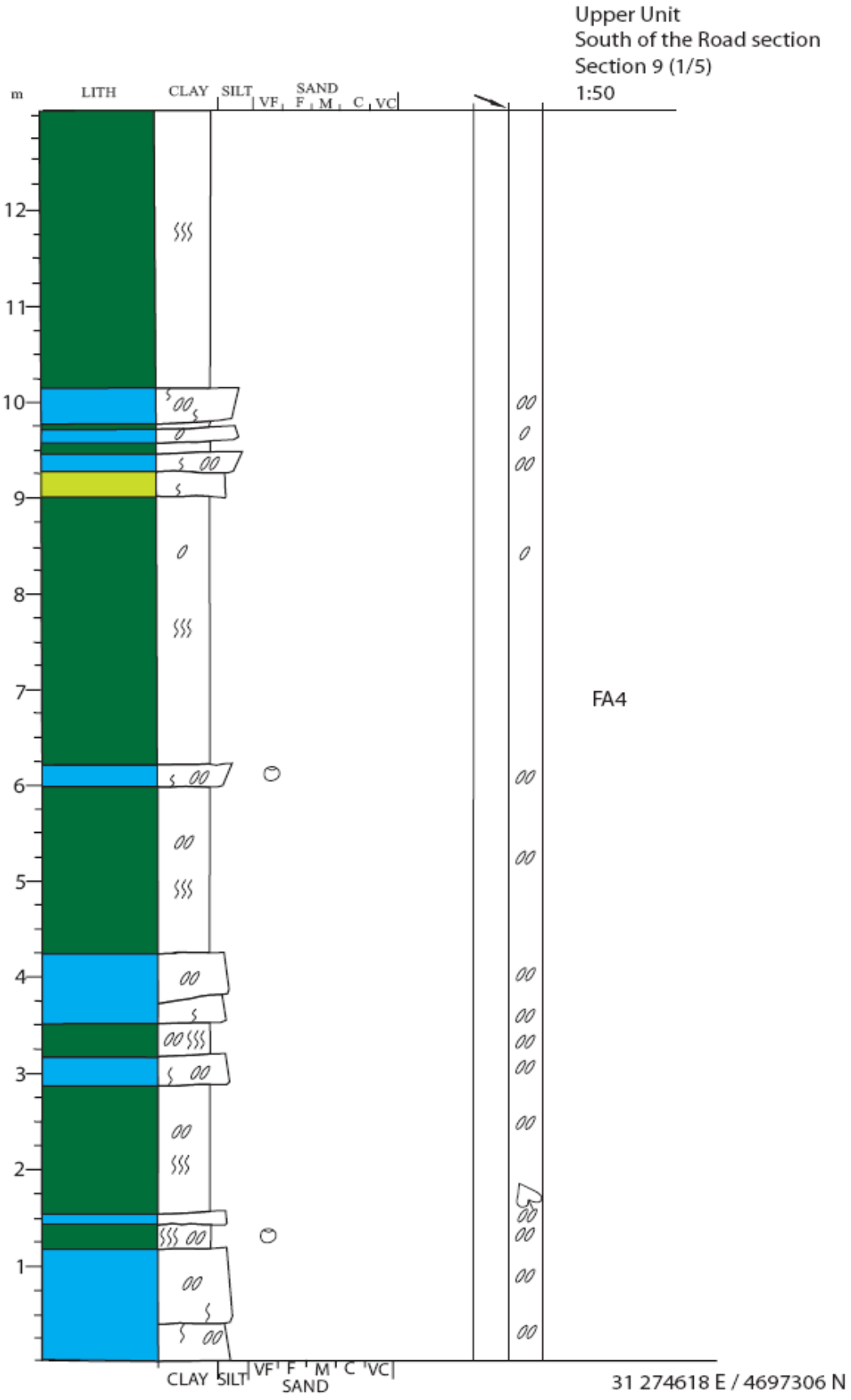
Upper Unit
South of the Road section
Section 9 (1/5)
1:50
m
LITH
CLAY
SILT
SAND
VF
F
M
C
VC
12
11
10
9
8
7
6
5
4
3
2
1
FA4
31 274618 E / 4697306 N

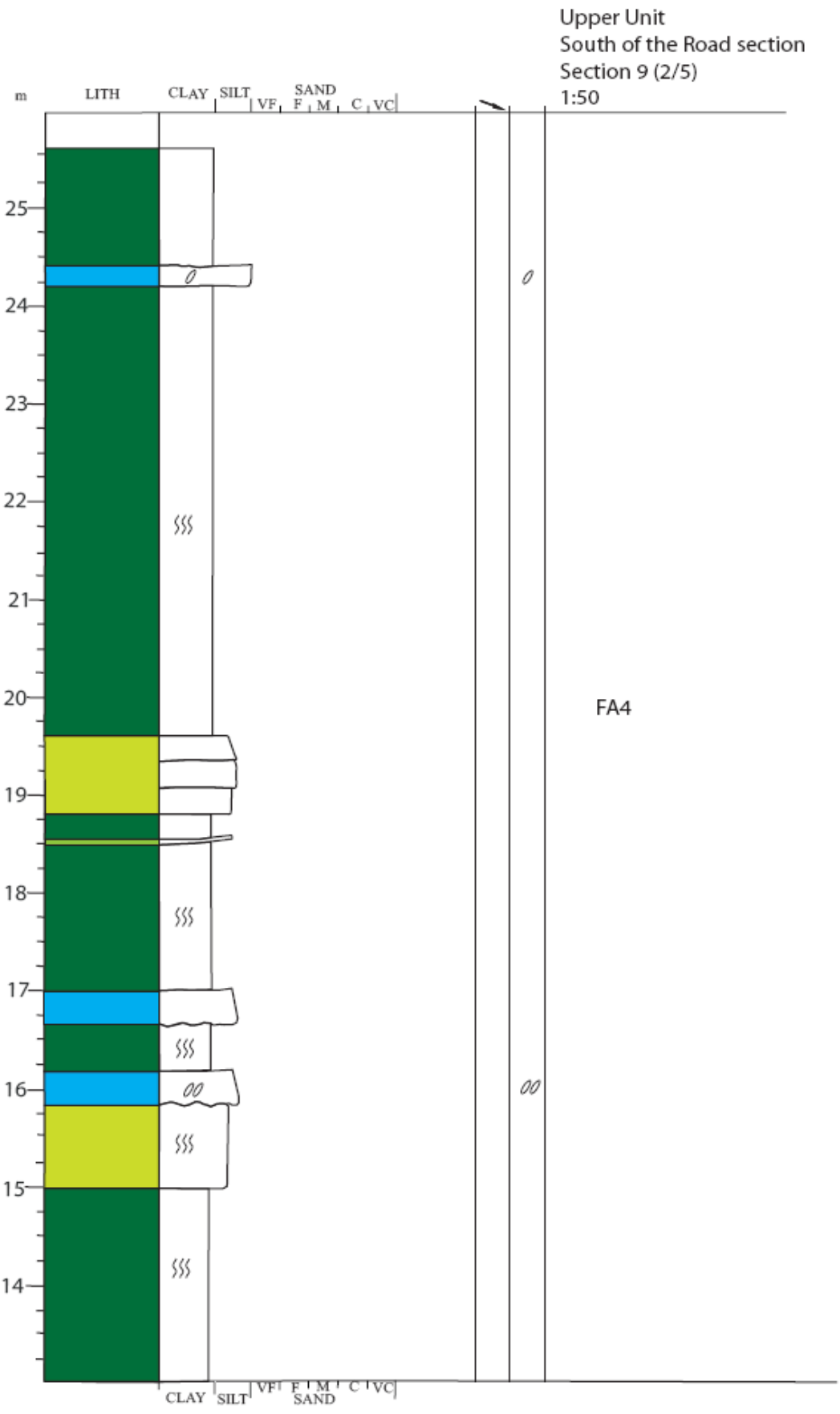
Upper Unit
South of the Road section
Section 9 (2/5)
1:50
m
LITH
CLAY
SILT
VF
SAND
F
M
C
VC
25
24
23
22
21
20
19
18
17
16
15
14
FA4

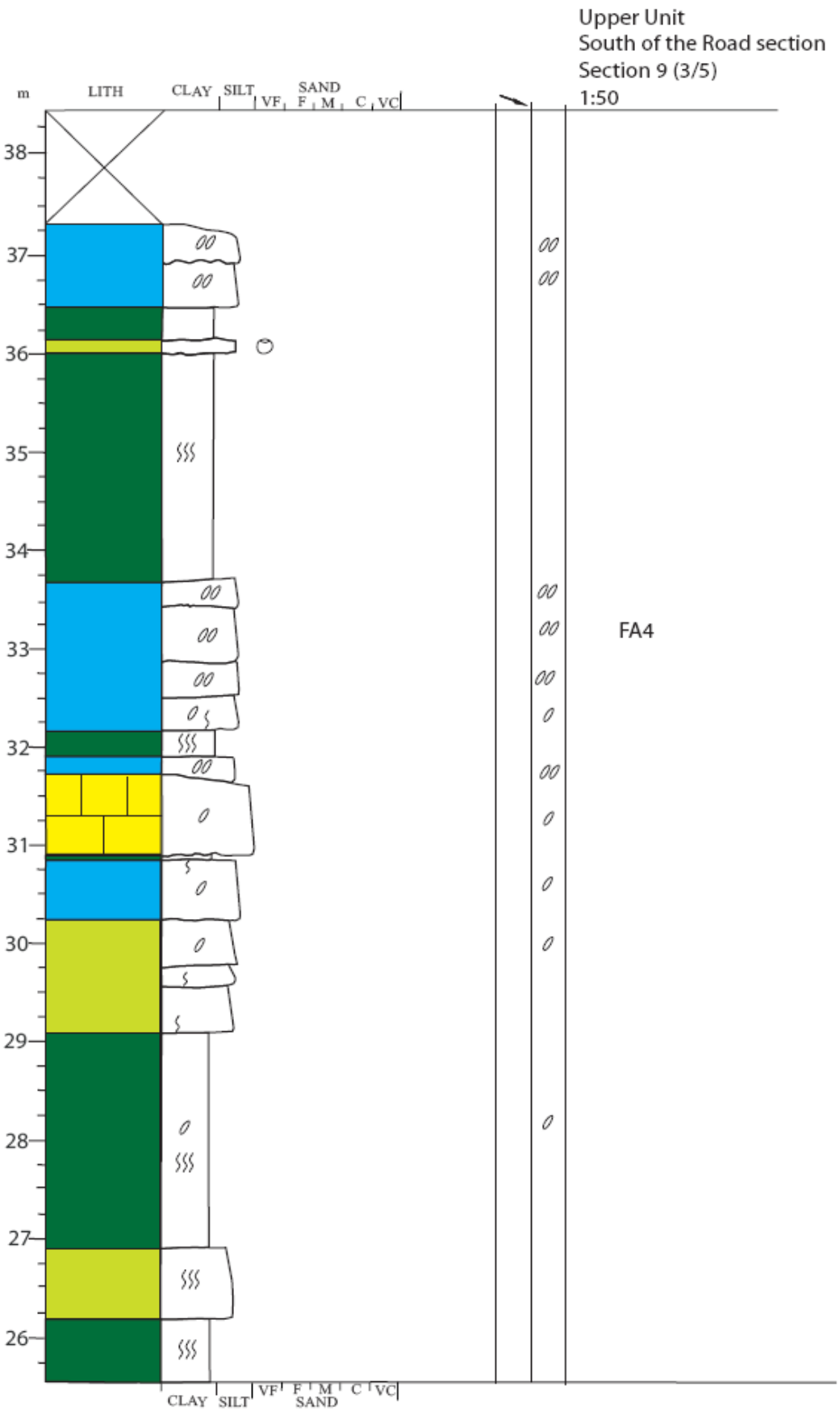
Upper Unit
South of the Road section
Section 9 (3/5)
1:50
m
LITH
CLAY
SILT
SAND
VF
F
M
C
VC
38
37
36
35
34
33
32
31
30
29
28
27
26
FA4

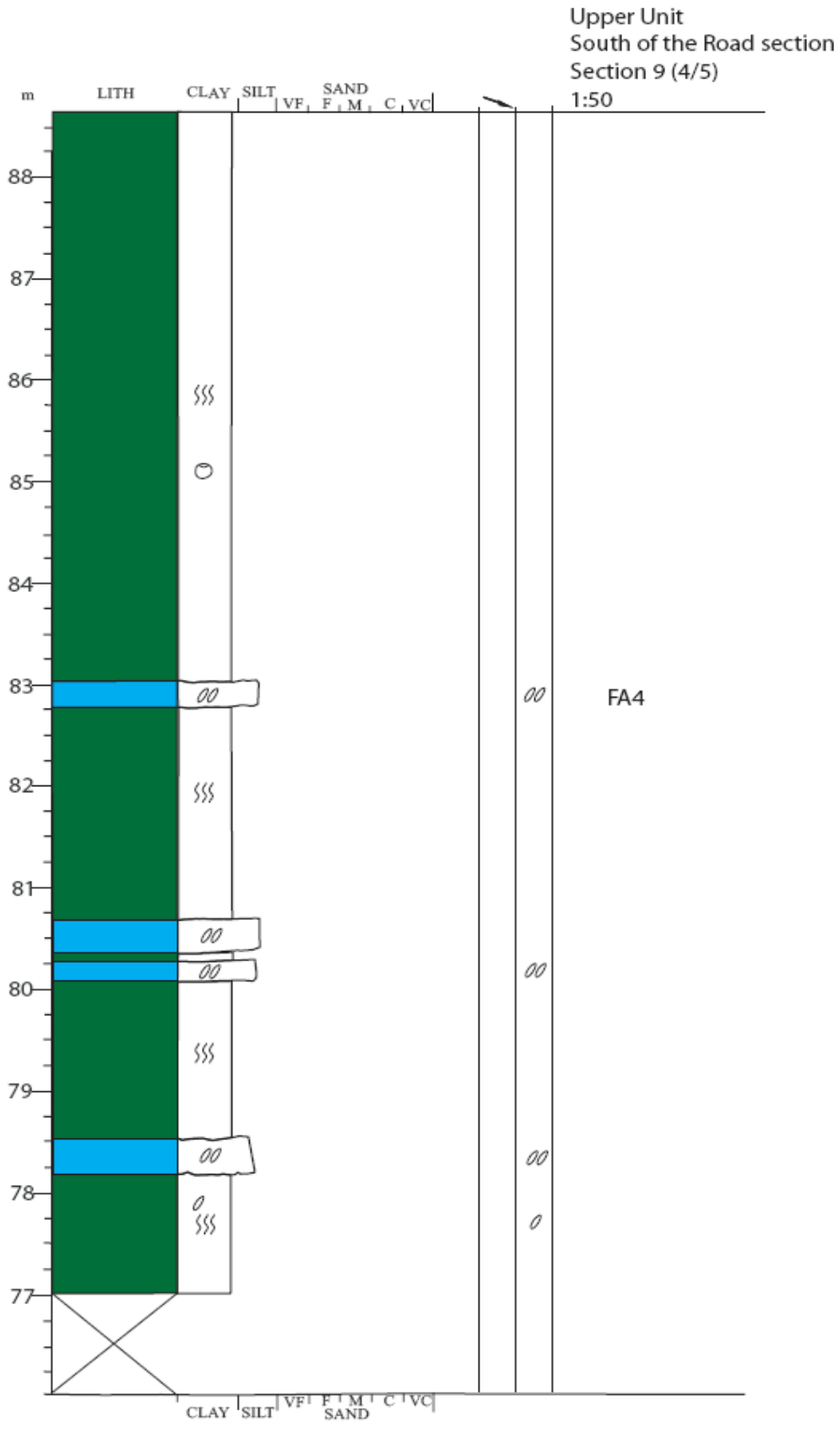
Upper Unit
South of the Road section
Section 9 (4/5)
1:50
m
LITH
CLAY
SILT
SAND
VF
F
M
C
VC
88
87
86
85
84
83
82
81
80
79
78
77
FA4

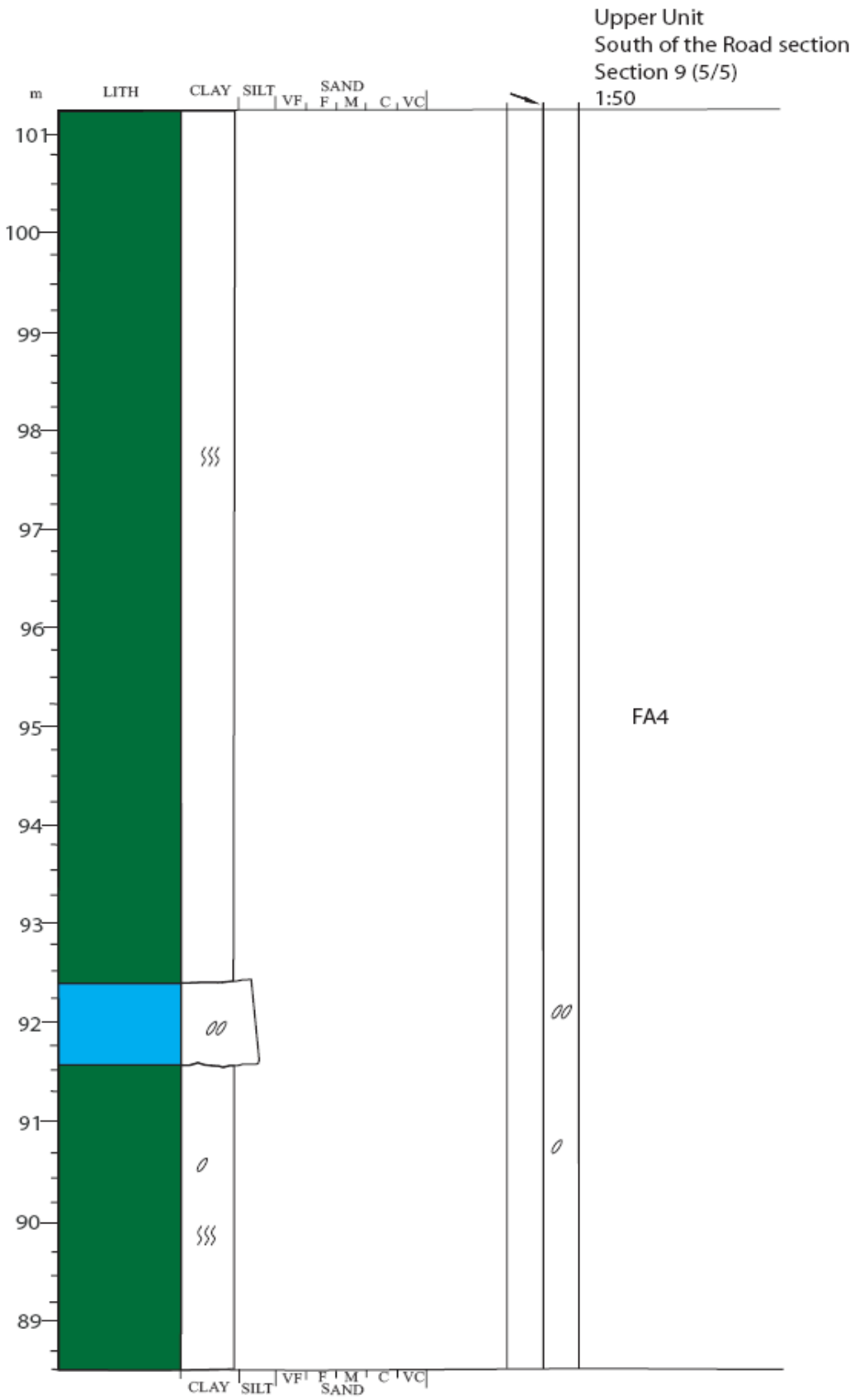
Upper Unit
South of the Road section
Section 9 (5/5)
1:50
m
LITH
CLAY
SILT
SAND
VF
F
M
C
VC
101
100
99
98
97
96
95
94
93
92
91
90
89
FA4